IPS Meeting 2026
28 - 30 October

Institute of Physics Singapore

Conference Program

The IPS Meeting 2026 thanks its sponsors
for their generous support

genetron

WE

OptoSigma®
SIGMAKOKI Group

AceXon
ACEXON TECHNOLOGIES PTE LTD

Y-LASER

World Scientific
Connecting Great Minds

EINST

IOP Publishing

ROHDE&SCHWARZ

ANALYTICAL
Technologies

WAVELENGTH
OPTO-ELECTRONIC

LASER21

ThermoFisher
SCIENTIFIC

Hakuto

PAEONIA
BLOCH

SPI
SingPhotonics International

Kyberlife

Institutional Supporters:

NUS
National University
of Singapore

NANYANG
TECHNOLOGICAL
UNIVERSITY
SINGAPORE

SUTD
SINGAPORE UNIVERSITY OF
TECHNOLOGY AND DESIGN

CQT
CENTRE FOR
QUANTUM
TECHNOLOGIES
SINGAPORE

NANYANG
TECHNOLOGICAL
UNIVERSITY
SINGAPORE
Institute of Advanced Studies

Agency for
Science, Technology
and Research
SINGAPORE

NUS
National University
of Singapore
Institute for Functional
Intelligent Materials

Quantum
Innovation
Centre
A*STAR Q.InC

1 Foreword

Dear fellow Physicists,

After quite some time, we are grateful to return to the campus of SUTD for this event, and welcome the new colleagues in physical sciences there.

As usual, this event aims to give all researchers in physical sciences in Singapore an opportunity to get updated with the quickly evolving research landscape in Singapore, to explore new collaborations, to hunt for new research team members, or just to finally catch up with your colleagues in a relaxed setting with a focus on physics rather than administrative tasks. Most importantly, we need to step out of our usual silos, and make ourselves aware what researchers in other institutions are up to.

We are very happy to welcome an increased number of international guests at this event over time, presenting an opportunity to network with physicists across national boundaries in a relaxed setting.

We try to highlight outstanding research activities in Singapore and beyond with plenary talks - from established researchers, newcomers to our Physical Sciences community in Singapore, and guests from abroad. On the first day, we start with Pan Feng from SUTD sharing how the emerging field of Quantum computing can tame complex physics problems, but switch to a more experimental topic with Ilya Belopolski from NTU sharing his work on semimetal optoelectronics. On the second day, a hot climate topic of the ongoing El Ninio and its consequences is shared by Yu-Heng Tseng visiting us from the National Taiwan University, but continue to look even further far out to a dusty disintegrating Planet, explained to us by Marc Hon from NUS. On the third day, we return back to device- and material related aspects of Quantum Nanophotonics, presented by DONG Zhaogang who recently joined SUTD, followed by a journey through unconventional antiferromagnets guided by Ho Pin from IMRE/A*STAR.

As last years, we also present the IPS awards to outstanding contributors to physical sciences through their accomplishments in research, education and communication in Singapore after the Plenary sessions on Wednesday.

Our technical programme covers a record of over 190 contributions, with 112 oral presentations. As of this writing, we have 81 posters, and encourage to join those who give a poster pitch in the Thursday slot, or nudge yourself to give one if you have not done so yet! As usual, the poster session in the middle of the meeting on Thursday afternoon is really a central part of this event, and as per tradition, of course transitions into a networking event with Pizza and Drinks to provide a proper setting.

We are, as always, grateful for our institutional supporters, the Department of Physics and the Department of Materials Sciences at NUS, the School of Physics and Applied Physics at NTU, the Graduate Studies Program at SUTD, the Center for Quantum Technologies, and the Institute for Functional Intelligent Materials at NUS. We also are grateful for the support by the Quantum Engineering Programme, the Institute of Advanced Studies at NTU, as well as A*STAR and Q.InC.

Last but not least, let's thank the huge number of exhibitors this year, who again help with their generous support to make this conference possible. Without their help, we would not be able to put up this conference – so do spend some time and visit their booths to see what products or services they can offer for your research. Make sure they find this conference useful as well, as they are a pillar for this event to happen!

With this, we wish you an inspiring conference, a refreshing look up from your daily work, new ideas, new contacts, new collaborations for a successful new year of research in physical sciences ahead!

Your organizing team of the IPS meeting 2026

(Notes)

Contents

1 Foreword 1

2 Schedule 4

3 Plenary sessions 6

P1: Taming Complex Systems in Quantum Computing . . . 6
P2: Semimetal optoelectronics . . . 6
P3: Predicting ENSO in a Changing Pacific: Physical insights from the triple-dip La Niño and Ongoing Development of 2026/27 El Niño . . . 7
P4: Discovery of a Dusty, Disintegrating Planet . . . 7
P5: Engineering Light at the Nanoscale: From Classical to Quantum Nanophotonics . . . 8
P6: Unconventional Antiferromagnets: From Fundamentals to Translation . . . 9

4 Posters 10

General poster presentation . . . 10

5 Technical Sessions 38

T1: Quantum Optics . . . 38
T2: Quantum Theory I . . . 40
T3: Condensed Matter I . . . 42
T4: Quantum Simulation I . . . 44
T5: Atoms and Ions . . . 47
T6: Quantum Theory II . . . 49
T7: Condensed Matter II . . . 51
T8: Quantum Simulation II . . . 53
T9: Quantum Algorithms I . . . 56
T10: 2D materials . . . 59
T11: Solid State Devices . . . 62
T12: Metamaterials and Photonics . . . 65
T13: Topologigal States . . . 68
T14: Nano-Optics . . . 70
T15: Physics and AI . . . 73
T16: Quantum Algorithms II . . . 75
T17: Quantum Communication . . . 78
T18: Quantum Devices . . . 80
T19: Quantum Algorithms III . . . 82
T20: Instrumentation and Processes . . . 84
T21: Astrophysics and Mathematical Physics . . . 87

6 Committees 89

Author List 90

2 Schedule

Wednesday, 28 October

8.30 AM	Registration (Near Lecture Theatre 2)			
8.50 AM	Opening Address (Lecture Theatre 2)			
9.00 AM	Plenary talk P1: Asst. Prof. PAN Feng (Lecture Theatre 2)			
9.45 AM	Plenary talk P2: Asst. Prof. Ilya Belopolski (Lecture Theatre 2)			
10.30 AM	IPS Awards presentation (Lecture Theatre 2)			
10.45 AM	Coffee/Tea Break + Exhibition (Multi-Purpose Hall)			
11.30 AM	Technical Sessions			
	T1 (Think Tank 2&3) Quantum Optics	T2 (Think Tank 4&5) Quantum Theory I	T3 (Think Tank 9&10) Condensed Matter I	T4 (Think Tank 11&12) Quantum Simulation I
1.00 PM	Lunch + Exhibition (Multi-Purpose Hall)			
2.00 PM	Technical Sessions			
	T5 (Think Tank 2&3) Atoms and Ions	T6 (Think Tank 4&5) Quantum Theory II	T7 (Think Tank 9&10) Condensed Matter II	T8 (Think Tank 11&12) Quantum Simulation II
3.30 PM	Coffee/Tea Break + Exhibition (Multi-Purpose Hall)			
4.15 PM	Technical Sessions			
	T9 (Think Tank 2&3) Quantum Algorithms I	T10 (Think Tank 4&5) 2D Materials	T11 (Think Tank 9&10) Solid State Devices	T12 (Think Tank 11&12) Metamaterials and Photonics
5.45 PM	End of Wednesday sessions			

Thursday, 29 October

9.00 AM	Plenary talk P3: Prof. Yu-Heng Tseng (Lecture Theatre 2)			
9.45 AM	Plenary talk P4: Asst. Prof. Marc Hon (Lecture Theatre 2)			
10.30 AM	Coffee/Tea Break + Exhibition (Multi-Purpose Hall)			
11.15 AM	Technical Sessions			
	T13 (Think Tank 2&3) Topological States	T14 (Think Tank 4&5) Nano-Optics	T15 (Think Tank 9&10) Physics and AI	T16 (Think Tank 11&12) Quantum Algorithms II
1.00 PM	Lunch + Exhibition (Multi-Purpose Hall)			
2.00 PM	Rapid Fire poster Pitch session (Lecture Theatre 2)			
3.15 PM	Coffee/Tea Break + Exhibition (Multi-Purpose Hall)			
4.00 PM	Poster session + Exhibition (Multi-Purpose Hall)			
5.30 PM	Poster awards + Pizza + Drinks (Multi-Purpose Hall)			
6.30 PM++	End of Thursday sessions			

Friday, 30 October

9:00 AM	Plenary talk P5: Assoc. Prof. DONG Zhaogang (Lecture Theatre 2)			
9:30 AM	Plenary talk P6: Dr. HO Pin (Lecture Theatre 2)			
10.30 AM	Coffee/Tea Break + Exhibition (Multi-Purpose Hall)			
11.15 AM	Technical Sessions			
	T17 (Think Tank 2&3) Quantum Communication	T18 (Think Tank 4&5) Quantum Devices	T19 (Think Tank 9&10) Quantum Algorithms III	T20 (Think Tank 11&12) Instrumentation and Processes
12.45 PM	Lunch + Exhibition (Multi-Purpose Hall)			
2.00 PM	Mixed Sessions			
	T21 (Think Tank 2&3) Astrophysics and Mathematical Physics	Quantum SG networking (Lecture Theatre 2)		
3.30++ PM	End of Conference			

3 Plenary sessions

We have several distinguished plenary speakers this year – with a nice overview of recent activities in physical sciences in Singapore.

P1: Taming Complex Systems in Quantum Computing

Asst. Prof. PAN Feng Science, Mathematics and Technology (SMT),
Singapore University of Technology and Design

Wednesday, 28 October, 9:00am, Venue: Lecture Theatre 2

Abstract

Quantum computing presents computational challenges ranging from the simulation of large quantum circuits to the inference of errors and the search for optimal solutions. Although these problems involve enormous spaces of possibilities, their structure can offer opportunities for more efficient computation. This talk presents recent advances in addressing these challenges using tensor networks, statistical mechanics, and machine learning.

I will discuss our work on classical simulation of quantum circuits, including benchmarks of quantum computational advantage and the validation of experimental outputs from Google's Sycamore circuits and IBM's doped-Clifford circuits. I will then explore how statistical-mechanical formulations, exact decoding, and learned noise models can improve quantum error correction. Extending these ideas to quantum-inspired optimization, I will introduce our physics-inspired Free Energy Machine framework and its application to combinatorial problems.

Finally, we will discuss how these computational methods can inform the design of quantum experiments and improve the reliability of logical qubits.

P2: Semimetal optoelectronics

Asst. Prof. Ilya Belopolski,
Nanyang Technological Univeraity (NTU)

Wednesday, 28 October, 9:45am, Venue: Lecture Theatre 2

Abstract

Semiconductors were first measured in the 1850s, and their counter-intuitive properties confused & frustrated scientists for nearly a century. The semiconductor transistor was only invented in 1947, making semiconductors useful for computers. With the discovery of graphene in 2004, scientists became fascinated by semimetals. Our community worldwide has now explored the compensated semimetal WTe_2, the Dirac semimetal Na_3Bi, the polar Weyl semimetal TaAs, the Weyl ring semimetal Co_2MnGa and a zoo of other materials [1-6]. Despite their fascinating physics, semimetals are not yet useful. I argue that driving materials across the phase transition—between semimetal and semiconductor—is the most natural way to operate a semimetal. We recently turned a Weyl semimetal 'on' and 'off' for the first time in $(Cr,Bi)_2Te_3$, using chemical doping & temperature to drive the phase transition to a semiconductor [7-8]. Now, we need to find more materials exhibiting a semimetal-semiconductor transition, drive the transition at high frequency [9], and understand how such 'semimetal switches' could surpass semiconductor transistors.

[1] M.Z. Hasan, G. Chang, I.B. et al., Nat. Rev. Mat. **6**, 784 (2021).

[2] Su-Yang Xu, I.B. et al., Science **349**, 613 (2015).

[3] D. S. Sanchez, I.B. et al., Nature **567**, 500 (2019).

[4] I.B. et al., Nature **604**, 647 (2022).

[5] I.B. et al., Science **365**, 1278 (2019).

[6] I.B. et al., Phys. Rev. Lett. **127**, 256403 (2021).

[7] Tokura, Yasuda and Tsukazaki, Nat. Rev. Phys. **1**, 126 (2019.

[8] I.B. et al., Nature **637**, 1078 (2025).

[9] Max. T. Birch, I.B. et al., Nature 633, **554** (2024).

P3: Predicting ENSO in a Changing Pacific: Physical insights from the triple-dip La Niño and Ongoing Development of 2026/27 El Niño

Prof. Yu-Heng Tseng
Distinguished Professor,
Institute Institute of Oceanography, National Taiwan University

Thursday, 29 October 9:00am, Venue: Lecture Theatre 2

Abstract

As the dominant mode of interannual climate variability, El Niño–Southern Oscillation (ENSO) significantly influences weather, marine and terrestrial ecosystems, and human society across the globe, making reliable prediction critically important. Predicting ENSO a few seasons in advance remains one of the major challenges in climate science, particularly across the Spring Predictability Barrier and for prolonged or atypical ENSO events. This presentation examines ENSO predictability within the broader context of Pacific climate variability, with an emphasis on the physical processes that govern ENSO evolution and provide sources of predictability. In particular, we explore the interaction among tropical ocean memory, ocean–atmosphere coupling, and extratropical forcing using a physically based statistical ENSO Prediction Model (EPM). The contrasting 1998–2001 and 2020–2023 triple-dip La Niña events illustrate how similar ENSO states can arise from different physical mechanisms: the former was largely sustained by negative equatorial Pacific heat-content anomalies following a strong El Niño, whereas the latter was strongly influenced by persistent extratropical forcing from the Southern Hemisphere. The EPM captures these distinct processes, demonstrating how physical understanding of tropical–extratropical interactions can improve ENSO prediction. Building on these insights, we examine the ongoing development of the 2026/27 El Niño to explore how evolving ocean heat content, atmospheric forcing, and tropical–extratropical interactions may provide early indications of its future evolution and test our current understanding of ENSO predictability.

P4: Discovery of a Dusty, Disintegrating Planet

Asst. Prof. Marc HON
Department of Physics, National University of Singapore

Thursday, 29 October, 9:45am, Venue: Lecture Theatre 2

Abstract

The planet BD+05 4868Ab is a world that is dying in a spectacular manner: by disintegration into dust that forms comet-like tails. In this talk, I will present its discovery, and how its dust tail offers the unprecedented opportunity to directly sample the geological composition of a rocky planet outside our Solar System.

P5: Engineering Light at the Nanoscale: From Classical to Quantum Nanophotonics

Assoc. Prof. DONG Zhaogang,
Science, Mathematics and Technology (SMT),
Singapore University of Technology and Design

Friday, 26 September, 9:00am, Venue: Lecture Theatre 2

Abstract

Engineering light at the nanoscale has opened exciting opportunities for exploring fundamental light–matter interactions and developing next-generation photonic and quantum technologies. By tailoring the geometry, composition, and electromagnetic resonances of nanostructures, it is able to achieve unprecedented control over optical confinement, scattering, absorption, and emission, far beyond the capabilities of conventional optical components.

In this plenary talk, I will present our recent advances in nanoscale light–matter interactions, spanning classical nanophotonics, nonlinear optics, and quantum photonic devices. First, I will discuss how advanced sub-10-nm nanofabrication enables precisely engineered dielectric and plasmonic nanostructures for strong optical confinement, tailored resonances, and enhanced light absorption, with applications in multifunctional optoelectronic devices. Next, I will highlight how Fano resonances and bound states in the continuum provide powerful platforms for enhancing nonlinear optical processes and manipulating light emission.

Finally, I will introduce our recent efforts in quantum nanophotonics, where engineered optical environments enable enhanced light–emitter coupling, controlled spontaneous emission, and tailored single-photon emission. Together, these developments demonstrate how nanoscale engineering bridges classical optical phenomena and quantum light–matter interactions, opening new opportunities for integrated photonics and emerging quantum technologies.

P6: Unconventional Antiferromagnets: From Fundamentals to Translation

Dr. HO Pin
Principal Scientist and Deputy Head
Electronic Materials Department, A*STAR Institute of Materials Research and Engineering (A*STAR IMRE)

Thursday, 25 September, 9:45am, Venue: Lecture Theatre 2

Abstract

Unconventional antiferromagnets (AFs), such as noncollinear AFs (NCAF) and altermagnets, have garnered significant interest due to their compensated spin structures and spin-splitting properties which enable functionalities beyond those of conventional ferromagnets (FMs) and AFs [1]. Notably, unconventional AFs combine the advantages of both FMs and AFs – offering field immunity, ultrafast spin dynamics, and energy-efficient operation – making them promising candidates for next-generation computing and sensing technologies.

First, we discuss NCAF material platforms based on hexagonal-close-packed (002)-oriented Mn_3Ga and face-centered-cubic (111)- and (001)-oriented Mn_3Pt thin films grown using magnetron sputtering [2-4]. In Mn_3Ga/Pt heterostructures, ultrafast spin current generation and THz signal arise from pulsed magnetization dynamics and transient spin currents associated with NCAF order [3]. In Mn_3Pt multilayers, modulation of the lattice parameter and dopant concentration enables control of the interplay between ferromagnetic canting and intrinsic antiferromagnetic contributions, providing tunability of the magnitude and polarity of the anomalous Hall effect and x-ray magnetic signatures [4].

Next, we further explore the translation of field-tolerant and magnetically compensated nature of NCAFs into magnetic-field sensing technology for demanding environments such as magnetic resonance imaging, where conventional magnetic sensors can be challenged by strong background fields and magnetic interference.

Finally, we discuss the development of altermagnetic thin films, including pyrite MnS_2 and rutile RuO_2, grown using chemical and physical vapour deposition, respectively. Combining density functional theory predictions of momentum-dependent spin-splitting near the Fermi level with experimental characterization of their chemical, structural, magnetic and electrical properties, we establish these materials as promising platforms for investigating and exploiting altermagnetic functionality [5].

[1] S. Chen et al., Mn-based noncollinear antiferromagnets and altermagnets, J. Phys. D: Appl. Phys. **57**, 443001 (2024).

[2] S. Chen et al., Crystalline and transport characteristics of ferrimagnetic and antiferromagnetic phases in Mn_3Ga films, APL Mater. **11**, 101126 (2023).

[3] Y. Song et al., Ultrafast spin current excitation and controlled terahertz radiation from noncollinear antiferromagnets, Adv. Opt. Mater. **13**, 2500210 (2025).

[4] S. Chen et al., Tailoring antiferromagnetic orders and spin transport in noncollinear Mn_3Pt multilayers, Adv. Func. Mater. e07406 (2025).

[5] J. Zhou et al., Symmetry-driven altermagnetism in the manganese sulphides family, APL Mater. (In press, 2026).

4 Posters

As previously, we have a full session (Thursday after lunch) with no parallel technical sessions where all IPS participants get your audience for a supershort (3 minutes) presentation on a poster if the authors want to participate. In order to encourage authors to participate, we will choose the Best Poster Award this year form those submissions where there was short presentation in this session.

For this, we just project your poster on the screen in the lecture hall (please provide us with a PDF file for that purpose). You can email this to us via posters@ipsmeeting.org, or leave it with the reception desk.

IPS Best Poster Award

During the conference the program committee will select the three best poster presentations for the IPS Best Poster Award. The award will be handed over to the winners at the Pizza session after the end of the poster session on Thursday evening, probably around 5.30pm-6.30pm.

General poster presentation

Format

The poster walls fit a A1 sized poster (portrait orientation).

Poster Abstracts

PO.9 Anomalous topological superradiant phases

Youqi Lu*

We present the a novel set of light-matter topology realized by implementing a finite-component quantum Rabi array with a photonic analog of the Su-Schrieffer-Heeger (SSH) configuration. We demonstrate how complex light-matter couplings with speciesependent phases lead to the closure of superradiance-induced band gap in a manner that differs from that in the SSH model. We uncover an topological superradiant phase transition from a normal phase to a topological superradiant electromagnet phase, which is characterized both by a local order parameter and a global topological invariant. Novel superradiance-enhanced edge states emerge with significantly amplified excitations superior to those in topological normal phase. Strikingly, anisotropic light-atom coupling restores the inversion symmetry, and induces a topological superradiant electric (magnetic) phase. It yields superradiant-enhanced chiral edge states, leading to unidirectional photon excitations in the left or right edge mode. Our proposed setup offers a tunable platform for topological quantum optics, advancing applications in topological superradiant lasers.

PO.11 The Cost of Removing Tunability in Quantum Data Re-Uploading

Anthony Yuezhang Liu*, Lirandë Pira* (National University of Singapore)

Fixed encoding data re-uploading quantum circuits provide a striking example of universality emerging from a highly constrained architecture. However, universality alone is insufficient for assessing the theoretical and practical value of fixed and tunable upload circuits. The resource cost of removing tunability remains poorly understood. In this work, we establish quantitative depth-error scaling for approximating tunable upload circuits with fixed upload circuits. We show that a tunable upload circuit can be approximated by a fixed upload circuit using depth $D = O_\sigma[(\log(1/\varepsilon))^\sigma]$ for every $\sigma > 1$, with a target dependent constant overhead, thereby improving the previously known polynomial dependence on $1/\varepsilon$ with the same overhead. Our proof is based on an auxiliary extension approximation mechanism that combines Gevrey class construction, Jackson's theorem and generalized quantum signal processing theorem. Thus, the expressive power lost by removing tunability can be recovered using only polylogarithmic growth in circuit depth with a target dependent constant overhead. We further identify a periodic mismatch obstruction intrinsic to fixed upload approximations and use Turán-Nazarov inequalities to prove logarithmic lower bounds $D = \Omega(\log(1/\varepsilon))$ for the approximation of mismatch class target tunable upload circuits. Conceptually, our analysis reveals two structural mechanisms underlying approximation in fixed upload architectures: auxiliary extensions and mismatch obstructions. These results provide a quantitative understanding

of how expressivity is transferred from tunable frequencies into circuit depth, and suggest a broader framework for studying approximation complexity in quantum signal processing and related quantum learning models.

PO.12 Spectral Differences Between Quantum Evolution and Stochastic Laplacian Dynamics

Pratham Tewari* (Cambridge Centre for International Research, Cambridge, UK and One World International School, Nanyang Campus, Singapore)

Both quantum systems and stochastic systems evolve through matrix exponentials, exhibiting a formal similarity in their mathematical structure. In quantum mechanics, time evolution is generated by the Hamiltonian operator. In stochastic processes, time evolution is determined by a Markov generator (Laplacian). Although both dynamics are expressed through exponential operators and appear structurally similar, the resulting dynamics display fundamentally different long-time behaviour. This work provides spectral and linear algebraic analysis to identify the source of this distinction. The qualitative difference arises not only from the spectrum of the generator, but also from the manner in which eigenvalues enter the exponential evolution. For quantum systems with Hermitian Hamiltonians, real eigenvalues lead to purely oscillatory dynamics. In contrast, non-Hermitian Hamiltonians, which represent open systems, possess complex eigenvalues with both real and imaginary parts, resulting in dynamics where the real part governs oscillation and the imaginary part induces exponential decay of state amplitude over long times. For stochastic systems, in a two-state Markov chain, eigenvalues are zero and real. Inserting real eigenvalues into the evolution leads to decay. In a three-state Markov chain, there is one complex eigenvalue also, which when substituted into the time evolution equation, leads to decay because of the eigenvalue's real part and oscillation due to its imaginary part. This behaviour is opposite to quantum evolution. Due to this distinction, it can be observed how the placement of the imaginary unit fundamentally alters the role of spectral components in determining time evolution across these systems.

PO.14 Size Generalization of Neural Network Potential Energy Surfaces for Gold Nanoparticles

Tianyu Gao*, Qinlan Luo*, Xuchen Yang, Qiyu Zeng, Jiayu Dai (national university of defense and Technology)

Machine learning interatomic potentials (MLIPs) have emerged as a powerful tool to bridge the accuracy of density functional theory (DFT) and the efficiency of classical force fields. However, their predictive reliability strongly depends on the completeness of the training dataset, especially for systems with diverse local atomic environments—such as metal nanoparticles (NPs) where bulk, surface, edge, and vertex sites coexist. In this work, we systematically investigate the size generalization capability of deep potential (DP) models for gold NPs by constructing three training sets with progressively expanded coverage: bulk only (DP-bulk), bulk + surface (DP-bulk+surface), and bulk + surface + small clusters (DP-all, clusters $\leq$ 212 atoms). Using SOAP descriptors combined with PCA, we map the atomic environments of decahedral Au NPs (2–14 nm) and compare the three potentials against DFT references for energy, forces, vibrational density of states, relative stability (Δ parameter), and ensemble-based force uncertainty. Our results demonstrate that DP-bulk fails completely for surface and edge atoms; adding surface data substantially improves planar surface predictions but still underestimates energies and cannot accurately describe edges/vertices. Only DP-all, which includes small clusters rich in under-coordinated and high-curvature sites, achieves uniformly low force uncertainties ($\approx$0.01 eV/Å) across all atomic environments, eliminates spurious peaks in vibrational spectra, and yields physically consistent size-dependent stability trends. We further show that while DP-bulk+surface performs adequately for medium-sized NPs ($\approx$4 nm), its errors diverge at edges and vertices in larger particles $\geq$8 nm), where DP-all maintains robust performance. This work establishes a practical data-coverage criterion for constructing transferable MLIPs for NPs and highlights the indispensable role of small-cluster data in capturing the complex local environments that govern melting and dynamical processes.

PO.20 Statistics-governed dynamical scaling in interacting anyonic chains

Xu-Chen Yang*, Botao Wang, Jianpeng Liu, Bing Yang, Jianmin Yuan, Yongqiang Li* (National University of Defense Technology)

Particle exchange statistics impose fundamental constraints on nonequilibrium quantum dynamics, yet it remains an open question whether anyonic statistics can lead to emergent dynamical scaling beyond the conventional Bose-Fermi paradigm. Here we investigate the far-from-equilibrium many-body relaxation of anyons in a one-dimensional lattice and uncover a statistics-governed dynamical scaling mechanism beyond the bosonic and

fermionic limits. Based on large-scale numerical simulations and scaling analysis, we find that fractional statistics leads to emergent superdiffusive scaling in both density transport and fluctuation dynamics, while the entanglement entropy remains ballistic and is essentially insensitive to exchange statistics. The anomalous dynamics can be interpreted intuitively from statistical-phase-induced quantum interference that suppresses coherent holon-doublon propagation, whereas the entanglement growth is dominated by its configurational component, which maintains ballistic spreading regardless of the statistical phase. Our results thus establish fractional statistics as a governing principle of universal dynamical scaling and provide experimentally accessible signatures for current quantum simulators.

PO.23 Spacetime as a Functional of Matter

Daniel Tan* (Independent Researcher)

Canonical quantisation of the spacetime metric as an independent dynamical variable retains a background-dependent ontology that general relativity's own machinery was built to displace. We take that displacement to its endpoint and propose that the metric is not an independent variable but a functional of the matter fields. Quantum mechanics and general relativity then integrate as coupled field equations (a Dirac equation on curved spacetime and a self-consistent metric functional whose classical limit recovers Einstein's equations).

PO.32 Supergroup Gauged Linear Sigma Models

Zhangcheng Liu* (e1105558@u.nus.edu)

We construct 2d $N = (2, 2)$ gauged linear sigma model with $U(1|1)^N$ supergauge group. Despite being nonunitary, one can still study their space of supersymmetric states and explore their applications to mathematics. In this presentation, we will focus on the physical realization of super-Grassmannian and physically derive the Calabi-Yau condition for these super manifold.

PO.33 Microscopic Theory of Temperature-Dependent Optical Rotation in Chiral Solutions

Pattarapon Tanalikhit*, Wittaya Kanchanapusakit* (KMUTT)

Optical activity describes the rotation of the plane of polarisation as light propagates through an optically active medium. The empirical Drude formula characterises the wavelength dependence of this rotation and also indicates an intrinsic temperature dependence. Earlier microscopic theories, pioneered by Rosenfeld, established the molecular origin of optical activity, but generally treated only a single chiral molecule or a small number of molecules and did not account explicitly for finite-temperature effects. Here, the Drude formula is derived from a microscopic model of chiral molecules in solution. Optical activity results from the coupled electric- and magnetic-dipole response; a purely scalar forced-dipole model cannot distinguish the two circular polarisations and therefore cannot describe optical activity. The Kubo formula extends the microscopic response to finite temperature, yields a temperature-dependent Drude relation, and connects the molecular dynamics directly with the macroscopic rotatory response. Comparison with the empirical formula, previous theoretical results, and experimental data is also discussed.

PO.36 Deciphering the many faces of Type-Ia supernovae and their remnants with 3-D hydrodynamic simulations and X-ray spectral synthesis

Herman Shiu-Hang Lee* (Kyoto University)

Supernovae (SNe) are long seen as one of the most important classes of astrophysical objects which do not only mark the end of stellar lives, but also serve as major factory of chemical elements, origin of space messengers like cosmic-rays, neutrinos and electromagnetic and gravitational waves, and distance ladders for cosmological investigations. One of the biggest mysteries surrounding SNe is the origin of their rich diversity. Explosions from the core-collapse of massive stars are intrinsically diverse, naturally expected from their different progenitor stars and circumstellar environments. Type-Ia SNe from the thermonuclear explosion of white dwarves are historically viewed as a more homogeneous class of objects, whose properties are scalable to serve as cosmological standard candles. However, recent observations and numerical simulations have revealed a number of outlier populations of Type-Ia SNe which do not fall into such a scalable category, indicating the existence of a variety of explosion mechanisms as well as surrounding environments are at play, just like their core-collapse counterparts. This poses a great impact on their usage in cosmology, as well as our fundamental understanding of the life cycle of stars.

I will introduce some recent activities in our group on using state-of-the-art three dimensional hydrodynamic simulations on the study of this mysterious diversity, as well as the predictions of spectroscopic observables usable as diagnostics of progenitor stars and explosion physics, from seconds to a few thousand years after the SN events.

PO.37 Progress Toward Laser-Based Smooth Gates in Trapped 138 Ba+ Ions

Jia-Yang Gao*, Jianwei Lee, Morteza Ahmadi, Jaren Gan, Manas Mukherjee (Centre for Quantum Technologies, National University of Singapore)

Recently, laser-free smooth gate, in which residual spin–motion entanglement errors are adiabatically eliminated by ramping the gate detuning, was experimentally demonstrated in trapped $^{40}Ca^{+}$ ions without ground-state cooling. In this work, we report progress toward implementing a laser-based smooth gate in trapped 138Ba+ ions using a narrow-linewidth 1762 nm laser, and discuss our preliminary results and current limitations.

PO.39 Comparative Study of Terahertz Photodetection in Two-Dimensional Platinum Dichalcogenides

Xuan Yi Ang*, Mengting Jiang, Zenn Tan, Piyush Agarwal, James Lourembam* (Institute of Materials Research and Engineering, Agency for Science, Technology and Research, Singapore 138634)

Terahertz (THz) radiation has significant potential in a wide range of applications from biomedical imaging to material characterisation. However, passive THz detection in ambient conditions remains challenging because of the low photon energy, which limits sensitivity of traditional photodetectors. Type-II Dirac semimetals offer a promising solution as its gapless band structure allows the generation of highly mobile carriers under THz excitation. In this study, we examine the photodetection performance in the continuous wave (CW) 0.1 THz regime of different two-dimensional (2D) type-II Dirac semimetals belonging to the platinum dichalcogenides family. Specifically, heterostructures based on graphene and platinum dichalcogenides were fabricated in the bow-tie antenna structure. Critical device performance parameter such as responsivity, noise-equivalent power and 3dB cutoff frequencies were systematically evaluated and compared. The results provide insights into the role of material selection and heterostructure design in determining THz detector performance and establish guidelines for the development of high-performance, room temperature passive THz detectors.

PO.40 Device-Architecture Engineering of Graphene/$PtTe_2$ Terahertz Detectors

Zenn Tan*, Mengting Jiang*, Xuan Yi Ang*, Piyush Agarwal*, James Lourembam* (Institute of Materials Research and Engineering, Agency for Science, Technology and Research, Singapore 138634)

Terahertz (THz) radiation offers unique advantages for non-destructive imaging and characterization, as well as high-speed wireless communication. However, passive room-temperature detection remains challenging because the inherently low photon energy (meV) limits the sensitivity of conventional semiconductor photodetectors. Dirac semi metals integrated in bow-tie antenna designed have shown significant promise for passive THz detection under ambient conditions although further improvements in detector performance are needed. In this work, we investigate Graphene/$PtTe_2$ photodetectors based on a novel multi-finger architecture. In contrast to the conventional bow-tie design, the proposed structure incorporates multiple interdigitated fingers to increase the active area and enhance photocurrent generation. Within the multi-finger design two different configurations symmetric and asymmetric are fabricated and systematically characterized. The photocurrent responses of the symmetric and asymmetric devices are compared over a range of operating frequencies, with particular emphasis on their modulation frequency dependence and cut-off frequencies. Dark current is also evaluated to assess the overall detector performance. These results demonstrate the potential of the multi-finger architecture as an effective approach for high-performance THz photodetection.

PO.43 Enhanced photon pair generation from silicon microring resonators via pilot laser locking

Jinyi Du*, En Teng Lim*, Si Hyung Kim*, Yiqiao Huang*, Hongwei Gao*, George Chen*, Dawn Tan*, Alexander Ling* (Centre for Quantum Technologies, NUS; Department of Physics, NUS)

We present a novel pilot-laser-based locking scheme for integrated photonic microring resonators, enabling stable operation of quantum photon-pair sources close to the optimum resonance condition. In conventional bistability-based locking [1,2,3], the pump is typically stabilized only on one side of the resonance fringe, which

restricts the accessible locking point to no more than about 90% of the resonance depth and therefore limits the efficiency of the photon-pair source. Moreover, when the locking point is pushed too close to the resonance minimum, the feedback loop becomes increasingly vulnerable to thermal drift. A more advanced approach is provided by Pound-Drever-Hall (PDH) locking [4], which can in principle stabilize the resonator closer to the resonance minimum. However, PDH generally requires more sophisticated electronics and additional components, including high-speed electro-optic modulation and error-signal demodulation. For microring resonators with relatively large full width at half maximum (FWHM), the required modulation speed can become even higher, further increasing system complexity and cost. In contrast, our approach introduces a low-power pilot laser as an independent monitoring channel for tracking the resonance state of the microring resonator. By setting the pilot-laser wavelength to be detuned from the on-resonance pump wavelength by an integer multiple of the free spectral range (FSR) minus half of the FWHM, the pilot laser provides a reliable and approximately linear readout of resonance movement, while temperature correction is implemented using a thermoelectric cooler (TEC) or a thin-film sheet heater. In this way, the pilot channel transforms the resonance response near the minimum from a non-monotonic behavior into a monotonic indicator of resonance drift, thereby preserving the correct feedback direction. The key advantage of this design is that it maintains valid PID feedback logic even when thermal drift drives the operating point across the resonance minimum. In conventional side-of-fringe locking, once the resonance dip drifts past the locking point, the local transmission slope reverses sign, causing the original PID response to become invalid and pushing the system further away from the desired operating point. In our scheme, the pilot laser continuously tracks the resonance position, allowing the control system to preserve a consistent error-signal direction and enabling the TEC to pull the microring back toward the target locking point. As a result, our locking scheme enables operation much closer to the resonance minimum than conventional bistability locking, allowing higher intracavity pump power and enhanced photon-pair generation. Because the pilot laser functions only as a low-power monitoring channel, the system avoids the high-speed modulation and demodulation electronics required in PDH-based implementations, making it simple and practical for long-term operation of integrated quantum photonic sources. The scheme is applicable to silicon, silicon nitride, and related integrated photonic platforms. [1] Guo, Kai, et al. ”Nonclassical optical bistability and resonance-locked regime of photon-pair sources using silicon microring resonator.” Physical Review Applied 11.3 (2019): 034007. [2] Wen, Wenjun, et al. ”Polarization-entangled quantum frequency comb from a silicon nitride microring resonator.” Physical Review Applied 20.6 (2023): 064032. [3] Kramnik, Danielius, et al. ”Scalable feedback stabilization of quantum light sources on a CMOS chip.” Nature Electronics 8.7 (2025): 620-630. [4] He, Yang, et al. ”Chip-scale high-performance photonic microwave oscillator.” Science Advances 10.33 (2024): eado9570.

PO.44 Highly stable hybrid interferometer with meter scale optical delay for time bin entanglement

Jinyi Du*, Bo Peng*, En Teng Lim*, Hongwei Gao*, George Chen*, Dawn Tan*, Alexander Ling* (Centre for Quantum Technologies, NUS; Department of Physics, NUS)

Optical interferometers with large path length imbalance are widely used in quantum optics. They are particularly important for time bin entanglement measurements. Conventionally, meter scale optical delays are implemented using optical fibre. However, environmental perturbations can induce substantial optical path variations and rapid phase fluctuations. This makes long term interferometric stabilization challenging. Here, we demonstrate a hybrid interferometer that combines the advantages of fibre and free space optical systems. Fibre beam splitters provide stable mode overlap and well controlled splitting ratios. The long optical delay is implemented using a free space Herriott cell, which provides a meter scale optical path in a compact geometry. Compared with a long fibre delay, the Herriott cell exhibits much slower phase drift and substantially reduces rapid phase fluctuations. Specially coated mirrors are used to minimize optical loss. This allows a several metre optical delay to be introduced without significantly compromising optical transmission. We implement the hybrid interferometer in a time bin entanglement experiment. The system achieves high two photon interference visibility and maintains stable phase operation over extended periods. No complex active compensation is required. These results provide a simple and practical approach to realizing low loss and highly stable interferometers with meter scale path length imbalance for quantum photonic experiments.

PO.45 Cross-Representation Analysis of Battery Degradation Trajectories: Linking Physics-Informed States with Equivalent-Circuit Signatures

Kaize Guo*, Sharon Xiaodai Lim, Puneet Gupta, Chorng Haur Sow* (Physics Dept, FOS, NUS)

Electrochemical impedance spectroscopy (EIS) provides a non-destructive, frequency-resolved probe of battery aging, but extracting physically meaningful degradation information from impedance spectra remains challenging because the inverse mapping from spectral response to degradation state is inherently non-unique. Here, we develop a physics-informed deep learning framework for degradation diagnosis in commercial silicon-containing lithium-ion cells. The architecture combines frequency-aware multi-SOC spectral encoding with a fixed physical-chemistry decoder containing no trainable parameters, so that the learned degradation representation is constrained through impedance reconstruction rather than optimized solely for prediction. Using 500 EIS spectra from eight cells aged under four protocols, the proposed model achieved a five-target macro normalized RMSE of 0.0631 under leave-one-cell-out validation, compared with 0.0756 for the strongest neural-network baseline. Matched ablation studies further showed that cycle-aligned physics context reduced prediction error by 23.4% relative to direct spectral readout, while cross-cycle and dimension-matched latent controls did not reproduce the improvement. In parallel, an independently fitted leakage-aware equivalent-circuit model achieved a mean curve NRMSE of 0.407%. Its parameter evolution showed consistent protocol-level trends with the learned degradation states, while spectral-sensitivity analysis revealed structured relationships associated with interfacial growth, connectivity loss, and distributed degradation processes. These results demonstrate how physics-informed data-driven modeling can improve battery degradation diagnosis while retaining interpretable links to the measured impedance response.

PO.46 Orbital Current Dynamics in Phase-Engineered W-based Ni/W/CuO_x Terahertz Emitter

Hrittik Kumar Roy*, Piyush Agarwal, Mukundadev Behera, Chandrasekhar Murapaka, Yogesh Kumar Srivastava*, James Lourembam* (Agency for Science Technology and Research (A*STAR))

The orbital angular momentum (OAM) has long been neglected as a functionality in spintronic devices due to its expected quenching inside a Ferromagnet (FM). However, recent discoveries of orbital current generation in spin-orbit-coupled FM have given the leverage to understand the dynamics and its implementation in next-generation electronics. Unlike spin current, the orbital current's propagation length, that is, the diffusion length, is still a debate, with some of the researchers claiming it has a large diffusion length (around 80-100 nm)and some of them claiming it has a sub-nanometric diffusion length. Meanwhile, tungsten (W) is a widely used heavy material (HM) that is used for orbital-to-charge and charge-to-orbital conversion and is of particular interest for orbital diffusion length studies. Here, we have made a spin-orbitronic THz emitter using Ni/W/CuO_x, varying the W phase and thickness via deposition parameters. In a typical spintronic THz emitter, upon excitation by a femtosecond laser pulse, the spin superdiffuses into the HM and undergoes the inverse Spin Hall effect (ISHE) to generate transient charge current, which is the source of the THz pulse. In our material system, Ni serves as both a spin and an orbital current generator: the spin current superdiffuses into the W for spin-to-charge conversion, and the orbital current also decays within the W, while W also serves as an orbital source due to spin-orbital interconversion. This generated orbital current enters the CuO_x interface, providing the inverse orbital Rashba Edelstein Effect and generating a THz pulse. The spin-to-charge conversion coefficient, or Spin Hall angle, is negative for W, but the orbital-to-charge conversion coefficient is positive for both inside the W and the Cu/CuO_x interface. Hence, the continuous competition between the spin and orbital current plays a crucial role in the emitted THz pulse amplitude and polarity. By performing thickness-dependent and phase-dependent THz emission through the W, we can understand the orbital current dynamics and its interplay with the lattice, which would provide a crucial platform for the upcoming spin-orbitronic-based memory devices.

PO.50 Non-Hermitian Four-Band Systems without Skin Effect: A New Invariant for Counting Edge States

Yang Ruan* (Southeast University)

Non-Hermitian topological systems have drawn great interest in condensed matter physics and optics. The non-Hermitian skin effect, ubiquitous in generic non-Hermitian models, overturns the conventional bulk-boundary correspondence. While topological invariants and edge state characterizations are well established for canonical two-band models, exact analytical solutions for open boundary conditions and rigorous edge-state counting rules

remain elusive for multi-band non-Hermitian lattices, especially for the special class of non-Hermitian systems free of the skin effect.In this work, we investigate a one-dimensional four-band anisotropic checkerboard non-Hermitian lattice with arbitrary complex couplings, which belongs to a family of non-Hermitian systems intrinsically free of the skin effect.We obtain the exact analytical solution to the open-boundary eigenvalue problem, and derive edge-state solutions that are independent of the number of lattice sites. By introducing the sublattice amplitude ratio M, we establish a strict criterion for physical edge states in the thermodynamic limit, and further propose a new invariant that realizes unambiguous counting of physical edge states without spurious solutions. All analytical conclusions are quantitatively verified by numerical diagonalization.These findings advance the topological theory of multi-band non-Hermitian systems, and provide a new framework for exploring non-Hermitian topology in skin-effect-free regimes.

PO.52 Time-bin interferometer for quantum networks

Emilien Lavie*, Arushi Sachan, Alexander Ling (NUS, CQT)

Photons are the most natural carriers of quantum information over long distance, and many quantum network architectures are designed around the use of photons to interconnect systems via interference at intermediate repeater stations. These stations can be thought of as application-specific Quantum Processing Units (QPUs) where universality is not necessary, but instead a few primitive quantum operations such as entangled state generation, distillation, and measurement are sufficient to establish or improve a quantum link. Time synchronisation and adaptivity are other important aspects of effective quantum repeaters, since they need to operate under link asymmetry and probabilistic link failure.

While it is in principle possible to convert back and forth between flying qubits and local computing qubits at the repeater station, the limited conversion efficiency might severely affect the network performance. Instead, we consider a fully photonic approach to the repeater station, where the repeater is a photonic QPU. Typically, photonic QPUs are developed on the integrated photonics platform owing to its many benefits in terms of stability, small footprint and perspective of scalability. However, adaptivity requires ultra-fast modulators and switches, and overall losses still remain a significant challenge.

Here, we explore the feasibility of a free-space optics time-bin interferometer to overcome these limitations. A QPU with a native time-bin encoding would more naturally be able to adapt and feedforward information with only moderate-speed modulators. While a bulk optics system would obviously not compete with an integrated system in terms of scalability, the overall system losses are usually lower, and we believe that it could be enough to implement an intermediate-scale QPU and to demonstrate elementary repeater capability.

We consider a potential implementation of the loop-architecture of Motes et al. (PRL 113 120501, 2014), and simulate various practical imperfections to study the feasibility of that scheme.

Using a Markov-Chain model, we estimated the compound losses and predicted success rates comparable to or exceeding state of the art implementations for circuits generating heralded Bell states and GHZ states. Since a free-space setup is non-guided, we implemented raytracing techniques to evaluate the requirements in terms of re-focusing and to estimate the expected visibility of interference due to spatial mode mismatch.

Preliminary results show that while this system would definitively be experimentally challenging to realise, it is still in the realm of feasible, and could result in a fairly flexible platform to implement various experiments such as graph state generation, measurement-based quantum computing, feedforward, heterogeneous light interference and multiphoton processing.

PO.54 Terahertz Emission Spectroscopy of TmIG/Pt heterostructures

Yuying Zhou*, Piyush Agarwal, Ganesh Ji Omar, Karen Ke Lin, Ariando Ariando, James Lourembam* (Institute of Materials Research and Engineering, Agency for Science, Technology and Research, Singapore 138634)

Ferromagnetic heterostructures have emerged as broadband and efficient sources of terahertz radiation enabled by ultrafast spin-current generation and spin-to-charge conversion. More recently, magnetic insulators such as yttrium iron garnet (YIG) have also been shown to generate THz radiation despite the absence of mobile conduction electrons, suggesting that magnons can mediate the underlying spin transport. Here, we investigate ultrafast magnetization dynamics in thulium iron garnet (TmIG)/platinum (Pt) heterostructures. As a magnetic insulator belonging to the garnet family, TmIG offers strong spin–orbit interactions and provides a promising platform for exploring ultrafast spin transport in insulating systems. We observe terahertz (THz) emission spectroscopy using

an 800 nm and 35 fs pulse-width optical laser. THz emission from the TmIG/Pt interface indicates arising from the inverse spin Hall effect (ISHE). It reverses sign upon magnetic field reversal and traces out a square hysteresis loop as a function of applied field, closely mirroring the sample's magnetometry. Fluence-dependent hysteresis measurements reveal a systematic increase in coercivity with increasing pump fluence, while the loop shape remains robust, indicating pump-tunable control over the switching threshold. Azimuthal polarisation-dependent measurements show a clear angular modulation of the emission amplitude upon sample rotation. Reference measurements on a CoFeB/Pt control sample reproduce the same fluence-dependent trends, validating the technique. Together, these results establish all-optical THz emission spectroscopy as a versatile route toward characterizing low-dissipation, insulator-based platforms for high-frequency magnonic memory and logic devices.

PO.58 Enhancing and optimising superheterodyne Rydberg atom sensors for RF detection using squeezed light

Jackson Phoong*, Lewis Clark, Wen Jun Wee, Syed Assad (NUS, Q.InC, CQT)

Rydberg atom sensors provide a platform for the detection of weak radio-frequency (RF) electric fields, offering direct SI-traceable measurement, broad tunability, small physical size, narrow selectivity and good sensitivity[1]. State-of-the-art sensors can achieve sensitivity limited by photon shot noise (PSN) arising from the optical readout[2]. Although increasing probe power reduces the relative PSN, it does not necessarily translate into improved sensitivity as it also depends on other system parameters. An alternative approach is to reduce the absolute PSN using non-classical resources such as squeezed light. We investigate the achievable enhancement in sensitivity, quantified by noise-equivalent field (NEF), by integrating squeezed probe light into a superheterodyne Rydberg atom sensor. A five-level model of Rb-87 is considered and we derive the NEF by considering the sensor responsivity together with PSN in the optical detection process. The effect of squeezed probe light is then incorporated through the corresponding reduction in quantum noise. Numerical optimisations are performed over experimentally relevant operating conditions to find the parameters that produce the largest reduction in NEF. For 10,dB of probe squeezing, we find that the NEF can be reduced by a maximum of approximately 36% relative to the corresponding unsqueezed case in the regime where PSN dominates. These results demonstrate that non-classical optical states can provide a practical route towards improving the sensitivity of Rydberg atom RF sensors beyond the conventional PSN-limited performance. This is especially important for applications where increasing the probe power is not possible.

[1] C. T. Fancher et al., IEEE Transactions on Quantum Engineering 2, 1 (2021). [2] S. Kumar et al., Sci Rep 7, 42981 (2017).

PO.59 From Sulfur Vacancies to Quantum Transport: A Multiscale Framework for Resistive Switching in Heterostructures

Vitalii Kapitan*, Andrey Ustyuzhanin (IFIM, National University of Singapore)

Molybdenum disulfide (MoS_2), an archetypal layered transition metal dichalcogenide, exhibits thickness-dependent electronic properties governed by quantum confinement and interlayer orbital hybridization. This work presents a first-principles density functional theory (DFT) study of the electronic structure, vacancy formation energetics, and local lattice relaxation of point defects in 2H-stacked bilayer MoS_2 supercells, using SIESTA 5.4.2 with the GGA-PBE functional and Grimme DFT-D3(BJ) dispersion corrections. The vacuum-padded pristine supercell reproduces the primitive bilayer unit cell, both treated as slabs, with high energetic fidelity and structural consistency. Vacancy defects in bilayer MoS_2 introduce deep in-gap states that substantially narrow the electronic band gap, with surface sites energetically favored over interlayer sites and divacancies producing a larger reduction than monovacancies. Calculations show that neighboring surface sulfur divacancies have a weak attractive binding energy of approximately 21 meV relative to isolated monovacancies, indicating a thermodynamic preference for defect clustering over random distribution. This clustering tendency is expected to influence the spatial distribution of localized in-gap states and, consequently, the electronic behavior of bilayer MoS_2. Based on these defect-level results, we propose a multiscale, data-driven framework that combines DFT with machine-learned interatomic potentials (MLIPs) to model memristive heterostructures, whose operation depends on coupled electronic and ionic processes across multiple spatial and temporal scales. Given the computational cost of DFT, MACE-type MLIPs implemented in LAMMPS are used to perform rapid structural relaxations, reducing the overhead of subsequent high-fidelity optimization in SIESTA. The quantum transport in the ON/OFF states of the device is then estimated

using nonequilibrium Green's function methods (TranSIESTA/TBtrans), which allows obtaining zero-bias transmission spectra and local density of states. This approach is benchmarked on Au-MoS_2-Au structure before being extended to unexplored heterostructure configurations. This research is supported by the Ministry of Education, Singapore, under its funding for the Research Centre of Excellence award to the Institute for Functional Intelligent Materials. Project No. EDUNC-33-18-279-V12-IFIM

PO.60 Two Time-local Approaches for Treating Non-Markovianity in Driven Open Quantum Systems

Zi Yao Lim*, Kelvin Onggadinata, Nelly H. Y. Ng, Teck Seng Koh (Nanyang Technological University)

Non-Markovian noise can arise from fundamentally different physical origins, yet formal treatments of these origins are often studied in isolation. In this work, we compare two master equations that model non-Markovian dynamics through distinct noise mechanisms but share a common derivation strategy – a second-order cumulant expansion. The first, pseudo-Lindblad master equation (PLME) [1], treats noise as classical fluctuations entering the control Hamiltonian, with no explicit environment or system-environment coupling. The second, time-convolutionless Born master equation (TCL-BME) [2], retains the full system-environment picture, with noise emerging from genuine quantum system-environment coupling. By applying the same expansion order to both approaches, we isolate how the origin of the noise – classical vs quantum – shapes the resulting non-Markovian signatures, through non-CP-divisibility of the dynamical maps and purity revivals of the system state. We present preliminary findings comparing these signatures across the two models.

PO.62 Cavity resonator for coupling superconducting qubit and Rydberg atom

Jeykanth Jaya Kumar* (Nanyang Technological University)

Superconducting qubits and atom ensembles provide an avenue for a physical realization of an integrated quantum processor and memory system. The qubit and atom subsystems can be coupled by a microwave resonator for the purpose of reading and writing quantum information. Here we propose a 3D cavity resonator design to facilitate the coupling between a superconducting transmon qubit and a Rydberg atom. The transmon and the Rydberg atom are modelled as electric dipoles that interact with the electromagnetic modes of the cavity resonator. This cavity aims to utilise two sets of metal posts that concentrate electric fields in the cavity to couple to the two sets of dipoles. The design properties were modelled and assessed using the HFSS simulator. The intended purpose of the cavity would then be to place it within a dilution refrigerator for cooling to superconducting temperatures. The atom would then have to be moved from a magneto-optical trap into the refrigerator and consequently into the cavity where it would be excited to its Rydberg state and coupled to the qubit.

PO.63 Mixed-radix representation of expectation values for classification tasks in quantum machine learning

Chee Kwan Gan*, Jun Yong Khoo, Stefano Carrazza, Jian Feng Kong (Institute of Advanced Intelligence and Computing)

Conventional multiclass classifiers typically associate output variables directly with class labels, while quantum classifiers often infer classes from the joint probability distribution of a set of measured qubits. We investigate an alternative representation in which the expectation value of each measured qubit is divided into multiple intervals and the corresponding interval indices are interpreted as mixed-radix digits. With radices $r_0, r_1, \ldots, r_{m-1}$, m measured qubits can therefore encode $\prod_{j=0}^{m-1} r_j$ classes, allowing the output representation to be adapted to the number of classes required. We implement this mixed-radix representation (MRR) in a hybrid convolutional-neural-network–quantum classifier for MNIST, where a classical convolutional encoder maps each image to quantum encoding parameters and a parameterized quantum circuit produces the measured expectation values. Classification is performed by assigning these expectation values to their corresponding mixed-radix intervals. We compare this approach with classification based directly on the measured joint probability distribution and examine its performance for multiclass problems including the eight-class MNIST task. The results establish MRR expectation-value encoding as a viable scheme for quantum multiclass classification using a small number of measured qubits.

PO.65 A Quantum-Enhanced Solver for the MaxCut Problem via Mean-Field and Transverse-Field Annealing

Ronit Dutta*, Pan Feng* (Singapore University of Technology and Design)

Combinatorial optimization is central to scientific and industrial decision-making, yet practical solvers must balance broad applicability, solution quality, and computational efficiency as problem size grows. We introduce the Quantum-enhanced Free Energy Machine (QeFEM), a classical, quantum-inspired framework for binary optimization that uses the method of variational optimization of a differentiable functional to obtain high-quality solutions. The algorithm uses automatic differentiation & gradient-based optimization. The formulation provides common optimization machinery for QUBO-representable problems and exposes dense, differentiable tensor operations that can be efficiently batched on graphics processing units and related parallel accelerators. We evaluate QeFEM on MaxCut using 71 tested G-set graphs of variying structural connectivities and the fully connected dense K2000 graph. Under a common budget of 1000 steps and 128 replicas, it recovers two stored best-known G-set cuts and achieves mean target-relative gaps of 0.985% (i.e. mean accuracy of 99.015%) on G1–G54 and 2.086% (mean accuracy of 97.914%) on the tested G55–G81 subset. Here gap refers to the relative difference between the obtained solution and the best known optimal solution. For K2000, the fixed and higher-budget runs reach gaps of 1.068% and 0.645%, respectively. These results support QeFEM as a unified, accelerator-ready approach to large-scale binary optimization.

PO.66 The Geometric Phase as a Diagnostic for Driven-Dissipative Oscillators

Zeen Sun*, Yuan Shen, Hai-Tao Ding, Yuancheng Zhan, Leong-Chuan Kwek (CQT)

Driven-dissipative quantum oscillators lock their phase, deform their limit cycles, and undergo dissipative phase transitions, yet these behaviors are read from unrelated quantities defined on the same steady-state density matrix. We show that a single geometric quantity organizes them. Winding the phase of the drive generates a closed loop of nonequilibrium steady states, and because the Liouvillian is covariant under number rotations, the kinematic mixed-state geometric phase of this loop reduces exactly to an eigensystem functional of a single steady state. Under weak driving, it is governed by the same nearest-neighbor coherences that produce phase locking and inherits the Arnold tongue of synchronization. Near the Hopf threshold, it registers the nonperturbative reorganization of the steady-state eigenvectors. And in the squeezing-driven Kerr resonator, it develops distinct signatures at the first and second order dissipative phase transitions. The geometric phase thus provides a unified and experimentally accessible characterization of steady-state reorganization.

PO.71 High-fidelity preservation of hyperentanglement in an optical delay line-based quantum memory

Yu Guo*, Arya Chowdhury, Pranay Tiwari, Jiaboon Chin, Anindya Banerji, Alexander Ling (Centre for Quantum technologies, NUS)

Photonic hyperentanglement refers to simultaneous entanglement across multiple degrees of freedom (DOFs) of a photon pair. It enlarges the accessible state space and supports multiplexing, high dimensional encoding, and more efficient entanglement distribution. Photonic quantum networks also require temporal synchronization, since entanglement generation and routing are probabilistic. A storage device for hyperentangled states must therefore preserve the state quality in each DOF without introducing coupling between them. Solid state quantum memories have stored hyperentanglement, but they require cryogenic cooling and have limited acceptance bandwidths. Free space optical delay lines offer an alternative approach to photonic storage. We previously demonstrated a delay line based on nested Herriott cells [1]. It achieved high transmission efficiency, ultrabroad bandwidth, a large time bandwidth product, and stable polarization propagation at room temperature. However, multiple mirror reflections can introduce polarization dependent phase shifts and losses. Their cumulative effects may degrade entanglement or couple different degrees of freedom. Whether this system could preserve hyperentanglement therefore remained unknown. We report the preservation of hyperentanglement in the polarization and energy time degrees of freedom after a delay of 647.0(6) ns over 160 reflections. After the delay line, the energy time interference visibility is 93.9(3)%, the polarization state fidelity relative to the input state is 99.5(4)%, and the CHSH parameter is 2.758(5). These results establish free space optical delay lines as a promising platform for the storage, synchronization, and multiplexing of hyperentangled photonic states.

[1] Guo, Yu, et al. ”Highly efficient and broadband optical delay line toward a quantum memory.” APL Photonics 11.2 (2026).

PO.73 Experimental evaluation of graph isomorphism algorithm on QPU and its applications

Marina Kolpakova*, Rainer Dumke (CQT)

Sub-graph isomorphism and other combinatorial problems are proven to be NP-hard. However efficient solving is required for many applications including compiler design. Efficient algorithms for graph isomorphism and token swapping allow employing quantum processors to transpile quantum programs for it, self-transpilation.

In this talk, we will show the current state of the technology in quantum computing with applications to efficiently solving sub-graph isomorphism matching on quantum processors. First we give an overview of available methods. Second, propose a VQE based algorithm to solve sub-graph isomorphism matching. Adjustment matrix for target and pattern graph features amplitude encoding and scales logarithmically, We address limitations of this scheme and evaluate its performance on a superconducting quantum processor available in-house and on cloud.In the end we showcase a potential application of the algorithm in the compiler domain and draw future directions.

PO.80 Coherent non-Markovianity: Inter-path memory effects in quantum compositions of channels

Jian Wei Cheong*, Andri Pradana, Lock Yue Chew (Nanyang Technological University)

In recent years, there are growing interests in higher-order quantum processes that can grant novel advantages in quantum information and thermodynamical tasks. For example, the quantum SWITCH is a quantum process that exhibits a superposition of causal orders in its operation, and can grant an advantage to a multitude of tasks such as communication and refrigeration. However, the underlying resources behind such quantum processes are often unclear due to their complex design. Particularly, the quantum SWITCH's advantages were often attributed to either its indefinite causality or to coherent control of superposition paths.

In this talk, I will provide an alternative by proposing a novel form of non-Markovian memory effect that we termed ”coherent non-Markovianity” or ”coherence-activated non-Markovianity”. I will first demonstrate that the quantum SWITCH and other quantum processes exhibit this novel non-Markovian effect, before demonstrating that the presence and amount of the ”inter-path memory effect” due to this novel non-Markovianity is tied to its indefinite causality, where its absence lead to a naive superposition of paths without any indefinite causality. This is achieved by augmenting the quantum SWITCH such that the presence and amount of this non-Markovianity is controllable. Lastly, I will give an example of a refrigeration cycle that utilize the quantum SWITCH to perform refrigeration in novel temperature regimes beyond what is achievable in classical settings, demonstrating its dependence on this novel non-Markovian memory.

This work attempts to connect the two disparate fields of indefinite causal order in higher-order quantum processes and non-Markovianity by proposing the novel ”coherent non-Markovianity”, that might offer a dual explanation beyond what were discussed in the literature on such processes.

PO.87 Strong atom-light coupling close to the concentric point

Wen Xin Chiew*, Jun Jie Chan, Christian Kurtsiefer (Centre for Quantum Technologies)

In the development of stationary nodes for quantum computing schemes, optical cavities strongly coupled to neutral atoms. Here, we explore the use of optical cavities in the near-concentric regime, where the cavity is operated at the edge of the resonator geometric stability criterion. While this regime offers small mode volume even with relatively large inter-mirror spacing, there is greatly added complexity in keeping the cavity aligned. We implement a low-noise near-concentric cavity design, utilizing solely tip/tilt control for transverse alignment of the cavity mirrors. We characterize the coupling between the cavity mode and a single 87Rb atom at a distance of 2.5 um from the concentric point, where the transmission shows a distinct vacuum Rabi Splitting spectrum. The fitted parameters $g, \kappa, \gamma = 2\pi \times 5.3(4), 3.2(2), 3.03$ MHz gives a cooperativity factor $C = g^2/2\kappa\gamma = 1.5$, therefore putting the system in the strong single-atom coupling regime.

PO.90 Realising different regimes of spin transport in a spin transistor with a quantum gate device

Gauthameshwar S.*, Heitor Casagrande, Noufal Jaseem*, William Munro, Vinitha Balachandran, Dario Poletti* (SUTD)

Controlling spin transport in interacting quantum systems is central to quantum transport and spintronics. We study a nonequilibrium spin transistor comprising a boundary-driven XXZ spin chain coupled to an auxiliary quantum-gate device. The gate coupling acts as the control parameter: varying its strength reorganises the composite steady state and switches the transport properties of the main chain. Using reservoir and bond-resolved spin currents together with magnetisation profiles, we show how the gate can suppress, enhance, or otherwise reshape transport without modifying the driving reservoirs.

Another interesting consequence is the emergence of a drag current through the gate. Although its two reservoirs are identical and impose no direct spin bias, coupling to the driven chain induces a finite current determined entirely by the chain's nonequilibrium steady state. This provides a clear signature of interaction-mediated quantum drag and demonstrates how transport in one subsystem can generate directed flow in another. We obtain the steady states using matrix-product-state and matrix-product-operator tensor-network methods. Their applicability is ultimately limited by operator-space entanglement growth, increasing bond-dimension requirements, and slow convergence in strongly coupled or slowly relaxing regimes. Our results establish the quantum gate as a tunable switch for controlling spin transport while identifying the numerical challenges in simulating such open quantum devices.

PO.91 Tantalum Nano-constriction Josephson Junctions for Low-Loss Superconducting Quantum Circuits

Ding Huang* (Institute of Materials Research and Engineering, A*STAR)

Superconducting constriction-based Josephson junctions offer a simple single-layer geometry, direct compatibility with the thin-film processes used for superconducting quantum circuits, and access to critical currents beyond those achievable with oxide tunnel junctions. However, integrating such junctions into low-loss superconducting microwave circuits has remained challenging. To date, superconducting resonators incorporating constriction-based junctions have exhibited internal quality factors below 1×10^4, far below those routinely achieved in state-of-the-art low-loss resonators. Here, we demonstrate constriction-based junctions and nanoSQUIDs in tantalum, the material platform underlying some of today's highest-coherence superconducting qubits, and improve the single-photon internal quality factor by more than an order of magnitude over previous constriction-integrated resonators. Tantalum constriction-based nanoSQUIDs exhibit well-behaved weak-link characteristics and clear flux-periodic voltage modulation. These results establish tantalum constriction junctions as low-loss, process-robust Josephson elements, enabling flux-tunable tantalum resonators and opening a path toward integrated nanoSQUID thermometry and magnetometry on a platform compatible with state-of-the-art coherent superconducting quantum circuits.

PO.93 Bosonic Non-linearity with Trapped Ions

Nigel Lee*, Eugene Koh*, Rongjie Zhang*, Jiacheng You*, Dzmitry Matsukevich*, Mu Young Kim (Centre for Quantum Technologies)

Mechanical oscillators encoded in the bosonic motional modes of trapped ions provide a promising platform for continuous-variable quantum information processing. Achieving universal control of these modes, however, requires nonlinear operations such as cubic phase gates and exponential-SWAP (E-SWAP) gates. Here, we report the experimental implementation of a cubic phase gate on a single motional mode using a sequence of spin-dependent displacement pulses [1]. We also present our progress toward realizing an E-SWAP operation between two motional modes, with the interaction controlled by the internal state of the ion. Finally, we describe the development of a new segmented blade trap designed for individual-ion addressing using two-dimensional acousto-optic deflectors (AODs). Together, these capabilities expand the toolbox for universal control and quantum information processing with trapped-ion motional modes.

[1] K. Park and R. Filip, npj Quantum Inf. 10 25 (2024).

PO.96 Photon-driven electron excitations in quantum materials

Xuan Dong* (SUTD)

Photon-driven electron excitation is a foundational mechanism underpinning the interaction between light and matter in quantum materials, including van der Waals materials, Dirac and Weyl semi-metals, topological insulators and other emergent phases. These enable next-generation optoelectronic, energy conversion and quantum information technologies. However, translating this mechanistic understanding into an engineering implementation is hindered by excitation efficiency, environmental stability and scalable fabrication. In this Review, we provide a mechanistic perspective on key photon-driven electron-excitation processes based on energy flow pathways, including electron–hole generation in semiconductors, high-mobility electron transport in semi-metals, photoemission from metals and low-dimensional materials, and light-induced thermoelectric effects. We examine engineering strategies to enhance the efficiency of these processes, including interface control, material selection and compatible integration. By bridging fundamental mechanisms with device-level metrics, this Review offers a unified framework and practical roadmap for advancing scalable, multifunctional optoelectronic devices that integrate sensing, data storage and computation.

PO.98 Entangling telecom-wavelength photons with neutral atoms and trapped ions

Ankush Sharma*, Zifang Xu, Chang Jian Kwong*, Christian Kurtsiefer, Alexander Ling (CQT)

Fully realizing large scale quantum networks would require multiple nodes of different stationary qubits, each performing the task they are uniquely suited to. Such a network requires interconnects that can allow entanglement distribution between these different quantum systems. A major challenge is that most atomic and ionic systems emit photons at different wavelengths, mostly around the visible range, resulting in significant transmission losses in traditional telecommunication fiber networks.

In this poster, we report our efforts to match the wavelengths of two different types of emitters: neutral atoms (Rb) and trapped ions (Ba). The initial step in this transfer process involves a spontaneous emission, which entangles a photon with the respective stationary systems. A wavelength conversion process then converts the visible-range wavelengths to the telecom band, enabling frequency matching between the different systems and low-loss transmission through optical fibers.

PO.99 Thermodynamic effects of a finite information tape in autonomous quantum machines

Yuhao Wang*, Jian Wei Cheong, Andri Pradana, Lock Yue Chew (Nanyang Technological University)

Autonomous quantum thermal machines can harness information as a thermodynamic resource. Many models based on information tapes assume an effectively unlimited sequence of fresh memory qubits, while in realistic settings the available information resource is finite. Here, we investigate how a finite information tape affects the thermodynamic operation of an autonomous quantum machine. We consider a finite tape composed of sequentially interacting memory qubits and characterize how the state of the tape evolves as the available information resource is progressively modified. We begin with the simplest case of a tape consisting of a single memory qubit and characterize its dynamics during the interaction with the machine. We further investigate how increasing the tape size and introducing correlations between memory qubits modify the accessible information resources and their conversion into thermodynamic tasks. Our study aims to provide a framework for understanding finite information reservoirs in autonomous quantum thermal machines and the role of memory structure in their operation.

PO.101 Orbital-selective Mott and antiferromagnetic phases in diagonally compressed kagome lattice

Jiewei Ding, Ho-Kin Tang*, Wing Chi Yu* (City University of Hong Kong)

Geometric deformation offers a controlled way to reshape frustration and correlations in the kagome lattice. In this work, we study the kagome lattice under diagonal compression, where the compression angle tunes the hierarchy of hopping amplitudes among neighboring sites. Using determinant quantum Monte Carlo simulations of the half-filled Hubbard model, we track charge and spin observables resolved on the individual sublattices. Compression breaks the sublattice equivalence and produces two distinct routes to a sublattice-selective Mott state. At weak compression, the A sublattice develops long-range hopping channels and remains metallic while electrons on the B and C sublattices localize at strong interactions. At strong compression, antiferromagnetic correlations

emerging along the B-C chains instead drive the A sublattice insulating. Mapping the plane of compression and interaction strength, we obtain a rich phase diagram hosting paramagnetic and antiferromagnetic metal and Mott regimes.

PO.105 Benchmarking electrical trace analysis methods for intrinsic photon number resolution in superconducting detectors

Ba Linh Nguyen*, Anton Vetlugin*, Cesare Soci* (NTU SPMS)

Superconducting nanowire single-photon detectors (SNSPDs) have traditionally been used as binary, on-off detectors. However, recent studies have shown that information about photon number can be extracted by analyzing the electrical readout trace generated in response to the absorption of an optical pulse. In this work, we systematically compare several trace-analysis methods for extracting photon-number information from SNSPD signals, including an arrival-time-based method, principal component analysis, K-means clustering, and mean-derivative projection. We quantitatively compare their performance using a criterion based on the overlap between neighboring photon-number clusters. In addition to photon-number distinguishability, we consider the computational complexity and implementation requirements of each method. Our results establish a framework for selecting electrical-trace analysis methods for extracting intrinsic photon-number information from SNSPDs and provide guidance for their implementation in applications requiring real-time photon-number-resolved detection.

PO.107 A Pockels cell as a voltage-tunable source of polarization-entangled photon pairs

Jia Boon Chin*, Euk Jin Alexander Ling (Centre for Quantum Technologies, National University of Singapore)

The wavelengths of photon pairs generated from spontaneous parametric down conversion (SPDC) sources are conventionally varied via angle-tuning or temperature-tuning of the nonlinear crystal. We predict and verify that the wavelengths can also be varied via voltage-tuning through the Pockels effect. We further demonstrate that, by using the less popular noncritical phase matching scheme, the geometry of a commercial thermally compensated double-crystal Pockels cell can be exploited to generate polarization-entangled photon pairs. Polarization-correlation visibility of more than 96% was observed after voltage-tuning while exhibiting a shift of 0.30(2)nm in the idler spectrum. These results demonstrate a simple approach to the generation and wavelength modulation of polarization-entangled photon pairs.

PO.109 Mechanical Phonon-Assisted Free Electron and Light Interaction Control

Sunjun Hwang*, Leong Chuan Kwek* (Centre for Quantum Technologies)

Free electrons provide a versatile platform for probing optical and material excitations, but their interaction with light is typically fixed by the electromagnetic environment and the electron trajectory. Here, we propose a mechanically controlled free-electron interaction in which transverse motion of a membrane dynamically modulates both the strength and momentum-space outcome of electron–light coupling. High-spatial-frequency mechanical modes reshape the optical field into evanescent sidebands carrying additional transverse momentum, thereby enabling efficient coupling to freely propagating electrons while simultaneously providing a mechanical degree of control over the interaction.

We show that changing the mechanical-mode amplitude modifies the electron coupling and redistributes the population among discrete momentum-recoil channels, allowing the electron state to follow the mechanical dynamics. Because different transverse mechanical modes carry distinct spatial momenta, their interactions can be selectively accessed by tuning the electron kinetic energy, providing a mode-resolved connection between mechanical motion and electron momentum evolution. This mechanism also enables sensing of external perturbations that modify the transverse mechanical response. We analyze the resulting electron readout using Fisher information, signal-to-noise ratio and force-referred imprecision, and compare it with conventional Gaussian optical detection for stochastic perturbations. The results establish mechanically modulated free-electron motion as a route toward programmable electron–light coupling and mode-selective sensing of high-spatial-frequency mechanical excitations.

PO.113 Single Atom-Photon Interfaces for Quantum Networks

Zifang Xu*, Ankush Sharma, Chang Hoong Chow, Boon Long Ng, Vindhiya Prakash, Alexander Ling, Christian Kurtsiefer* (Centre for Quantum Technologies; Department of Physics, National University of Singapore)

Building a distributed quantum network is a promising way for scaling quantum information processing beyond a single node by connecting multiple quantum systems. This requires efficient interfaces between stationary qubits at distant nodes via photonic links, and one promising approach is to generate entanglement between the internal electronic state of a stationary qubit and the polarization of the spontaneously emitted photon.

Here we present our results in generating atom-photon entanglement using a single optically trapped ^{87}Rb atom, achieving a detection rate of 600 pairs per minute with a fidelity of 81(2)%, and discuss paths to improving both metrics. We also explore time-bin encoding as an alternative to polarization encoding for long-distance entanglement distribution. To extend towards metropolitan distances, we convert the 780 nm emitted photons to the telecom O-band (1310 nm) via three-wave mixing in a periodically poled lithium niobate waveguide, reaching 37.3% fiber-to-fiber conversion efficiency. We discuss the challenges of preserving state fidelity through conversion and our outlook for a practical quantum network node.

PO.119 Dynamics-based nonclassicality witness under dissipative dynamics

Nguyen Huynh* (Centre for Quantum Technologies)

AA dynamics-based test, originally proposed by Tsirelson for the harmonic oscillator, provides a method for certifying quantumness under the assumption of a known Hamiltonian. These tests, however, are typically proposed for isolated systems, an assumption that breaks down in experimental implementation. In this paper, we extend the protocol to the harmonic oscillator coupled to standard models of dissipation: thermal relaxation, pure dephasing, and the Caldeira–Leggett model. Using the Moyal-Wigner formalism of quantum mechanics in phase space, we show that the introduction of dissipation requires a dissipation-dependent shift of the classical bound, and provide the threshold under which the nonclassicality witness retains its validity.

PO.121 Sub-Degree Interference Phase Stabilization in a 2D Optical Lattice Using a Hybrid RF-PZT Scheme

Rishav Koirala*, Haotian Song, Kai Dieckmann (Centre for Quantum Technologies)

Precise control of interference phase Φ between optical lattice beams is essential for engineering tunable Hamiltonians in quantum simulation experiments. Direct interferometric schemes can require lattice dithering or auxiliary optical paths, whereas heterodyne schemes employing RF-based phase correction require dynamically frequency- or phase-programmable radio-frequency (RF) sources. We present a hybrid architecture that decouples phase detection from phase correction, combining carrier-independent heterodyne RF phase detection with piezoelectric (PZT)-mirror-based path-length correction. We separately demodulate the roundtrip phase of each lattice beam and apply feedback using a home-built integral-only controller, thereby stabilizing the differential lattice interference phase Φ. Over five minutes of continuous locked operation, we infer an in-loop root-mean-square (RMS) interference phase fluctuation of $\sigma_\Phi = 0.65^\circ$ with suppression of low-frequency error signal noise by up to 25,dB, as well as 180° tunability in the inferred value of Φ while maintaining approximately constant in-loop interferometric phase fluctuations. Our design is well-suited for optical lattice-based experiments that need a static or slowly-adjustable Φ with reduced optical and electronic complexity.

PO.124 Exponential Speed-ups for Structured Goemans-Williamson relaxations via Quantum Gibbs States and Pauli Sparsity

Haomu Yuan*, Daniel Stilck França*, Ilia Luchnikov, Tobias Haug, Leandro Aolita (University of Copenhagen)

Quadratic Unconstrained Binary Optimization (QUBO) problems are prevalent in various applications and are known to be NP-hard. The seminal work of Goemans and Williamson introduced a semidefinite programming (SDP) relaxation for such problems, solvable in polynomial time that upper bounds the optimal value. Their approach also enables randomized rounding techniques to obtain feasible solutions with provable performance guarantees.

In this work, we identify instances of QUBO problems where matrix multiplicative weight methods lead to quantum and quantum-inspired algorithms that approximate the Goemans-Williamson SDP exponentially faster than existing methods, achieving polylogarithmic time complexity relative to the problem dimension. This speedup is attainable under the assumption that the QUBO cost matrix is sparse when expressed as a linear combination of Pauli strings satisfying certain algebraic constraints, and leverages efficient quantum and classical simulation results for quantum Gibbs states.

We demonstrate how to verify these conditions efficiently given the decomposition. Additionally, we explore heuristic methods for randomized rounding procedures and extract the energy of a feasible point of the QUBO in polylogarithmic time. While the practical relevance of instances where our methods excel remains to be fully established, we propose heuristic algorithms with broader applicability and identify Kronecker graphs as a promising class for applying our techniques. We conduct numerical experiments to benchmark our methods. Notably, by utilizing tensor network methods, we solve an SDP with $D = 2^{50}$ variables and extract a feasible point which is certifiably within 0.15% of the optimum of the QUBO through our approach on a desktop, reaching dimensions millions of times larger than those handled by existing SDP or QUBO solvers, whether heuristic or rigorous.

PO.129 Continued Development of a Compact and Stable Laser-Induced-Thermal-Ablation Cold Atom Source

Hajime Watanabe*, Chengmeng Wang*, Chang Chi Kwong*, David Wilkowski* (Nanyang Technological University)

Cold atoms are vital to the development of quantum technologies such as quantum computing, sensing, and simulations. Currently the development of compact and portable setups is gaining more attention, as practical use demand increases. In this work we report on our progress in the development of a laser ablation source for cold strontium experiments, which could pave the path towards further miniaturization, increased efficiency, and portability of setups.

Our strontium source is generated by laser induced thermal ablation (LITA) [1] of strontium. This method eliminates the need for the oven, Zeeman slower, and 2D MOT. A laser is focused onto a strontium disc, vaporizing a tiny portion while the large unheated fraction acts as a heat sink. The rapid diffusion of heat rapidly stops the ablation once the laser is switched off, restoring the ultra-high vacuum environment, necessary for most of the applications. An in-vacuum mirror is placed inside the vacuum chamber to reflect the ablation laser, breaking the direct line of sight between the viewports, strontium, and 3D MOT. This prevents the coating of viewports by strontium while also preventing fast strontium particles from disturbing the MOT, protecting lifetime. A fluorescence lock was also implemented which precisely controls the laser to ensure the pressure does not increase beyond a certain point. This ensures that the background pressure remains low enough, also protecting lifetime. Our current setup loaded 1.2 million atoms within 400 ms, with a lifetime of 1.5 s. Currently the setup is limited by background pressure from inadequate baking and an unalterable magnetic field. Thus, a new setup is currently under development with a similar design but with proper bake-out, modified mirrors, and modified magnetic field preparation. Once the entire setup is complete, it will advance the miniaturization of MOT setups, opening a practical path to portable setups that could potentially be used for more compact neutral atom quantum computers, optical lattice clocks, and more.

[1] C. C. Hsu, R. Larue, C. C. Kwong, and D. Wilkowski, ”Laser-induced thermal source for cold atoms”, Sci. Rep. 12, 868 (2022)

PO.131 Magic-wavelength matter-wave interferometry with optical clock states

Swarup Das*, Jianing Li, Xinyuan Ma*, Thomas Zanon, Shau-Yu Lan, Chang Chi Kwong*, David Wilkowski (Nanyang Technological University)

Combining optical atomic clocks and matter-wave interferometry unlocks unprecedented precision in testing fundamental gravity and sensing forces. However, integrating optical internal energy without introducing systematic phase shifts requires state-independent manipulation. Here, we demonstrate a simultaneous dual matter-wave interferometer operating on both states of the ^{88}Sr optical clock transition ($^1S_0$ and $^3P_0$). By driving the interferometer with Bragg pulses at the 813 nm ”magic wavelength,” both clock states experience identical optical coupling. With a differential phase sensitivity of 30 mrad, we observe zero differential phase shift in free fall, bounding state-dependent differential acceleration to$< 10^{-5}$. Furthermore, by probing state-dependent dipole forces, we determine the $^3P_0$ tune-out wavelength to be 478.95(8) nm. These results establish magic-wavelength clock-state interferometry for excited-state polarizability metrology and next-generation quantum-clock tests of gravity.

PO.132 Energetics of non-Gaussianity in single mode cavities

Sahil Sardar Jafar* (NTU)

Non-Gaussian states are key resources for quantum technologies, making the quantification of non-Gaussianity a fundamental challenge. We introduce an energetic framework for characterizing non-Gaussianity in single-mode bosonic states by decomposing the total energy into Gaussian and non-Gaussian contributions. For pure states, we show that the non-Gaussian energy defines a bonafide measure of non-Gaussianity and establish a direct connection with the relative entropy of non- Gaussianity. As an illustration, we consider non-Gaussian states generated from coherent states with tunable amplitudes using a SNAP gate. We find that the resulting non-Gaussian energy and Wigner negativity are maximized at similar input amplitudes. For mixed states, we demonstrate that the non-Gaussian energy provides a faithful witness of non-Gaussianity. Our results uncover an energetic fine structure of non-Gaussian quantum states and offer new insights into the efficient generation and manipulation of non-Gaussian resources.

PO.133 Characterization of Josephson Junction Aging and Annealing Under Different Environmental Conditions

Rangga Perdana Budoyo*, Rasanayagam Kajen, Lilis Rachel Yohana, Bing Wen Cheah, Long Hoang Nguyen, Rainer Dumke (Centre for Quantum Technologies)

Understanding the aging behavior of Josephson junctions and the effect of annealing on junction resistance is important in building large-scale superconducting quantum processors. We report the aging behavior of Al/AlO$_x$/Al Josephson junctions under different storage conditions up to 3 months after fabrication. The aging curve follows a logarithmic curve, with the aging amplitude determined by fabrication conditions and aging rate determined by both fabrication and storage conditions. Junctions stored at ambient laboratory conditions aged faster compared to junctions stored in a nitrogen atmosphere or vacuum, with changes in the aging trajectory when the storage condition changed. We also report on the effect of voltage and thermal annealing of Josephson junctions under different annealing and prior storage conditions.

PO.134 Single-realization Pauli twirling for suppressing coherent error accumulation in structured quantum circuits

Dihang Sun* (National University of Singapore)

Pauli twirling is conventionally understood as an ensemble-level noise-tailoring procedure which suppresses coherent components of the error channel by averaging over randomized compilations. This picture does not by itself determine whether a single Pauli-dressed circuit can outperform its bare counterpart, nor does it predict when such an advantage should occur. In this work, we develop a single-realization framework for the standard Pauli dressing of two-qubit Clifford gates in structured quantum circuits. For weak coherent errors, we show that the leading state-preparation infidelity is governed by the variance of the accumulated first-order error generator. Through numerical simulation, we illustrate that coherent errors accumulated at different entangling gates can produce $\Theta(L^2)$ variance growth in a bare circuit, whereas independent Pauli dressing eliminates the cross-layer contribution on average and gives an $O(L)$ variance bound at any fixed confidence level for a randomly sampled realization. We also develop a covariance diagnostic that predicts when this mechanism is effective. We find a strong PT advantage for coherent errors whose transported generators have large off-diagonal covariance, and little advantage when the covariance matrix is nearly diagonal. Hardware experiments on IBM superconducting processors demonstrate fidelity improvements for GHZ-state preparation and reduced observable errors in Trotterized transverse-field Ising dynamics. These results indicate that this PT method is a useful coherent-error suppression technique for structured circuits containing repeated nontrivial two-qubit operations.

PO.135 Topologies in three-photon entanglement states

Honglin Xie*, Yijie Shen*, Zhenyu Guo* (NTU)

Topological structures in structured light provide new ways to describe and encode information in optical fields. Here, we extend these ideas to multiphoton entangled systems demonstrated using three-photon entanglement state, where topology is encoded non-locally in correlations between spatial and polarization degrees of freedom. Conditional measurements on one photon can prepare topological states in the remaining photons, enabling the

realization and control of structures such as nonlocal skyrmions and Hopfion-like configurations.

PO.136 AI-assisted Slepian-Pollak Imaging

Eng Aik Chan*, Taeyong Chang, Benquan Wang, Giorgio Adamo, Nikolay Zheludev (Nanyang Technological University)

The diffraction limit restricts the recovery of subwavelength information in conventional far-field imaging. We present an AI-assisted imaging approach that represents coherent far-field measurements of finite-sized nanostructures in the Slepian–Pollak basis which uses correlations between robust low-order modes and noise-sensitive high-order modes to recover subdiffraction features. In a proof-of-principle study, nanostructures are illuminated from four orthogonal directions by total internal reflection at a wavelength of 638 nm. Complex Slepian–Pollak coefficients are processed using a residual U-Net trained on 1,000 randomly generated nanostructures. Evaluation on 100 unseen samples yields a median resolution of $\lambda/13$, with an interquartile range from $\lambda/11$ to $\lambda/14$, within a field of view below 0.8λ. This resolution is achieved without increasing the collection numerical aperture, structured illumination, or nonlinear fluorescent contrast, demonstrating a promising route towards robust far-field super-resolution imaging.

PO.141 Compact Single-Shot Incoherent Edge Detection With a Polarization-Multiplexed Metalens

Weiyan Li*, Xiaotong Li, Youngsun Jeon, Zhaogang Dong, Chunying Guan*, Jinhui Shi*, Junsuk Rho* (Pohang University of Science and Technology)

Edge detection under incoherent illumination is highly desirable for compact vision systems but remains challenging due to the lack of phase control and the difficulty of implementing high-pass filtering in intensity-based imaging. Here, we propose and experimentally demonstrate a polarization-sensitive metalens that enables single-shot incoherent edge detection by constructing a second-order high-pass optical transfer function (OTF). The metalens imparts distinct phase profiles to left- and right-handed circularly polarized components, producing a pair of spatially separated images that encode complementary object information. Through digital alignment and subtraction, an effective second-order high-pass OTF is realized, enabling robust edge enhancement while requiring only simple pixel-wise operations. We experimentally validate this approach using USAF resolution targets and further demonstrate a compact imaging module by directly integrating the metalens with a complementary metal-oxide-semiconductor (CMOS) sensor, enabling real-scene single-shot operation. This work establishes a practical optical preprocessing strategy for incoherent edge detection, providing a pathway toward miniaturized, low-power, and computation-efficient vision front-ends for machine vision, autonomous sensing, and portable imaging systems.

PO.143 Ultimate sensitivity of multi-parameter estimation in quantum sensing with undetected photons

Sanjeet Swaroop Panda*, Lorcan O. Conlon*, Li Gong*, Ping Koy Lam*, Jie Zhao*, Young-wook Cho*, Ruvi Lecamwasam* (A*star, NUS)

Quantum sensing with undetected photons is a technique where photons of one wavelength probe a sample, but information is extracted by measuring photons of another wavelength that never interacts with the sample. This has seen significant experimental advances in applications such as spectroscopy, microscopy, and bio-sensing. However, a detailed theoretical analysis using the tools of quantum metrology is currently lacking. Thus it is unclear how far away current schemes are from fundamental limits, and what the optimal measurement strategies are. We apply a multiparameter quantum estimation framework to quantify the error when estimating the unknown transmission and phase shift of a sample. The optimal measurement scheme is shown to require only a single controllable phase shift, easily implementable in existing setups. We also study how to use multipass interactions to maximise information gain. In general the optimum number of passes scales inversely with the log of the transmission of the sample. This work clarifies the metrological power of quantum sensing with undetected photons, and provides guidance for the design of experiments requiring high sensitivity.

PO.146 High spectral purity photon source on thin-film lithium niobate

Ran Yang* (Centre for Quantum Technologies)

High-purity photon sources on fully integrated platforms are essential for optical quantum information pro-

cessing. Here, we demonstrate a high-spectral-purity photon source on thin-film lithium niobate based on cavity-enhanced spontaneous parametric down-conversion. By engineering the resonances, linewidths, and nonlinear interaction in two linearly decoupled resonators, we generate photon pairs with strongly suppressed spectral correlations. The generated photons exhibit high spectral purity without narrowband external filtering, thereby preserving source brightness and enhancing multi-photon interference performance. We measure a spectral purity of 96.4 $\pm$ 1.3%. This work highlights thin-film lithium niobate as a scalable platform for high-purity photon-pair generation and integrated quantum photonic processing.

PO.147 Integrated polarization-entangled photon source for wavelength-multiplexed quantum networks

Xiaodong Shi*, Yue Li, Jinyi Du, Lin Zhou, Ran Yang, En Teng Lim, Sakthi Mohanraj, Mengyao Zhao, Xu Chen, Xiaojie Wang, Guangxing Wu, Hao Hao, Veerendra Dhyani, Sihao Wang, Alexander Ling*, Di Zhu* (CQT)

Entangled photons are fundamental resources for quantum communication, computing, and networking. Among them, polarization-entangled photon pairs play an important role due to their straightforward state manipulation and direct use in quantum key distribution, teleportation, and network protocols. However, realizing compact, efficient, and scalable polarization-entangled sources that meet the requirements of practical deployment remains a major challenge. Here, we present a simple yet high-performance on-chip polarization-entangled photon-pair source on thin-film lithium niobate (TFLN). Our device employs dual quasi-phase matching (D-QPM) that sequentially supports type-0 and type-I spontaneous parametric down-conversion in a single nanophotonic waveguide, eliminating the need for interferometers, polarization rotators, or other complex circuits. The source directly produces high-fidelity Bell states with broad bandwidth, high brightness, and low noise. Using this integrated platform, we realize wavelength-multiplexed entanglement distribution in a four-user quantum network deployed over metropolitan fiber links up to 50 km. These results establish a robust and scalable pathway toward practical quantum communication systems and multi-user quantum mesh networks based on integrated photonics.

PO.151 Wide-Range 3D Magnetic Field Sensing in a 90°-Bent Geometry Enabled by Spin-Orbit Torque

Pinkesh Kumar Mishra*, Hasibur Rahaman, Ramu Maddu, Bilal Jamshed, Subhakanta Das, S.N. Piramanayagam* (Nanyang Technological University Singapore)

Magnetic-field sensors are essential for applications spanning transportation, industrial automation, and biomedical diagnostics. Nevertheless, compact three-dimensional (3D) magnetic-field detection remains difficult because conventional solid-state sensors typically require multiple sensing elements and intricate device configurations. In this work, we demonstrate a compact 3D magnetic sensor based on a 90°-bent domain-wall device (see Fig. 1c) fabricated from a Co/Pt heterostructure (see Fig. 1a) on a CMOS-compatible Si/SiO_2 substrate. The device utilizes spin-orbit torque to drive domain-wall motion within a single Hall-bar architecture, enabling the simultaneous detection of in-plane and (OOP) magnetic-field components through anomalous Hall resistance measurements. By optimizing the Co-layer thickness and device stack, we achieve an in-plane sensing range of $\pm$200 Oe and an OOP range of $\pm$9.5 kOe (Fig. 1e), while maintaining a low operating power density of 1.22 GW/cm^3 and excellent repeatability. Furthermore, the device supports in-plane angular magnetic-field scanning (Fig. 1d), expanding its capability for vector-field measurements within a single integrated structure. These results demonstrate a scalable spintronic approach toward compact, high-dynamic-range 3D magnetic-field sensors for next-generation integrated sensing technologies.

PO.154 Onset of Localization in 3D to 2D Crossover in Disordered Ultracold Fermi Gas

Song Haotian*, Rishav Koirala, Kai Dieckmann* (Center for quantum technologies)

We investigate how dimensionality modifies disorder-induced transport in an ultracold Fermi gas. An accordion lattice controls the vertical confinement by varying the lattice constant from 2.5 to 18.1 μm, while optical-speckle disorder drives localization and diffusion dynamics. Transport is characterized through the time evolution of the cloud width variance. Under strong vertical confinement, the cloud shows initial expansion followed by strongly suppressed variance growth. At weaker confinement, continued expansion is observed. These measurements reveal a dimensional crossover in disorder transport and suggest localization as the system approaches the quasi-two-dimensional regime.

PO.156 Generating and detecting photon pairs on a single integrated chip

Hao Hao* (National University of Singapore)

Thin-film lithium niobate (TFLN) combines a strong $\chi^{(2)}$ nonlinearity with an electro-optic response that remains efficient at cryogenic temperatures, making it an attractive host for circuits in which quantum light generation and superconducting single-photon detection coexist on one chip. Bringing the two together, however, requires simultaneously reconciling superconducting-detector and lithium niobate process flows, suppressing a pump that exceeds the generated single-photon flux by many orders of magnitude, and preserving the performance of the source and passive circuitry at the temperature the detectors demand.

Here we demonstrate a TFLN photonic chip on which spontaneous parametric down-conversion, pump rejection, passive linear-optical routing and waveguide-coupled single-photon detection all operate on the same substrate at approximately 1 K. A 780 nm pump is delivered through apodized grating couplers to a periodically poled waveguide that generates telecom-band photon pairs; the residual pump is removed by a monolithic amorphous-silicon absorptive filter; and the photons are distributed by a passive splitter network to four niobium nitride superconducting nanowire detectors integrated by deterministic transfer printing, which decouples the superconducting and lithium niobate fabrication processes. We characterise the cryogenic response of the grating couplers and of the quasi-phase-matching condition, and measure photon-pair correlations, heralded single-photon statistics and the end-to-end source-to-detector efficiency entirely on chip.

PO.160 Discrete Simulation of Nonlinear Schrödinger Dynamics in a Two Coupled Fiber Loop Temporal Photonic Lattice

Yuchun Wang* (SUTD)

The nonlinear Schrödinger equation can describe rich wave phenomena such as soliton formation, modulational instability, and nonlinear localized states. Here we investigate a two coupled fiber loop temporal photonic lattice as a discrete platform for simulating novel nonlinear Schrödinger type propagation, where the effective spatial and evolution dimensions are constructed through time multiplexing and the nonlinear response is introduced through intensity gradient-dependent phase modulation. Theoretical simulations show that, under suitable nonlinear strength and initial conditions, a Gaussian beam can form a stable localized cusp soliton structure and approximately maintain its spatial distribution during propagation. For a flat-top initial beam, the considered topological nonlinearity can preserve the sharp edges of the beam and stabilize localized structures near the boundaries. Our results indicate that the two coupled fiber loop platform can serve as an experimentally realizable system for studying novel discrete nonlinear Schrödinger dynamics, soliton formation, and nonlinear boundary localized states.

PO.161 Flux-activated resonant control of a bosonic quantum memory

Hector Calero Mas*, Seungwon Jin*, Aleksandr Dorogov*, Yvonne Y. Gao* (Centre for Quantum Technologies, National University of Singapore, Singapore)

Abstract. Bosonic modes in circuit quantum electrodynamics (cQED) are high-dimensional and hardware-efficient systems for quantum information processing and the study of light-matter in- teractions [1, 2]. Here, we implemented universal control of bosonic degrees of freedom through dynamic access to resonant Jaynes-Cummings interactions [3]. This was enabled by an architec- ture that integrates a flux-tunable transmon with a filtered on-chip flux line, providing protected broadband control while preserving long cavity lifetimes [4]. Nanosecond scale flux pulses en- able rapid switching between the dispersive and resonant interaction regimes, giving on-demand access to number selective cavity transitions. Using these capabilities, we demonstrated deterministic preparation of Fock states and their superpositions within hundreds of nanoseconds, together with efficient rotations between arbitrary pairs of Fock levels. Furthermore, we are extending this architecture toward a single-atom maser using AC parametric flux modulation to generate sidebands with tunable effective coupling. In this system, a single transmon serves as an artificial gain medium for the microwave cavity field [5, 6]. Cavity state tomography will provide access to quantum signatures of lasing, including sub-Poissonian photon statistics and phase space bistability, with potential applications in quantum metrology and sensing [7]. To- gether, these results and ongoing developments highlight the potential of protected flux-tunable bosonic cQED as a versatile platform for quantum control and for exploring light-matter physics across a broad range of interaction regimes.

References [1] A. Joshi, K. Noh, and Y. Y. Gao, "Quantum information processing with bosonic qubits in circuit QED," Quantum Sci. Technol. 6, 033001 (2021). [2] B. M. Terhal, J. Conrad, and C. Vuillot, "Towards scalable bosonic quantum error correction," Quan- tum Sci. Technol. 5, 043001 (2020). [3] F. Valadares et al., "Flux-activated resonant control of a bosonic quantum memory," arXiv:2602.18122 (2026). [4] F. Valadares, "Dynamical Light–Matter Coupling with Protected Superconducting Oscillators," Ph.D. thesis, National University of Singapore (2026). [5] A. A. Sokolova, G. P. Fedorov, E. V. Il'ichev, and O. V. Astafiev, "Single-atom maser with an engineered circuit for population inversion," Phys. Rev. A 103, 013718 (2021). [6] A. A. Sokolova, D. A. Kalacheva, G. P. Fedorov, and O. V. Astafiev, "Overcoming photon blockade in a circuit-QED single-atom maser with engineered metastability and strong coupling," Phys. Rev. A 107, L031701 (2023). [7] S. Fernández-Lorenzo and D. Porras, "Quantum sensing close to a dissipative phase transition: Sym- metry breaking and criticality as metrological resources," Phys. Rev. A 96, 013817 (2017).

PO.164 Classical and Quantum Heuristics for the Binary Paint Shop Problem

V Vijendran*, Dax Enshan Koh, Ping Koy Lam, Syed M Assad (A*STAR Quantum Innovation Centre)

The Binary Paint Shop Problem (BPSP) is an APX-hard optimisation problem arising in automotive manufacturing: given a sequence of 2n cars, comprising n distinct models each appearing twice, the task is to decide which of two colours to paint each car so that the two occurrences of each model are painted differently, while minimising consecutive colour swaps. Performance is measured by the paint swap ratio—the average number of colour changes per car—which directly affects production efficiency and cost. Prior work showed that the Quantum Approximate Optimisation Algorithm (QAOA) at depth p = 7 achieves a ratio of 0.393, outperforming the then-best-known classical heuristic, Recursive Greedy, with a proven asymptotic expected ratio of 0.4 [Phys. Rev. A 104, 012403 (2021)]. More recently, the Recursive Star Greedy (RSG) heuristic was proposed with a conjectured expected ratio of 0.361. Here, we formally reduce BPSP to weighted MaxCut, yielding an exact Ising formulation, and benchmark two state-of-the-art low-depth QAOA variants—eXpressive QAOA and Recursive QAOA—at p = 1 (denoted XQAOA1 and RQAOA1) against four classical BPSP heuristics. Across instances ranging from 128 to 4096 cars, XQAOA1 achieves an average paint-swap ratio of 0.357; in our instance-wise benchmarks, it outperforms RQAOA1 on almost all instances and each of the four classical baselines, including RSG, on every instance. Surprisingly, RQAOA1 deteriorates with problem size despite employing provably near-optimal QAOA1 parameters at each recursive step, eventually falling behind RSG at the largest sizes. To our knowledge, this is the first report of size-dependent performance degradation of RQAOA1 at scale. In contrast, XQAOA1 remains stable across all tested sizes, with no evidence of size-dependent degradation.

PO.165 Bridging Quantum Physics and the Technology Community: Lessons from the Singapore Computer Society Quantum Technologies Special Interest Group

Jing Yan Haw* (Centre for Quantum Technologies)

Quantum technologies are advancing across computing, communication and sensing, yet their underlying physics, technological maturity and practical relevance remain difficult to communicate to non-specialist technology professionals. The Singapore Computer Society Quantum Technologies Special Interest Group (SCS QT SIG) was established to create strategic platform for professionals to collaborate, share knowledge, and explore real-world applications. Since the launch of the initiative, QT SIG has organised activities spanning quantum computing, quantum communication, quantum sensing, financial applications and quantum-safe cybersecurity.

We reflect on the SIG experience engagement and activities thus far, and the lessons learned from communicating quantum concepts across disciplinary and sectoral boundaries. These include distinguishing theoretical capability from present maturity, connecting physical principles with applications and limitations, and addressing common misconceptions without sacrificing scientific accuracy. We discuss how professional societies can complement formal education by connecting quantum researchers with industry, government and the wider technology community.

PO.167 Exceptional-Point Winding for Topological Control of Resonant Photonic Systems

Arnab Laha*, Lin Wu (SUTD)

Exceptional points (EPs) provide a powerful framework for topological control in non-Hermitian photonic systems, where their branch-point topology enables coupled states to exchange their spectral identities through para-

metric winding. Beyond state permutation itself, an important direction is to translate this topology into control over the functional characteristics of resonant photonic systems. Here, we explore EP winding as a general strategy for reconfiguring amplification and absorption while controlling resonance linewidth and quality factor in open non-Hermitian microcavities.

Using scattering-matrix descriptions of gain–loss-engineered Fabry–Pérot microcavities, we construct two-parameter non-Hermitian landscapes in which coupled scattering states exhibit characteristic branch-point topology. Parametric winding around EPs drives deterministic permutation of the interacting states and simultaneously reorganizes their spectral characteristics. Within this framework, a pair of conjugate EPs connects the pole and zero branches associated with amplification and absorption, thereby enabling controlled access to distinct threshold-lasing and coherent-perfect-absorption (CPA) conditions via topological-state evolution. At the same time, tailoring the surrounding resonance landscape enables branch-selective linewidth suppression, such that the winding-induced state exchange can transfer narrow-linewidth, high-Q characteristics between coupled resonances. Thus, the topology governing state permutation also provides a route for controlling which resonant state approaches a lasing or absorption condition and how its linewidth and Q factor evolve during the reconfiguration.

These results establish EP winding as a versatile mechanism for translating non-Hermitian topology into controllable photonic operation. Rather than using winding solely to exchange modal identities, the approach connects the evolution of the topological state to the functional properties of the participating resonances, encompassing lasing and CPA operation, as well as reconfiguration of linewidth and Q-factor. This perspective provides a route toward reconfigurable resonant photonic systems in which both the selected optical state and its operating characteristics can be manipulated within a common topological framework, with potential applications in mode-selective lasers, coherent absorbers, narrow-linewidth resonators, and other non-Hermitian photonic devices.

PO.168 Collective Multimode Interference and Chiral Exceptional Points in a Dielectric Metasurface

Fangzhou Shu, Sergei Reva*, Lin Wu* (SUTD)

Handedness-dependent optical responses in metasurfaces have attracted considerable interest for polarization control, sensing, and optical information processing. Importantly, strong circular-conversion asymmetry can arise even in geometrically achiral structures. Here, we study a mirror-symmetric dielectric terahertz metasurface formed by a square lattice of rectangular apertures rotated within the unit cell. The rotation breaks the in-plane mirror symmetries while preserving the out-of-plane reflection symmetry, producing a strong circular-conversion asymmetry and several chiral exceptional-point conditions which are coalescence points of the transmission matrix eigenvalues. Reduced coupled-mode models are often used to interpret resonant metasurface responses, but their applicability becomes less transparent when several resonances have noticeable spectral overlap. Here we employ a quasinormal-mode (QNM) pole expansion of the scattering matrix, where the complex resonance frequencies and mode-to-channel coupling amplitudes are obtained directly from the Maxwell eigenproblem. The preserved out-of-plane mirror symmetry separates the QNMs into TE and TM families, while their radiation contributions remain free to interfere in the common far-field channels. In the spectral range of interest, four QNMs together with a smooth effective background reproduce well the full-wave scattering simulations. The cluster of four modes generates two spectrally separated bands of strong circular dichroism through far-field interference. Within this multimode response, several chiral exceptional points are observed. Their pole-resolved decomposition reveals qualitatively different interference mechanisms underlying the transmission response at these points: one exceptional point exhibits a broadly distributed contribution from all four QNMs, whereas another involves substantial interference between the resonant response and the effective background. The results demonstrate that both broadband chiral functionality and chiral exceptional points in realistic metasurfaces can emerge from collective multimode interference beyond minimal coupled-mode descriptions.

PO.169 Stabilization of Granovskii-Zhedanov scars of the XYZ quantum spin chain via non-Hermitian spin relaxation

Dhiman Bhowmick* (Nanyang Technological University)

The Granovskii–Zhedanov (GZ) states are exact scar states of the spin-S XYZ chain for $S \geq 1$. As a result, local quantum information encoded in a GZ state remains preserved under the unitary dynamics of the XYZ Hamiltonian; thus, these states evade thermalization and violate ergodicity despite the system being otherwise non-

integrable and chaotic. However, in realistic experimental settings, the realization of an ideal XYZ Hamiltonian is not possible, as perturbations are inevitable. These perturbations ultimately lead to the decay and thermalization of the GZ state. We study the stability and dynamics of GZ states in the presence of generic perturbations and propose physically realistic mechanisms to stabilize them. We show that the product structure of the GZ state allows its lifetime to be enhanced in the presence of an external helical magnetic field, which slows down thermalization but does not prevent it at long times. We further demonstrate that the inclusion of effective non-Hermitian spin relaxation processes can substantially stabilize the GZ states, leading to a nonequilibrium steady state with finite fidelity with GZ state. Such dissipative processes can naturally originate from mechanisms such as Purcell-enhanced spontaneous emission or spin–lattice relaxation in the presence of the helical magnetic field. Using infinite time-evolving block decimation (iTEBD) and exact time evolution, we systematically analyze the dynamics and robustness of the GZ states in the perturbed non-Hermitian XYZ model. To connect with experimental platforms, we introduce a Hubbard model that maps onto the XYZ spin system and propose that ring-shaped optical lattices may provide a viable route for realizing and stabilizing GZ states. Finally, we present an equivalent Lindblad description of the effective non-Hermitian dynamics.

PO.171 Integrating QKD/PQC with Network Layer VPN Technologies

Zeyu Zhu*, Matthew Wee*, Ruyi Xu*, Jeff Lee*, Jing Yan Haw*, Hao Qin*, Alexander Ling* (Centre for Quantum Technologies)

IPsec and WireGuard are distinct virtual private network (VPN) technologies that operate at Layer 3 (network-layer) of the Open Systems Interconnection (OSI) model, providing encryption and encapsulation of IP traffic. In this work, we integrate these network-layer VPN technologies with NQSN in-house Key Management System (KMS), exploring the use of Quantum Key Distribution (QKD), and Post-Quantum Cryptography (PQC) as key sources.

We first implement a QKD-key mode. For IPsec, both hardware-based (Fortinet FortiGate) and software-based (Juniper vSRX) solutions are configured to retrieve QKD key material locally from the KMS via the standardized ETSI GS QKD 014 interface and incorporate it into the IKEv2 key-derivation process. For WireGuard, QKD-key supplied by the same KMS is used to derive the pre-shared key protecting the tunnel. We then extend the implementation to a hybrid QKD + PQC mode on both FortiGate and WireGuard, examining the respective key-injection points and key-combining mechanism.

To validate these implementations under real network traffic, two virtual machines (VMs) were deployed at two different sites, acting as end users to generate bidirectional data flow. Performance of different configurations will be assessed through throughput testing across the tunnel.

PO.172 Temperature-Tunable Yoneda-Like Anomalous Soft X-Ray Reflection at the Al L3 Edge

Muhandis Shiddiq*, Pengtao Song, Russell Kwan Jie Wen, Caozheng Diao, Yvonne Y. Gao, Andrivo Rusydi* (NUS)

We report an unusual anomalous soft x-ray reflection at the Al L3 edge that exhibits several characteristics reminiscent of the Yoneda effect. At 300 K, neither anomalous nor specular reflection is observed at very low incident angles below approximately 6 degrees. As the incident angle increases, a broad anomalous reflection emerges, reaches a maximum, and subsequently weakens, while conventional specular reflection becomes prominent above approximately 14 degrees. The anomalous peak consistently occurs at a scattering angle smaller than the incident angle and suppresses the specular reflection. The enhanced anomalous reflection is accompanied by strongly reduced absorption, indicating redistribution of the incident x-ray intensity between absorption and scattering channels. A striking feature is its strong temperature dependence. Cooling from 300 K to 37 K suppresses the anomalous reflection at lower incident angles, while at higher incident angles it suppresses the specular component and enhances the anomalous reflection. This behavior effectively shifts the angular evolution of the anomalous reflection toward larger incident angles. These observations reveal a temperature-tunable, Yoneda-like reflection regime at the Al L3 edge that is distinct from both conventional specular reflection and classical Yoneda scattering.

PO.175 Spatial Superposition of a Large Mass in an RF Trap

Jackson Tiong* (National University of Singapore)

We provide a proposal to create a spatial superposition of a massive charged silica nanoparticle, co trapped with an ion in a dual frequency Paul trap. Ion cat states rely on state-dependent optical kicks on internal levels, unavailable in a dielectric nanoparticle. We instead co-trap a charged nanoparticle (slow RF) with a $^{40}Ca^{+}$ ion (fast RF) at 43–55 μm, and use the Coulomb coupling to map the ion superposition onto a correlated displacement $\Delta z \sim$ nm $\gg \Delta z0 \approx 0.01$ nm. Spatial superposition of a massive object probes the quantum–classical boundary: it bounds collapse models (CSL, Diósi–Penrose) and, since gravitational coupling scales with mass, enables gravitational entanglement tests.

PO.176 Complete Hypergraph States as a Resource for Quantum Metrology

Hoe Kin Mooi*, Leong Chuan Kwek* (CQT)

Quantum metrology exploits uniquely quantum resources to achieve parameter-estimation precision beyond classical limits. Multipartite entangled states, including graph states, can provide substantial metrological enhancement. Hypergraph states extend graph states by incorporating many-body interactions through multi-controlled-phase gates, but their metrological performance and noise robustness remain incompletely understood. We derive exact analytical expressions for the quantum Fisher information (QFI) of complete hypergraph states with respect to the collective-spin generators J_x and J_y. For a set of hyperedge orders K sharing an entangling phase ϕ, the noiseless QFI reduces to three finite binomial averages requiring $O(n|K|)$ arithmetic. At $\phi = \pi$, the pointwise order-optimized J_x envelope approaches the unit Heisenberg prefactor, whereas the corresponding J_y envelope has lower and upper accumulation values of $1/2$ and 1, respectively, as the system size n increases. We extend the analysis to particle erasure using an exact Dicke-basis representation of dimension $n - e + 1$, where e particles are erased. For independent phase-flip dephasing before parameter encoding, a radial Krawtchouk reduction yields the exact QFI with $O(n^2)$ arithmetic. At $\phi = \pi$, we prove that, for every fixed hyperedge order $k \geq 3$, both transverse generators retain a positive asymptotic Heisenberg coefficient after any fixed finite number of erasures. Under independent phase flips with any fixed probability $p < 1/2$, the noiseless coefficient is reduced by the factor $(1 - 2p)^2$ but remains positive. Complete hypergraph states therefore provide a structured family of metrological probes that retain Heisenberg scaling under fixed-count erasure and fixed-rate independent phase-flip noise.

PO.178 Syndrome-driven code adaptation for multicycle quantum error correction

Tejas Acharya* (National University of Singapore)

General-purpose Quantum Error Correction (QEC) codes, such as surface codes, are designed to correct arbitrary errors on sufficiently few qubits, without requiring detailed knowledge of the underlying noise. However, if the noise is highly asymmetric and well-calibrated, it is possible to design smaller, noise-aware codes that correct these specific errors rather than general ones, thereby reducing the required qubit count. When the noise structure is more complicated—e.g. due to the bath retaining memory—the effective noise on the system can change after a QEC cycle, and this change can depend on the QEC process itself. The original noise-aware code may then perform poorly on subsequent cycles, making noise-aware codes useless beyond a single cycle of correction when applied naively. However, when the error-detection syndrome sufficiently constrains the post-measurement support of the bath, this information can be used to track the relevant change in the noise. One can then design dynamically adapting noise-aware codes, where adaptation is driven only by classical memory (the syndrome data), thereby retaining the qubit-count advantage of smaller codes across multiple QEC cycles. In this paper we (i) characterize how QEC itself can alter the effective noise on the system, (ii) provide a Knill–Laflamme-type theorem giving conditions under which a code can be validly adapted at each cycle while maintaining correctability, and (iii) demonstrate these concepts through analytical examples and numerical code searches on small systems, including cases where syndrome-dependent adaptation succeeds across multiple cycles while static reuse fails.

PO.179 Tensor Networks for Diffusion Simulations: QTT Tensor Cores, High-Order Time Integration, and Implicit vs Explicit Schemes

Bernard Yim*, Dario Poletti (SUTD)

Tensor Networks (TN), also called Matrix-product states or Tensor Train, has been shown to be able to compute

numerical solutions to classical computational problems, such as those found in Computational Fluid Dynamics and PDEs. In this project, we explore using modern techniques such as Quantics Tensor Train to perform diffusion simulations in 2d (can be extended to 3d), using various differentiation time-stepping schemes such as Explicit/Implicit Euler, Crank-Nicolson and higher order Linear Product Expansion approximations. We also benchmark them against their equivalent classical methods and solvers

PO.180 Subharmonic photonic interband transitions through virtual multiband pathways in a doubled moving-basis coupled-mode theory

Divij Ramesh Nalge* (NTU)

Coupled-mode theory for time-modulated photonic structures is commonly formulated in the eigenmodes of an unmodulated reference system. Here we instead expand the electromagnetic field in the instantaneous eigenmodes of the time-dependent Maxwell operator, retaining both positive and negative-frequency branches. Mode coupling is governed by a geometric connection evaluated directly from a Hellmann-Feynman identity involving the instantaneous modes and the explicit time derivative of the permittivity, avoiding finite differences of eigenvectors and any expansion in modulation depth.

We identify photonic-band pairs whose first-order coupling vanishes by a momentum selection rule, yet undergo nearly complete transfer when driven at half their frequency splitting. The transition is a two-quantum process: in a static-mode description it arises from a combination of higher harmonics of the exact Maxwell operator and coherent virtual pathways through off-resonant intermediate bands. A linearised two-mode fixed-basis theory therefore predicts no transfer, and restoring the intermediate modes recovers the dynamics only non-monotonically, since each added mode also shifts the resonance. A two-mode moving basis, by contrast, reproduces full-wave Yee-FDTD dynamics to a root-mean-square error below 10^{-3}, because the instantaneous eigenmodes are already dressed by the intermediate bands and carry the multiband virtual processes in their geometric coupling. The result gives a compact description of higher-order photonic transitions and shows that subharmonic driving can access interband transfer at modulation frequencies below the bare mode splitting.

PO.181 Theoretical Scaling Laws of Geodesic Acoustic Modes in Shaped Tokamak Plasmas

Thura Kaung Htet*, Kyungtak Lim, Xavier Garbet (School of Physical and Mathematical Sciences, Nanyang Technological University)

Geodesic Acoustic Modes (GAMs) play a critical role in the regulation of cross-field transport in modern tokamaks[1]. As contemporary devices move towards non-circular and highly shaped configurations[2], there is a pressing need for a robust treatment of the interplay between plasma geometry and GAM dynamics. This work investigates the theoretical scaling laws of the GAM frequency and growth rate with respect to key shaping parameters: triangularity δ), elongation (κ), Shafranov shift gradient (Δ'), and aspect ratio (ϵ)). While earlier analytical studies[3,4,5] have been foundational in establishing GAM scaling laws in shaped plasmas, these approaches have often relied on fluid models or simplified gyrokinetic approximations, and have generally not been benchmarked against nonlinear simulations or experimental data. In our work, we address these limitations by employing a dual-track methodology to bridge the gap between analytical predictions, numerical results, and experimental observations.

Using gyrokinetic theory and the Miller local equilibrium model, we derive from first principles an analytical dispersion relation that incorporates the effects of non-circular magnetic equilibria. This model also includes extended poloidal mode coupling by retaining the $m = 2$ harmonic, and accounts for drift resonances up to the second order of the smallness parameter.

These analytical results are benchmarked against data from the global, full-f, flux-driven gyrokinetic code GYSELA[7], using custom-tailored magnetic equilibria. Protocols used to mitigate numerical artefacts and ensure physical fidelity are also detailed, along with post-processing techniques and additional benchmarking. Our results from GYSELA, showcased in Figure 2, demonstrate that the GAM damping rate increases moderately with triangularity, which shows good agreement with analytical results from Wahlberg[3] and Chen[5]. Additional analysis, hitherto lacking in the literature, is also provided for the scaling of GAM parameters with respect to the gradient of the Shafranov shift Δ'. By comparing the theoretical scaling laws from the analytical model with numerical results from flux-driven simulations, this work provides a unified picture of GAM scaling across a wide range of shaping parameters.

References [1] G.D. Conway et al 2022 Nucl. Fusion 62 013001 [2] Marinoni, A., Sauter, O. & Coda, S. Rev. Mod. Plasma Phys. 5, 6 (2021). [3] C Wahlberg and J P Graves 2019 Plasma Phys. Control. Fusion 61 075013 [4] Sorokina E.A., Lakhin V.P., Konovaltseva L.V. and Ilgisonis V.I. 2017 Plasma Phys. Rep. 43 271 [5] Zhe Chen and Haijun Ren 2023 Nucl. Fusion 63 066004 [6] Gao Z. 2013 Phys. Plasmas 20 032501 [7] Virginie Grandgirard, Jérémie Abiteboul, Julien Bigot, Thomas Cartier-Michaud, Nicolas Crouseilles, et al Computer Physics Communications, 2016, 207, pp. 35-68.

PO.183 Heralded Narrowband Photon Pair Generation from a Cold Rubidium Ensemble

Raghav Sah*, Christian Kurtsiefer* (CQT)

Quantum networks, relying on atomic ensembles as quantum nodes, require narrowband photons for efficient atom-photon interaction. We demonstrate two schemes to generate narrowband, time-correlated photon pairs at the atomic transitions in ^{87}Rb. Further, we propose a scheme to generate photon triplets that can be used in multi-node quantum communication.

PO.185 Tools and methods for security certification of quantum key distribution (QKD) systems.

Wastu Wisesa Ginanjar*, Bibhuti Thapa*, Hou Shun Poh*, Christian Kurtsiefer*, Michael Kasper* (Fraunhofer Singapore Research Center, NTU)

With an ongoing global effort in certifying the security of quantum key distribution (QKD) systems, we are developing the tools and methods to characterisatise their vulnerability against implementation attacks. We looked at the vulnerabilities of InGaAs single-photon avalanche detectors (SPAD) to blinding and faked-states attacks. The SPAD responses under bright light and engineered optical pulses were characterised. We applied continuous-wave optical power of $\approx$7 nW to a SPAD, suppressing the detector counts. This is combined with optical trigger pulses at 1310 nm with a pulse width of $\approx$5 ns and a peak power of $\approx$220 μW, over a range of repetition rates. We demonstrated that these pulses deterministically generate clicks of the SPAD up to repetition rates of 1 MHz.

PO.191 Toward Digital and Analog Quantum Processors Using Cesium Atom Arrays

Subrahmanyam Sai Gurunath Mantha* (CQT)

We report progress toward developing 200-qubit quantum processors based on reconfigurable arrays of neutral Cs atoms. Several experimental setups will be constructed, targeting state-of-the-art performance in qubit coherence, atom shuttling, quantum gate fidelity, and fast qubit-state readout. We have completed assembly of a 3D MOT and achieved a loading rate of $\approx 2 \times 10^9$ atoms per second. We also loaded a 21x21 tweezer array and measured a tweezer limited lifetime of 2 minutes. Towards the end of this year, we aim to demonstrate atom sorting to obtrain a defect free array. Over the next two years, we will implement quantum error correction and quantum simulation experiments on our Cs processors and further scale the array to thousands of qubits while maintaining robust control and high fidelity.

PO.192 Field-Effect Switchable Type-III Band Alignment in InSe/BP Heterostructures for Low-Power Tunneling Field-Effect Transistor Applications

Yufan Kang, Su Tong*, Sanchali Mitra, Yee Sin Ang* (SUTD)

Van der Waals heterostructures with tunable band alignment are promising candidates for low-power tunneling field-effect transistors (TFETs). In particular, heterostructures that are intrinsically close to a broken-gap band alignment are highly desirable because they can be driven into a type-III alignment under relatively small external perturbations. In this work, we systematically investigate the layer-dependent electronic structures of 1L/2L InSe, 1L/2L BP, and their corresponding heterostructures using first-principles calculations. Our results show that the band alignment in InSe/BP heterostructures is highly sensitive to the layer number. Among the studied configurations, the 2L-InSe/2L-BP heterostructure exhibits a near-broken-gap alignment while retaining relatively small effective masses, making it particularly attractive for TFET applications. Under an external electric field, this bilayer heterostructure undergoes a transition from type-II to type-III band alignment at a relatively low critical field of 0.05 V/Å compared with many previously reported systems. We further examine the influence of representative point defects by constructing defective heterostructures based on the most stable defects in bilayer InSe and bilayer BP. Although the defects modify the electronic structure and increase the critical field required for the

transition, the field-induced evolution toward the type-III regime is still preserved. These results demonstrate that layer-engineered InSe/BP heterostructures provide a promising platform for low-field-accessible broken-gap band alignment and TFET devices.

PO.195 LIDAR with optically amplified thermal light

Darren Koh*, Christian Kurtsiefer, Peng Kian Tan* (Centre for Quantum Technologies)

Thermal light exhibits intensity fluctuations or photon bunching characteristic that has been used as a source of entropy or correlation. However, its low spectral density limits its use in practical application. One method of remedying this is optical amplification to boost its brightness. In this paper, we show that the normalized second order coherence function of a thermal light source is preserved after amplification. We then show that amplified thermal light is a suitable light source for LIDAR by demonstrating a LIDAR raster scan of a building at 1.3km with a depth resolution of 2cm.

PO.196 One Aperture, Two Colors: Independently Fed Vertically Stacked Silicon Nitride Gratings for Trapped-Ion Addressing

Gyanendra Yadav* (Centre for Quantum technologies, National University of Singapore)

Scaling integrated optical control for trapped-ion processors is constrained by chip area: each additional wavelength ordinarily requires separate routing, emission structures, and electrode openings near the ions. This work numerically demonstrates an alternative architecture in which two independently fed, vertically stacked silicon nitride gratings synthesize separate narrowband wavefronts through one $24 times 24$ μm^2 aperture. The device targets the 729.4 nm qubit and 854.2 nm repump transitions of ^{40}Ca$^+$.

A hierarchical design strategy combines differentiable optimization of three-level scattering cells, analytical focusing-phase synthesis, and discrete depth allocation using two etches per photonic layer. This construction implements graded radiation envelopes while maintaining a 125 nm propagation-axis feature floor. Full-stack phase registration then aligns the independently generated wavefronts at the ion position.

Mesh-converged simulations using Tidy3D and Lumerical independently reproduce the device response. At the trap-compatible plane 72.13 μm above the upper photonic layer, the focal maxima are separated by only 0.05 μm, and the common coordinate retains 99.93% of each beam's peak intensity. The corresponding focusing efficiencies are approximately 0.41 and 0.17 for the 729 and 854 nm channels. At 5 μm ion spacing, the qubit channel provides -23.6,dB point crosstalk. Analytic surface-electrode placement preserves a 15.3 μm clearance from the radio-frequency rails.

The architecture converts multi-wavelength delivery from a lateral chip-area penalty into a vertically integrated wavefront-design problem, enabling lithographically locked multicolor alignment for compact quantum-control interfaces.

PO.199 TOPO2: Recovering topological information of light by topological learning

Benquan Wang* (NTU SPMS)

The evolution of modern-day communication networks towards optical solutions with enhanced capacity and robustness is driving interest in topological light waves, exploiting their stability against perturbations through a topological invariant, e.g., the skyrmion number. However, detecting the underlying topology remains a computationally intense process even under ideal conditions, becoming intractable after passing through strongly disordered channels, where the degradation into unrecognisable speckle appears to destroy the topology.

Here, we propose and demonstrate a topology-enhanced artificial intelligence (AI) approach to recover and classify such apparently lost topological information by computationally leveraging topological invariants in the data across many length scales. By aligning the topological classification of information with the topology of light, our topology-enhanced learning protocol, termed TOPO2, achieves highly efficient recognition of the topological states of light, even from speckle, without the need for any prior learning. Our approach outperforms benchmark tests against standard computational algorithms and has the benefit of requiring just a single intensity pattern as the input, facilitating single-shot operation. To demonstrate this, we leverage the skyrmion number as a robust data carrier of images through a disordered channel, using TOPO2 to accurately reconstruct the transmitted images.This work synergises topological photonics and topological AI for unravelling hidden topological signatures in light, opening a pathway towards robust communications even in extreme disordered environments.

PO.200 Nonlinear Spatial Pulling and Walk-off Quenching of Light Drag in Counter-Propagating Four-Wave Mixing

Lin Cheng* (member)

The greatly enhanced Fresnel-Fizeau transverse optical drag in slow-light media has been regarded as a linear kinematic effect of a single beam. Here, we study this effect in phase-matched four-wave mixing (FWM) and show that the third-order nonlinearity $\chi^{(3)}$ acts as an effective spatial restoring force, mutually pulling the simultaneously generated forward and backward signal beams. Based on the evolution of the centroid trajectories, we identify three distinct dynamical states: (i) Walk-off quenching, where the medium motion exponentially suppresses nonlinear energy exchange. (ii) Mutual spatial trapping, forming bound pairs. (iii) Asymmetric drag driven by Doppler-induced group velocity mismatch. This work introduces a nonlinear framework for controlling nonlinear optical states through macroscopic mechanical motion, which is significant for ultrasensitive motion sensing and nonreciprocal optical signal manipulation.

5 Technical Sessions

Please observe the technical instructions for talks to comply wiht regulations. We will leave a copy for each chair in the rooms.

T1: Quantum Optics

Time: Wednesday 28 Oct, 11:30am; Venue: Think Tanks 2&3; Chair: (TBD)
Time allocated for invited talks is 15 min speaking time, plus 5 min Q&A, and time allocated for contributed talks is 12 min speaking time plus 3 minutes Q&A.

T1.106 (INVITED) Giant Photon Superbunching from Weak Nonlinearity

You Wang*, Timothy C. H. Liew, Yidong Chong* (Nanyang Technological University)
11:30am – 11:50am

Photon superbunching, which occurs when the second-order correlation satisfies $g^{(2)} > 2$, is typically associated with strong optical nonlinearities or collective multi-photon emission processes. We predict that extreme superbunching can also arise in systems of weakly-nonlinear photonic cavities, via the creation of a squeezed vacuum through interference engineering by fine-tuning inter-cavity couplings and drive parameters. We present numerical calculations indicating that a system of four photonic resonators containing representative Kerr media can achieve $g^{(2)}(0) = 135$ with a 80 kHz emission rate. Unlike earlier superbunching schemes, this mechanism is highly compatible with integrated photonic platforms constructed using conventional optical media.

T1.123 Experimental violation of multipartite Bell-type correlation witnesses using few-body symmetric correlations

Mengyao Hu* (National University of Singapore)
11:50am – 12:05pm

Certifying Bell correlations in increasingly large multipartite quantum systems is challenging because conventional Bell inequalities often require access to high-order correlations that become experimentally demanding with increasing system size. Here we demonstrate that multipartite Bell correlations can be certified using low-order permutation-invariant (PI) correlations with a fixed maximal correlation order, using Dicke states as an experimentally accessible platform. We experimentally test PI Bell-type witnesses containing only two- and four-body correlators and show that introducing four-body correlations substantially enhances the noise tolerance compared with previously studied two-body witnesses. For six photons, the optimized witness tolerates a white-noise fraction of $p_c \approx 0.301$, compared with $p_c \approx 0.048$ for a representative two-body inequality. Using high-fidelity six- and eight-photon Dicke states with fidelities of $0.933(4)$ and $0.916(11)$, we observe Bell-correlation violations of 32 and 8.9 standard deviations, respectively. Notably, the eight-photon experiment achieves Bell certification while retaining the same four PI correlators and maximal correlation order as the six-photon case. These results demonstrate an experimentally accessible approach for certifying multipartite Bell correlations in larger Dicke systems without requiring full-body correlation measurements.

T1.112 On the Impossibility of Complete Absorption of Vector Beams

Sauvik Roy*, Nirmalya Ghosh, Ayan Banerjee, Subhasish Dutta Gupta (Nanyang Technological University, Singapore)
12:05pm – 12:20pm

Complete absorption of an optical beam is conventionally associated with either coherent perfect absorption (CPA) or critical coupling (CC). However, these concepts are predominantly formulated within scalar or coupled-mode descriptions, which do not fully account for the vectorial nature of structured optical beams. Here, we investigate the possibility of complete absorption of monochromatic vector beams, including Gaussian and Laguerre–Gaussian beams with and without orbital angular momentum, using a full vectorial treatment. We consider both coherent counter-propagating illumination satisfying the CPA condition and single-sided illumination under critical-coupling conditions in planar absorbing multilayer structures. In both cases, we find that the conditions required for perfect absorption can be satisfied only for a specific spatial harmonic, while the remaining off-axis components

experience different reflection, transmission, and polarization transformations. Consequently, complete absorption of a finite vector beam cannot be achieved, despite substantial suppression of the reflected and transmitted fields. Our results establish a fundamental limitation on extending the concepts of CPA and critical coupling from plane waves to realistic vector beams and highlight the necessity of retaining the full polarization and angular-spectrum information in the analysis of beam absorption.

T1.122 Demonstration of tripartite cat states in two distinct classes of entanglement

May Chee Loke, Jonathan Schwinger, Kehui Yu, Yingshan Zhang, Amon Maria Kasper, Tanjung Krisnanda*, Yvonne Gao* (Centre for Quantum Technologies)

12:20pm – 12:35pm

Entanglement is a cornerstone of quantum mechanics and an essential resource for quantum computation, communication, and metrology. While bipartite entanglement is extensively studied, genuine multipartite entangled states remain largely inaccessible in the macroscopic continuous-variable domain. Here, we experimentally realize macroscopic tripartite entangled cat states of the two distinct classes with fundamentally inequivalent properties, namely GHZ-cat and W-cat states, encoded across three microwave resonators coupled to an ancillary superconducting transmon. We develop one-to-all conditional controls on the three oscillators by fully utilizing three energy levels of the transmon to generate these states in a single piece of hardware and employ an efficient subspace tomography protocol for state reconstruction. The reconstructed state fidelities are 0.83 ± 0.02 for GHZ-cat and 0.70 ± 0.02 for W-cat after correcting for independently calibrated measurement errors, exceeding the thresholds that certify genuine multipartite entanglement in the GHZ and W classes, respectively. We further validate the distinct entanglement classes by experimentally demonstrating that pairwise entanglement is present in the W-cat state but absent in the GHZ-cat state. Our technique for the on-demand generation and characterization of inequivalent classes of tripartite continuous-variable entanglement provides a valuable testbed for future studies of macroscopic many-body entanglement and fault-tolerant quantum information processing with multipartite bosonic codes.

T1.138 Multi-parameter quantum metrology with an entangled cat state

Celine Trieu*, Xiang Li*, Adrian Copetudo, Ni-Ni Huang, Amon Kasper, Tanjung Krisnanda*, Yvonne Gao* (CQT)

12:35pm – 12:50pm

A fundamental principle of quantum mechanics is the Heisenberg uncertainty relation, which sets a lower bound on the product of the uncertainties of two non-commuting observables, precluding their simultaneous determination with arbitrary precision. Multi-parameter quantum metrology seeks to optimize the joint precision with which such incompatible observables can be estimated.

Here, we introduce a scheme that leverages a two-mode non-Gaussian entangled cat state to estimate a coherent displacement through its two conjugate quadrature components, whose generators do not commute. We experimentally realize this protocol on a bosonic cQED device, using a Josephson element operated in the transmon regime to generate and disentangle two harmonic-oscillator modes on demand. We show that the simultaneous estimation of the two conjugate quadratures each beats the standard quantum limit set by coherent states, while their product falls below the bound imposed by the Heisenberg uncertainty relation. Furthermore, thanks to its greater robustness against experimental imperfections, our scheme outperforms one based on a two-mode squeezed vacuum state, the optimal Gaussian resource in the ideal case. Our results chart a practical route toward non-Gaussian, entanglement-enhanced sensing of multiple incompatible observables.

T1.150 Super-resolution label-free imaging of limited-size objects

Taeyong Chang*, Giorgio Adamo, Nikolay Zheludev (Nanyang Technological University)

12:50pm – 1:05pm

We experimentally achieved $\lambda/8$ label-free far-field super-resolution imaging using prior knowledge of the object size limit, a problem that has remained challenging for more than 60 years. Our breakthrough is based on determining the achievable resolution as a function of photon budget and object size limit through quantum Fisher information analysis, and on the development of an experimental multi-parameter estimation framework that compensates for the optical distortion in the microscope.

T2: Quantum Theory I

Time: Wednesday 28 Oct, 11:30am; Venue: Think Tanks 4&5; Chair: (TBD)
Time allocated for invited talks is 15 min speaking time, plus 5 min Q&A, and time allocated for contributed talks is 12 min speaking time plus 3 minutes Q&A.

T2.118 (INVITED) Falsifying direct causation for quantum correlations

Valerio Scarani* (National University of Singapore)
11:30am – 11:50am

According to Reichenbach's criterion, correlations arise from two basic processes: common cause, or direct causation; and their combination. For the case of correlations obtained by measuring entangled systems, Bell famously excluded any explanation relying solely on a common cause ("local variables"). It is less widely known that one can falsify also a lot of models that supplement local variables with direct causation in the form of some hidden nonlocal influence. The technical result is that any model featuring a communication at finite speed, even superluminal, would be extremely problematic, as it would allow even the users to communicate faster-than-light in some situations [1-5]. This leaves basically Bohmian mechanics and retrocausation, which are unfalsifiable insofar as we know, as mechanisms for "how nature does it" in spacetime (after which, for your interpretation, you should look outside spacetime or in even more radical departures from usual physics). The argument requires more than two parties. Recently, we have also simplified and improved the setup, bringing it closer to a possible experimental test [6]. The foundational narrative could be twisted to make it seem slightly more applied, but I think we have more than our fair share of applications these days.

[1] VS, N. Gisin, Phys. Lett. A 295, 167 (2002) https://arxiv.org/abs/quant-ph/0110074 [2] VS, N. Gisin, Braz. J. Phys. 35, 328 (2005) (Proceedings of DICE 2004) https://arxiv.org/abs/quant-ph/0410025 [3] J.D. Bancal et al., Nature Physics 8, 867 (2012) https://arxiv.org/abs/1110.3795 [4] T. Barnea et al. Phys. Rev. A 88, 022123 (2013) https://arxiv.org/abs/1304.1812 [5] VS et al., Found. Phys. 44, 523-531 (2014) https://arxiv.org/abs/1304.0532 [6] W. Li, M. Hu, D.L. Deng, VS (2026) https://arxiv.org/abs/2608.05271

T2.57 (INVITED) What Does Prediction Mean in a Quantum World?

Graeme Berk*, Jayne Thompson*, Mile Gu* (Nanyang Technological University & National University of Singapore)
11:50am – 12:10pm

Prediction is a foundational task across the quantitative sciences and is precisely understood in the classical world. The universe, however, is fundamentally quantum. What, then, does it mean to 'predict' a future whose proper description is neither a definite outcome nor a probability distribution, but a quantum state, and what resources are required?

The first question turns out to be unexpectedly problematic. Classically, prediction can be understood as per-realisation faithfulness: a model outputs the correct probability distribution of what will happen next, given a past, and it does so in almost every realisation in which that past is observed. Quantum mechanically, this final clause is ill-defined, because given a density matrix, there is no privileged answer to which ensemble of pure states produced it. We are thus compelled to require that the model outputs the correct future quantum state for every pure state in every decomposition consistent with the memory density matrix. However, doing so appears to deprive our quantum notion of per-realisation faithfulness of its operational meaning, because these ensemble decompositions are not distinguishable from one another. We resolve this tension by proving the equivalence of our notion of quantum prediction to the property that the model contains no 'oracular' information pertaining to its own future beyond that already in the past, mirroring a equivalent characterisation of classical predictive models. Unlike per-realisation faithfulness, non-oracularity is equally concrete in the classical and quantum theories.

For the second question, we bound the minimum average memory required to implement a quantum model of a quantum process in terms of the forecasting advantage yielded by knowing the past. We then decompose quantum memory into four operationally distinct contributions. From this, the goal of memory-efficient quantum prediction emerges as a constrained optimisation task over all four of these quantities.

T2.158 Tomographic Limits of the Petz Recovery Map

Peter Sidajaya*, Clive Cenxin Aw, Liu Mingxuan, Valerio Scarani (Centre for Quantum Technologies)
12:10pm – 12:25pm

The Petz recovery map is considered one of the key candidates for the quantum analogue of Bayesian inference and Jeffrey's conditionalization. Since, there seems to be a natural connection between Bayesian inference and the notion of state tomography, it is natural to ask if the Petz recovery can be used for this latter task. In this paper, we discuss such recent results on iterated Petz recovery and relate them to Bayesian approaches to quantum state tomography. We highlight the limitations of direct Petz iteration and show how an extended Petz construction, by lifting the inference problem to a classical distribution over candidate quantum states, recovers the structure of Bayesian and maximum likelihood tomography. This provides perspective on the modifications or nuances required for a Petz approach to quantum retrodiction to perform quantum state tomography.

T2.83 A physical framework for optimal transport of quantum states

Matt Hoogsteder-Riera*, John Calsamiglia Costa, Andreas Winter (Centre for Quantum Technologies, National University of Singapore)
12:25pm – 12:40pm

How costly is it to transform one quantum state into another when physical structure such as energy, locality, or restricted dynamics matters? Conventional measures of quantum-state distinguishability do not directly answer this question. We develop a quantum version of the primal formulation of classical optimal transport by assigning a cost jointly to an initial state and the channel used to transform it. We encode their temporal correlations in a Jordan-product state over time: a Hermitian two-time object with the correct initial and final marginals and the classical joint distribution as its commuting limit. Minimizing a linear cost over all channels that realize a prescribed state transformation gives a semidefinite program. We establish structural properties of the resulting transport cost and show that basis independence, positivity, and zero cost for the identity channel determine a unique cost matrix up to scale. Although weak membership in the general cone of states over time is NP-hard, we construct an outer SDP hierarchy whose dual levels certify cost matrices with nonnegative transport costs. In the unitary-invariant case, we obtain analytical results for pure and commuting states, show that coherence can reduce the cost below the minimum for classical channels, and relate an asymptotic limit to entanglement fidelity.

T2.61 An Irreducible Quantum Advantage in Aligning World Models with Reality

Josep Lumbreras*, Hailan Ma*, Jayne Thompson*, Mile Gu* (Nanyang Technological University)
12:40pm – 12:55pm

World models provide digital simulacra of the true world, allowing agents to be trained and tested before costly real-world deployment. At each time step, they receive an action and generate an observation and reward matching the statistics of the true world. In complex environments where present outcomes depend on events far in the past, this requires memory. One might expect that, by increasing memory, we can always build a model accurately enough to align the optimal agent policies of the real and virtual worlds. We show that this is false for classical world models, even when the true world itself is classical. We construct true worlds for which every finite classical model fails along the same possible trajectory: it either loses the ability to distinguish actions when the true world clearly prefers one, or repeatedly assigns the highest expected reward to suboptimal actions. Its expected-reward estimates also retain a nonvanishing average error. In contrast, each such true world admits a quantum world model using a single qutrit that reproduces it exactly: its reward estimates and preferred actions always match those of the true world, ensuring that the optimal policies of the real and virtual worlds remain perfectly aligned.

T3: Condensed Matter I

Time: Wednesday 28 Oct, 11:30am; Venue: Think Tanks 9&10; Chair: (TBD)
Time allocated for invited talks is 15 min speaking time, plus 5 min Q&A, and time allocated for contributed talks is 12 min speaking time plus 3 minutes Q&A.

T3.186 (INVITED) Ferroelectric Band Twinning from Pair-State Symmetry

Shibo Fang*, Yee Sin Ang* (SUTD)
11:30am – 11:50am

Ferroelectric switching provides a nonvolatile way to control electronic structures, but a general symmetry rule connecting the full Bloch bands of two switchable polarization states is still lacking. Here, we introduce band twinning as a pair-state relation in which two interconvertible states preserve the same lattice while their Bloch bands are mapped onto each other by a non-inversion state-exchange symmetry. Using dichromatic groups, we identify 22 band-twinning point-group classes, including five ferroelectric classes in which the state exchange reverses the polarization. Screening the Ferroelectric Materials Database yields two ferroelectric band-twinning candidates, bulk γ-Ag_3SI and $BaAl_2O_4$, which are validated by first-principles calculations. For γ-Ag_3SI, we further show that the same pair-state symmetry controls the transformation of shift-current tensor components under polarization reversal. These results establish band twinning as a general symmetry framework for switchable electronic structures, with ferroelectric band twinning providing a nonvolatile realization.

T3.29 Current-Free Creation, Annihilation, and Optical Transport of Antiferromagnetic Antiskyrmions

Fan Wang* (Southeast University)
11:50am – 12:05pm

Antiferromagnetic antiskyrmions combine a compensated net magnetic moment, weak stray fields, and an anisotropic topological structure. These properties make them promising information carriers for fast and low-power spintronic devices. However, a unified method for current-free creation, annihilation, and directional transport is still lacking. Here, we propose a magnetoelectric–optical control scheme for antiferromagnetic antiskyrmions in two-dimensional MnI_2. First-principles calculations and atomistic spin-dynamics simulations show that MnI_2 has strong spin-induced polarization, finite Dzyaloshinskii–Moriya interaction, and magnetic parameters close to a topological phase boundary. Electric-field pulses with opposite polarities can write and erase an antiskyrmion. Circularly polarized light couples to the nonuniform spin-induced polarization and generates a finite cycle-averaged magnetoelectric force. This force drives steady antiskyrmion translation. Reversing the laser helicity reverses the motion, while in-plane electric and magnetic bias fields continuously tune the speed and trajectory. We further propose a device concept that integrates electric writing, optical transport, and electrical readout. These results provide a current-free and programmable route for controlling antiferromagnetic topological textures.

T3.27 Chiral anomaly and planar Hall conductance in pseudospin-1 Fermions

Azaz Ahmad* (Indian institute of technology Bombay)
12:05pm – 12:20pm

Positive longitudinal magnetoconductance (LMC) and planar Hall conductance (PHC) are widely regarded as hallmark transport signatures of the chiral anomaly in Weyl semimetals. Recent theoretical advances have generalized the concept of Weyl fermions to multifold Fermionic systems characterized by higher-pseudospin quasiparticle excitations, motivating a systematic investigation of their anomaly-induced transport responses. In this work, we employ semiclassical Boltzmann transport theory within the relaxation-time approximation to study magnetotransport in pseudospin-1 Weyl semimetals, incorporating momentum-dependent scattering, orbital magnetic moment corrections, and charge-conservation constraints. To study PHC, we explicitly break the azimuthal symmetry of the system through two mechanisms: (i) a generic tilt of the quasiparticle dispersion and (ii) a finite misalignment between the electric and magnetic fields. We find that, in the untilted case, the PHC is positive and exhibits a quadratic dependence on the magnetic field strength. Remarkably, increasing the scattering strength drives a sign reversal of the PHC, resulting in a transition from positive to negative values. Furthermore, the PHC displays the

characteristic angular dependence $\sin 2\gamma$, where γ denotes the angle between the applied magnetic field and the x-axis. The introduction of tilt qualitatively modifies this behavior: tilt along the x- and z-directions transforms the angular response into $\sin\gamma$ and $\cos\gamma$ forms, respectively, thereby inducing pronounced anisotropy in the planar Hall signal. In addition, the PHC exhibits a nonmonotonic dependence on the tilt magnitude, highlighting the intricate interplay between tilt-induced symmetry breaking and chiral-anomaly-driven transport in higher-spin Weyl systems. Our results provide experimentally accessible signatures of multifold fermions and establish a theoretical framework for interpreting magnetotransport measurements in candidate materials belonging to space groups 199, 214, and 220.

T3.103 Continuum Landau Modes and non-Hermitian anomaly in a non-Hermitian Weyl semimetal

Shuxin Lin* (Nanyang Technological university)
12:20pm – 12:35pm

A prominent example of 3D topology is the Weyl semimetal, which hosts a gapless topological phase with Fermi arc surface states connecting chiral pairs of topological nodes. The non-Hermitian(NH) Weyl phase displays fundamentally different behavior, such as unpaired chiral channels in the long time limit characterized by a 3D winding number. While the bulk topology of the NH Weyl semimetal is relatively well understood, the complementary surface states have been little studied. In this paper, we discover a rich variety of surface states in the NH Weyl semimetal in both y-PBC (Periodic Boundary Condition) and full-OBCs (Open Boundary Conditions). For y-PBC, the NH Fermi arc surface states with complex dispersion $\pm k_x - ik_y$ transforms into localized modes on only one side of the lattice. The modes are shown to be the recently-discovered Continuum Landau Modes (CLMs), with a Gaussian field profile width that scales inversely with the square root of the magnetic field. Interestingly, the localization of CLMs results in a particle imbalance that matches the field-theoric predictions of the NH anomaly. In full-OBC, skin effect sets in due to non-reciprocal coupling in the y direction. Despite this, our calculations find that under a magnetic field CLMs defy the skin effect. Furthermore, we calculate the transmission spectrum to compare the transport behavior of CLMs versus the NH Fermi arc. Finally, we discuss possible experimental realization of both CLMs and the NH anomaly. One potential realization is via photonic lattices using an imaginary synthetic potential, which is the topic of ongoing research.

T3.189 Spin Splitting Coupled Visible-Light Driven Injection Photocurrent in Bilayer Altermagnets

Huanhuan Yang*, Xiao Jiang*, Yee Sin Ang* (SUTD)
12:35pm – 12:50pm

Altermagnets host symmetry-protected spin splitting without net magnetization, offering a new platform for spin-dependent transport and optical responses. Here we demonstrate that bilayer altermagnets enable efficient and tunable second-order injection photocurrents in the visible regime via interlayer coupling. Using a multiorbital tight-binding model, we show that interlayer coupling lifts the spin degeneracy and enables the normal injection current (NIC), while both the normal and magnetic injection currents (NIC and MIC) evolve in opposite directions as the interlayer hybridization increases. This contrasting behavior reflects distinct microscopic mechanisms: magnetic symmetry governs the emergence of the NIC, whereas the interlayer hybridization strengthens the Berry-curvature-weighted optical transitions and thereby enhances their magnitude. By contrast, the evolution of the MIC is primarily governed by band geometric effects. First-principles calculations for a realistic MnPTe3 bilayer candidate confirm our predictions. Notably, moderate interlayer compression enhances the visible normal injection current by nearly a factor of five. Our results uncover a direct link between altermagnetic spin splitting and nonlinear photocurrent generation and establish interlayer engineering as a general route toward tunable nonlinear optoelectronics.

T4: Quantum Simulation I

Time: Wednesday 28 Oct, 11:30am; Venue: Think Tanks 11&12; Chair: (TBD)
Time allocated for invited talks is 15 min speaking time, plus 5 min Q&A, and time allocated for contributed talks is 12 min speaking time plus 3 minutes Q&A.

T4.159 From Haldane Excitations to the Anderson Tower in a Long-Range Spin-1 Chain

Mohitha Adira*, Pinaki Sengupta, Sibin Yang (SPMS, NTU)
11:30am – 11:45am

Long-range interactions provide a route to spontaneous breaking of continuous symmetries in one-dimensional quantum systems. We study the spin-1 Heisenberg chain with unfrustrated power-law interactions, $J_r \sim -1^{(r-1)} r^{(-\alpha)}$, which undergoes a transition from the symmetry-protected topological Haldane phase to a Néel-ordered phase at $\alpha_C \approx 2.48$. Using quantum Monte Carlo simulations (QMC) combined with stochastic analytic continuation (SAC), we track the dynamical structure factor $S(k, \omega)$ across the interaction range. Our results reveal a progressive reorganization of the characteristic Haldane excitation structure with increasing interaction range, culminating in gapless, highly coherent Goldstone excitations in the Néel phase.

We further examine the low-energy finite-size spectrum within the Néel phase and identify an Anderson tower of states associated with spontaneous SU(2) symmetry breaking. Finite-size scaling of the tower and spin-wave energy scales reveals two regimes within the ordered phase. Deep in the Néel phase, the conventional rotor hierarchy is recovered, with the tower-of-states scale collapsing faster than the spin-wave scale. Closer to the critical point, the tower collapses more slowly while the spin-wave scale collapses more rapidly, bringing the two energy scales closer while they remain asymptotically distinct. Together, these results trace the reorganization of the dynamical excitation spectrum across the Haldane–Néel transition, the emergence of an Anderson tower with long-range order in one dimension, and an unusual evolution of the hierarchy between tower and spin-wave energy scales on approaching quantum criticality.

T4.97 Probing Phase Transitions in Non-Hermitian Systems with Quantum Entanglement

Ling-Feng Zhang, Wing Chi Yu* (City University of Hong Kong)
11:45am – 12:00pm

Quantum information concepts have proven powerful for characterizing quantum phase transitions without prior knowledge of order parameters, yet their applicability to non-Hermitian systems remains an open question. In this work, we investigate quantum phase transitions in the non-Hermitian spin-1/2 XXZ model with a staggered imaginary field and the anisotropic XY model with complex spin-spin couplings, using exact diagonalization and analytical methods, respectively. We examine both self-normal and biorthogonal entanglement measures, including concurrence, negativity, mutual information, and quantum coherence. Most measures successfully detect the first-order and PT transitions in the XXZ model, as well as the Ising and RT transitions in the XY model. The concurrence and negativity also reveal the Berezinskii-Kosterlitz-Thouless (BKT) transition of the XXZ model at weak non-Hermiticity. Notably, we find that Hermitian critical points in the XXZ model evolve into exceptional points as non-Hermiticity increases, with the first-order transition being more robust against non-Hermiticity than the BKT transition.

T4.114 Anyon-Induced Criticality and Dynamical Stability in Non-Hermitian Many-Body Systems

Yi Qin* (NUS)
12:00pm – 12:15pm

We show that anyonic statistics fundamentally reshapes non-Hermitian many-body physics by intrinsically breaking pseudo-Hermiticity, leading to a unique real-complex spectral transition with characteristically dense states in ImE. This anyon-induced transition occurs even when bosonic and pseudofermionic counterparts remain entirely real, revealing a form of non-Hermitian criticality driven purely by exchange statistics. The resulting spectrum features a near-degenerate pair of dominant states with a small splitting in ImE, separated from the rest of the spectrum by a much larger imaginary-energy gap, thereby producing anomalously stable short-time quench dynamics for anyons. Our results show that the occupation-dependent statistical string of anyons, together with the

effective nonlocality of the quasi-one-dimensional system, provides a mechanism for generating unconventional non-Hermitian critical behavior usually associated with strongly nonlocal systems. We further verify the predicted dynamical stabilization on IBM quantum hardware, where encoded-state measurements reproduce the characteristic anyonic quench dynamics.

T4.115 Quantum-enhanced sensing in a driven-dissipative system via chiral waveguide

Yan Xi Foo*, Saubhik Sarkar, Leong Chuan Kwek, Abolfazl Bayat, Davit Aghamalyan (Nanyang Technological University)
12:15pm – 12:30pm

Quantum sensors can achieve precision unattainable by classical sensors. However, dissipation coming from interaction with the environment can greatly degrade the performance of quantum sensors. Therefore, it is crucial to attempt harnessing dissipation to our advantage and investigate the sensing performance of driven-dissipative systems to gain practical quantum advantages. Here, we study a simple system of two-level systems driven coherently at a detuned frequency, and importantly, connected to a chiral waveguide that serves both as an interaction mediator and a bath. We show analytically that the steady state of such a system shows enhanced sensitivity to estimate weak detuning strength while the probe preparation time only grows linearly with system size. Therefore, the enhanced sensitivity is sustained even when the preparation time is incorporated. Underlying this is a mechanism for quantum-enhanced sensing explicitly leveraging open-systems, rather than criticality. We further establish measurement protocols to achieve such sensitivity that are experimentally implementable. The chirality of the waveguide helps us to control both precision and range of enhanced sensitivity and can be used for adaptive sensing.

T4.157 Solving hard optimization problems with quantum-optical analogue spin simulators.

Wouter Verstraelen* (NTU-Majulab-CQT)
12:30pm – 12:45pm

Finding the ground states of frustrated spin models is believed to be an exponentially (NP-) hard problem, even on a quantum computer. On the other hand, it maps to many problems of similar complexity, such as the traveling salesman problem; which would make the ability to solve such models explicitly useful.

It has been recognized that analogue simulation, especially via an optical or polaritonic setup, would be a promising approach to a device that could achieve this task.

In such previously proposed spin simulators, there have typically been a number of problems though, that we have addressed. In previous work[1,2], we have addressed how to keep the amplitude homogeneous (and thus the light-to-spin-mapping sincere) and allow for arbitrary connectivity between Ising spins, but the operation was still very brute force pulsed scheme.

We have now extended this framework beyond mean-field into quantum-optical phase-space methods [3], and show (1) operation in continuous time and (2) highlight a speedup thanks to genuine quantum fluctuations: a longstanding topic of debate on such simulators [4].

[1,2] WV, TCH Liew et al, Phys. Rev. Applied 21, 024057 (2024); Phys. Rev. B 111, 014307 [3] S. Świerczewski, WV et al, arXiv:2507.07684 (2025); ... [4] N. Berloff et al., Nat Mat 16, pages 1120–1126 (2017); Yamamoto et al, npj QI 3:49 (2017) ;Cao et al, arXiv:2511.04223

T4.190 Pure Spin Photocurrent in Altermagnetic Photovoltaic Battery

Qiang Li*, Yee Sin Ang* (Singapore University of Technology and Design)
12:45pm – 1:00pm

Altermagnets, featuring momentum-dependent spin splitting without net magnetization, provide a promising platform for spintronic functionalities beyond conventional ferromagnets and antiferromagnets. Here, we propose an altermagnetic photovoltaic battery composed of a nonmagnetic centrosymmetric semiconductor sandwiched between two altermagnetic electrodes. Using first-principles quantum-transport simulations, we demonstrate that a V_2Te_2O/ZnSe/V_2Te_2O junction with opposite Néel vectors in the two electrodes generates nearly equal and oppositely directed spin-up and spin-down photocurrents, yielding a vanishing charge photocurrent but a finite pure

spin photocurrent. The effect persists under both linearly and circularly polarized light and can be tuned by photon energy and polarization angle. These results demonstrate a viable device concept for light-driven pure spin-current generation based on altermagnetic junctions.

T5: Atoms and Ions

Time: Wednesday 28 Oct, 2:00pm; Venue: Think Tanks 2&3; Chair: (TBD)
Time allocated for invited talks is 15 min speaking time, plus 5 min Q&A, and time allocated for contributed talks is 12 min speaking time plus 3 minutes Q&A.

T5.149 (INVITED) Hahn echo in a qutrit atom interferometer using direct SU(3) gates

Chirantan Mitra*, Lucas Gabardos, Francois Impens, David Guéry-Odelin, David Wilkowski, Chang Chi Kwong* (Nanyang Technological University)
2:00pm – 2:20pm

Scaling qubit-based quantum systems requires effective strategies to suppress errors arising from inhomogeneous interactions with the environment. For qubits, commonly used techniques include the Hahn echo, which employs an intermediate Pauli-X gate to refocus inhomogeneous dephasing, as well as multi-pulse dynamical decoupling sequences. Extending such error-suppression methods to higher-dimensional systems is of key interest, as qudits promise significant advantages for quantum simulation, quantum information processing and quantum sensing. In this work, we extend the Hahn echo concept to a qutrit using direct SU(3) control. The qutrit states are encoded in the ground-state Zeeman manifold of an ultracold strontium gas in free space and are manipulated using direct SU(3) gates. These gates are subsequently used to realize the qutrit Hahn echo, extending the coherence time by more than an order of magnitude. The qutrit Hahn echo sequence also realizes a three-path Mach-Zehnder atom interferometer, whose phase is sensitive to both rotations and two-dimensional forces, providing a promising platform for multidimensional quantum sensing.

T5.116 Proposal for creating spatial superpositions of a large mass in ion traps

Martine Schut*, Jackson Tiong*, Valerio Scarani* (National University of Singapore)
2:20pm – 2:35pm

Engineering coherent spatial superpositions of levitated large masses is an ongoing challenge. Borrowing from recent experimental work and inspired by improvements in cooling, we consider a charged mass of hundreds of nanometers size ("nanoparticle") co-trapped with an ion in a Paul trap, and propose a scheme to manipulate its spatial state through the Coulomb interaction with the ion. We focus on the achievable delocalisation and sketch the other challenges of the protocol: initial cooling, preservation of coherence for long-enough times, and detection. We show that our scheme can coherently displace the nanoparticle by a few nanometers based on parameters borrowed from experimental setups; we give an estimate of the allowed noise and compare it to the state-of-the art noise shielding. Although smaller than the nanoparticle's size, the nanoparticle displacement is much larger than the wavefunction of the trap's ground state. Thus the co-trapping scheme is in principle able to demonstrate the delocalisation of a charged nanoparticle if the required noise isolation can be realised.

T5.102 Coupling strength and motional quantum state exchange between trapped ions

Noah Van Horne* (Florida Atlantic University)
2:35pm – 2:50pm

Interfacing ion qubits in separate traps is among the challenges towards scaling up trapped ion quantum computing. This theoretical study focuses on using a conducting wire to couple the motional quantum states of ions in separate planar traps. This approach of interfacing ion traps provides an alternative to coupling distant qubits with lasers or via ion shuttling. We develop a detailed model for the coupling strength γ, which in turn allows us to calculate the time required to exchange motional quantum states between two ions, t_{ex}. To maximize the coupling strength γ, a rule of thumb is developed to relate the distance d_{eq} between a trapped ion and a nearby pickup disk, to the optimal radius r_{opt} of the disk: $d_{eq}/\sqrt{2} < r_{opt} < d_{eq}$. We include a coefficient ζ which describes three self-capacitances connected in series, relating the capacitances of each part of the coupling system, which corrects an oversight common to several previous works. Our analytical model for the coupling strength is then compared with other existing analytical models in the literature. This requires a standardization of the coupling systems and mapping them to a common set of parameter values. Similarities, differences and limitations of the various models are discussed. Although necessary for a complete description of the exchange of motional states between trapped

ions, models for decoherence and noise in the system are not discussed here. These subjects are treated in their own right in a separate work.

T5.34 Trapped ion chains - Quantum simulation and characterization

Manoj Kumar Joshi* (Singapore University of technology and design q)
2:50pm – 3:05pm

Quantum simulation of many-body physics is one of the key applications of noisy intermediate-scale quantum systems. In such devices, quantum simulation is carried out via the available toolset of a universal quantum computer or via engineered interactions in analog quantum simulators. Trapped-ion chains with available high-fidelity single-qubit gates, along with motional-mode-mediated long-range interactions, allow us to engineer a large set of Hamiltonians to simulate complex many-body physics models. At this conference, I will present some recent experimental demonstrations of many-body quantum physics models with a spin chain realized on a trapped-ion quantum simulator. Furthermore, I will present verification and characterization methods such systems demonstrated with a spin chain of N=51ions.

T6: Quantum Theory II

Time: Wednesday 28 Oct, 2:00pm; Venue: Think Tanks 4&5; Chair: (TBD)
Time allocated for invited talks is 15 min speaking time, plus 5 min Q&A, and time allocated for contributed talks is 12 min speaking time plus 3 minutes Q&A.

T6.128 (INVITED) Towards certifying entanglement in quantum field simulators at finite temperature and out of equilibrium

Taufiq Murtadho*, Stefan Aimet, Marek Gluza, Matteo Fadel, Giuseppe Vitagliano, Jens Eisert, Janet Anders, Jörg Schmiedmayer, Nelly Ng* (Nanyang Technological University)
2:00pm – 2:20pm

Entanglement is a defining feature of quantum mechanics and ubiquitous in quantum field theory, yet directly certifying it in quantum field simulators remains an outstanding challenge. The difficulty is fundamentally operational: experiments access only finite sets of coarse-grained observables. Here we develop an operational framework for detecting and quantifying entanglement in quantum field simulators at finite temperature and out of equilibrium. We formulate finite continuous-variable sectors generated by smeared equal-time field observables and show how different choices of accessible degrees of freedom give rise to real-space, momentum-space, and field-space entanglement. We develop entanglement criteria directly in terms of experimentally accessible second moments, including covariance-matrix, partial-transpose, and variance-based witnesses, and formulate optimised covariance-matrix witnesses as semi-definite programs. This provides a systematic route from reconstructed correlation functions to statistically robust entanglement certification, while making explicit the limitations of finite resolution, finite statistics, and incomplete access to the underlying field. We apply the framework to one-dimensional ultracold Bose gases, where phase correlations can be measured spatially and the covariance matrix of an accessible field sector reconstructed through dynamical tomography. We consider tunnel-coupled thermal states, their evolution after decoupling, and states prepared by coherent splitting, and determine the temperature and mode-access regimes in which entanglement remains experimentally certifiable, including its statistical significance under finite experimental sampling. Our results provide a roadmap for directly observing entanglement in analogue quantum field simulators.

T6.117 (INVITED) Quantum coherence in dissipative systems

Vincenzo Vespri* (università di Firenze)
2:20pm – 2:40pm

The emergence of quantum coherence in dissipative systems raises a fundamental mathematical question: how can ordered, coherent behaviour persist or arise in systems whose macroscopic dynamics are affected by noise, irreversibility and energy exchange with the environment? This talk addresses this question from the viewpoint of nonlinear evolution equations, dissipative mechanisms and asymptotic dynamics. Starting from models inspired by open quantum systems and ultracold atomic platforms, we discuss how classical-looking dissipative structures may encode genuinely quantum features, and how tools from the analysis of PDEs, semigroups, diffusion, memory effects and long-time behaviour can help clarify this transition. Rather than focusing on a specific experimental mechanism, the aim is to identify robust mathematical principles behind the formation, persistence and loss of coherence. The talk is intended as a bridge between mathematical analysis and quantum physics, highlighting how dissipative dynamics can become a natural setting for understanding coherence, transport and irreversibility in emerging quantum technologies.

T6.1 Unifying Quantum Smoothing Theories with Extended Retrodiction

Mingxuan Liu*, Ge Bai, Valerio Scarani (CQT, National University of Singapore)
2:40pm – 2:55pm

Estimating the state of an open quantum system monitored over time requires incorporating information from past measurements (filtering) and, for improved accuracy, also from future measurements (smoothing). While classical smoothing is well understood within a Bayesian framework, its quantum generalization has been challenging, leading to distinct and seemingly incompatible approaches. In this work, we demonstrate that quantum state

smoothing hinges on a uniquely quantum feature: the fundamental dependence of retrodiction on prior correlations. We introduce auxiliary systems into the prior belief to capture correlations formed during preparation and evolution and develop a comprehensive framework for quantum state smoothing based on extended Bayesian retrodiction. This framework identifies all previous approaches as different choices of the extended prior, and naturally extends it to other choices that have not been considered before. We also give an information-theoretic characterization of the choices of prior, in terms of the average entropy of the smoothed states. Our results establish quantum state smoothing as a fundamentally retrodictive process just like classical smoothing, with proper quantum features clearly identified.

T6.145 The Quantum Central Limit Theorem: Rényi Divergences and Generalized Free Energies

Milad Goodarzi*, Salman Beigi, Marco Tomamichel (National University of Singapore)
2:55pm – 3:10pm

Gaussian states underpin much of quantum optics and continuous-variable quantum information. The Cushen–Hudson quantum central limit theorem explains their emergence through the mixing of independent bosonic systems: combining many identical, centered input states through passive linear optics produces a collective output approaching the Gaussian state with the same covariance matrix. When this limiting state is thermal, the approach to Gaussianity also raises a thermodynamic question: when do generalized free energies approach their equilibrium values, and how rapidly?

In this talk, I will present a complete characterization of convergence in sandwiched Rényi divergences for each fixed order. We prove that convergence occurs if and only if the divergence is finite at some finite stage of mixing and the input's quadrature moment-generating function satisfies a strict sub-Gaussian bound determined by the input state and the Rényi order. Under these conditions, we establish an $O(1/n)$ convergence rate, where n is the number of input copies. For a thermal Gaussian limit, this gives the same rate for the decay of excess generalized free energies. These results identify the role of fluctuation tails in the emergence of Gaussian behavior and connect quantitative quantum central limit theory with quantum thermodynamics.

T6.21 Quantum ring all-reduce: communication and privacy advantages for distributed learning

Maria Gragera Garces*, Lirandë Pira* (National University of Singapore)
3:10pm – 3:25pm

Machine learning models have scaled to unprecedented sizes, making training across distributed devices the de facto standard in the field. In this work, we explore how quantum communications can make distributed training both more communication-efficient and information-theoretically private, for both classical and quantum learning models. Ring all-reduce is the foundational communication primitive for large-scale distributed training. We present a quantum version that reduces per-link *online* communication by a provably optimal factor of two (a saving on the synchronisation critical path; total lifetime channel use is unchanged) using pre-shared entanglement and superdense coding, without requiring the learning model or gradient computation to change. Beyond bandwidth, the primitive enables privacy guarantees that are information-theoretically impossible for any classical protocol, achieving composable ε-secure aggregation, via verified entanglement, at a $2\times$ overhead in GHZ copies. Our hybrid quantum-classical communication architecture yields simultaneous communication and security advantages for large scale distributed training, regardless of whether the learning itself is quantum or classical. Finally, we characterise quantum advantages in gradient conflict detection for server-to-client communication under bandwidth constraints, a setting that arises after ring all-reduce is completed, when full gradient broadcast to external clients is infeasible due to bandwidth constraints. Two variants of the problem admit qualitatively different separations. For margin-based alignment testing ($\textsc{GapIP}_\tau$), the quantum advantage is quadratic in the margin parameter: $\widetilde{O}(\tau^{-1}\log P)$ qubits versus $\widetilde{O}(\min(\tau^{-2}, P))$ bits classically. For sign-consistency auditing against a private parameter matching ($\textsc{TieAudit}_\varepsilon$), the advantage represents an exponential separation in communication complexity: classical one-way communication requires $\Omega(\sqrt{P})$ bits whereas $O(\varepsilon^{-2}\log P)$ qubits suffice.

T7: Condensed Matter II

Time: Wednesday 28 Oct, 2:00pm; Venue: Think Tanks 9&10; Chair: (TBD)
Time allocated for invited talks is 15 min speaking time, plus 5 min Q&A, and time allocated for contributed talks is 12 min speaking time plus 3 minutes Q&A.

T7.8 (INVITED) Physical properties and correlated electron behavior of the kagome metal $Cu_3V_2Sb_4$

Mengqin Liu* (Southeast University)
2:00pm – 2:20pm

We report the successful synthesis and comprehensive characterization of the kagome metal Cu_3V_2 Sb_4. This material exhibits a quadratic temperature dependence of resistivity over a broad temperature range, indicative of strong electron-electron interactions, as confirmed by the fact that specific heat measurements with the Kadowaki-Woods ratio lie between those of transition metal and heavy fermion systems.Magnetoresistance measurements reveal a linear magnetic field dependence at low temperatures,while Hall effect measurements display nonlinear behavior describable with a semiclassical two-band model. The angle-dependent magnetoresistance further reveals twofold symmetry. These results collectively suggest an evolution of the band structure within the temperature range of 50–80 K. Magnetic susceptibility measurements indicate paramagnetic behavior with evidence of short-range magnetic correlations emerging near 25 K. Our findings broaden the material landscape of kagome metals and provide a promising platform for exploring correlated electron states and topological quantum phenomena in novel quantum materials.

T7.7 Positive exchange bias in $LaFeO_3/Ni_{81}Fe_{19}$ bilayers

Xiaojing Li* (School of Physics, Southeast University)
2:20pm – 2:35pm

In recent years, the longitudinal spin Seebeck effect and magnonic spin swapping have been observed in canted antiferromagnetic insulator $LaFeO_3$ bulk single crystal [1-3]. In this work, $LaFeO_3$ thin films were grown on $SrTiO_3(110)$ single crystal substrates via off-axis radio-frequency magnetron sputtering. We observed positive exchange bias in $LaFeO_3/Ni_{81}Fe_{19}$ bilayers after field-cooling by measuring the anomalous Nernst effect under vertical temperature gradient and in-plane field. As temperature decreases, exchange bias field increases with a maximum near 150 K and then decreases. The exchange bias field is larger for the thicker $LaFeO_3$. These unusual behaviors indicate special antiferromagnetic configuration of $LaFeO_3$ thin film exchange coupled to $Ni_{81}Fe_{19}$ at low temperatures.

T7.182 Electron-electron interactions and the nonlinear Hall effect

John Tan* (NTU SPMS)
2:35pm – 2:50pm

Nonlinearities have become powerful diagnostics of a material's symmetry and quantum geometry. A prime example is the nonlinear Hall effect that depend intricately on its Berry curvature distribution. These however, have predominantly been explored in primarily non-interacting materials with the nonlinear Hall conductivities depending on single particle band geometry. Here, we discuss the role of electron-electron interactions in driving the nonlinear Hall effect as well as how interactions modify quantum geometry; we compare it with single particle counterparts that include the Berry curvature dipole as well as the Berry connection polarizability induced intrinsic nonlinear Hall effect providing means to understand the role of interactions in shaping the geometry of quantum matter.

T7.47 Microscopic Origin of Loop Currents in the Kagome Hubbard Model

Jun Wei Tan*, Christian Alexander Baum, Ching Hua Lee, Ronny Thomale, Lennart Klebl (National University of Singapore)

2:50pm – 3:05pm

We find loop current order in the Hubbard model on the kagome lattice around Van Hove filling. Loop currents emerge as subsequent instability in a charge bond order phase. The driving force for loop currents are antiferromagnetic spin fluctuations at intermediate temperature/energy scales. As the charge bond order phase is seeded by the same fluctuations, loop currents are generically subleading to charge bond order and absent without translational symmetry breaking. Longer-ranged interactions do not alter the picture significantly. Our results imply that multi-orbital, three dimensional, or strong-coupling physics must be taken into account to make the loop currents the leading instability.

T7.77 Reconciling Mottness and Hundness in Infinite-Layer Nickelate Superconductors: Role of the Interstitial-s Band

Ao Zhang* (Department of Physics, Southeast University, Nanjing, China)

3:05pm – 3:20pm

Infinite-layer nickelates provide a promising platform for unconventional superconductivity, yet their minimal effective model remains debated. Using first-principles density-functional theory combined with dynamical mean-field theory, we systematically compare effective models for $LaNiO_2$, ranging from a single Ni-dx2-y2 band to multi-orbital models including all Ni-3d states and an interstitial-s band. We show that Ni-3d five-band models without the interstitial-s orbital tend to overestimate Hund-metal behavior, producing artificial multi-orbital correlations. In contrast, six-band models including the interstitial-s band recover an orbital-selective Mottness picture, where strong correlations are mainly confined to the Ni-dx2-y2 orbital. After properly accounting for the self-doping effect induced by the interstitial-s band, the single-band Hubbard model and filling-adjusted five-band model reproduce the essential dx2-y2 correlation physics. However, optical conductivity and Drude spectral weight require explicit inclusion of the interstitial-s band. These results clarify the applicability of minimal models for nickelate superconductors and provide guidance for efficient modeling of correlated functional materials.

T7.152 Harnessing Pt/W Multilayers for Efficient Field-Free Spin-Orbit Torque Switching

Bilal Jamshed*, Subhakanta Das, Durgesh Kumar, Hasibur Rahaman, Ramu Maddu, S.N. Piramanayagam* (Nanyang Technological University Singapore)

3:20pm – 3:35pm

Spin-orbit torque (SOT) offers a promising route to achieve energy-efficient magnetisation switching. However, materials with a perpendicular magnetic anisotropy (PMA) require an external magnetic field for deterministic magnetisation switching. Achieving SOT-driven field-free switching of PMA materials is crucial for next-generation spintronic devices. Here, we demonstrate the field-free SOT switching in Co/[Pt/W]n heterostructures using Pt/W multilayers. The competing spins from the Pt and W bilayer generate an out-of-plane SOT field that enables magnetisation switching without the need for an external in-plane magnetic field. These multilayers generate unconventional spin currents, as confirmed by anomalous Hall resistance loop-shift measurements. We observed a maximum field-free switching of 92% in domain wall devices. In addition, the sample with 15 multilayers exhibits a 2.7-fold enhanced damping-like efficiency compared to a single Pt layer. This work advances practical SOT device development and deepens understanding of deterministic perpendicular magnetisation switching.

T8: Quantum Simulation II

Time: Wednesday 28 Oct, 2:00pm; Venue: Think Tanks 11&12; Chair: (TBD)
Time allocated for invited talks is 15 min speaking time, plus 5 min Q&A, and time allocated for contributed talks is 12 min speaking time plus 3 minutes Q&A.

T8.42 (INVITED) Classical Simulation and Design Frontiers for IBM's Doped Clifford Sampling Experiment

Hidetaka Manabe*, Hanfeng Gu, Feng Pan (Singapore University of Technology and Design)
2:00pm – 2:20pm

We classically simulate the IBM doped Clifford random circuit sampling experiment, comprising 70 qubits, 70 entangling layers, and 468 inserted T gates. A deterministic temporal-boundary tensor network contraction approach is specifically designed to tackle such open-boundary one-dimensional brickwork circuits with operator-Schmidt-rank-2 entangling gates. For an n-qubit circuit of depth d, the resulting unsliced path evaluates an exact amplitude with contraction width $\lceil d/2 \rceil$; Ratcatcher calculations certify that no smaller width is possible for the tested instances. Because one-qubit gates are absorbed without changing the network topology, the width and dense scheduled contraction cost are independent of their values and of the number and placement of T gates. For the IBM instance, its largest intermediate tensor contains 2^{35} complex64 entries (256 times smaller than IBM's estimation), corresponding to a tensor payload of 256 GiB, and is distributed across eight GPUs within a node. Using 32 nodes, with eight NVIDIA H100 GPUs per node, we completed all 2051 amplitude batches corresponding to IBM's published output bitstrings in 37.3 minutes. The resulting probabilities yield a log-XEB estimate of 0.35034 with a 95% interval of [0.29763, 0.40305]. Under the Porter–Thomas and scrambled-noise assumptions, this is numerically compatible with IBM's fidelity lower bound; separately, fidelity-weighted resource accounting projects a 583-contraction workload with a 10.6-minute makespan on the same 32 nodes. More broadly, the approach provides a practical diagnostic for experimental outputs and a quantitative tool for designing future doped Clifford sampling experiments.

T8.144 (INVITED) Quantum Metamorphosis: Topology in Multiscale systems

Daniel Leykam* (Singapore University of Technology and Design)
2:20pm – 2:40pm

Many physical systems are governed by the interplay of structures and dynamics that occur across widely different length, time, and energy scales. From moiré quantum materials and ultracold atoms to photonic and networked systems, this multiscale interplay can generate collective phenomena that do not exist at any individual scale. Here we introduce a scale-programmable approach based on hierarchically nested lattices that enables quantum metamorphosis (QuMorph): a continuous transformation between distinct physical regimes controlled by a single dimensionless parameter.

As a concrete example, we demonstrate a system whose spectral and topological properties evolve from those characteristic of the integer quantum Hall effect to those of an anomalous quantum Hall phase. Between these limits lies a rich intermediate "cocoon" regime where multiple scales strongly hybridize, generating dense mini-gap structures and new emergent states. This multiscale mixing gives rise to phenomena with no counterpart in conventional single-scale systems, including hybrid edge-bulk states, scale-dependent topology, topologically embedded flat bands, and isolated edge bands.

We further outline an experimentally feasible implementation using coupled photonic resonator arrays and discuss observable spatial and spectral signatures of quantum metamorphosis. More broadly, our results establish multiscale structure as a new design principle for engineering emergent quantum and wave phenomena, opening opportunities in topological photonics, synthetic quantum matter, and nonlinear dynamics.

T8.140 Towards Quantum Advantage for Validated Simulation of Interacting Many-Body Systems

Roberto Ruiz*, Alejandro Sopena, Thaís de Lima Silva, Renato M. S. Farias, Leandro Aolita (Centre for Quantum Technologies)

2:40pm – 2:55pm

Quantum computing promises access to tasks in many-body systems beyond efficient classical simulation. Validating their outputs remains challenging nonetheless. We analyse the interplay between classical simulatability and validation in the folded XXZ model. This integrable spin-1/2 chain is the strong-coupling limit of the anisotropic Heisenberg model. Its eigenstates are based on shifted Slater determinants and admit efficient preparation by quantum circuits. We identify classes of eigenstates whose entanglement, non-stabiliserness, and fermionic non-Gaussianity grow extensively. Representing these states using matrix-product states, stabiliser formalisms, and fermionic-Gaussian formalism incurs exponentially growing costs. Yet their determinantal wave functions render both sampling in the computational basis and the computation of selected observables classically tractable, providing a foundation for validation. We analyse these eigenstates under a sudden quench at the free-fermionic point of the anisotropic Heisenberg model. The quench is implemented at a fixed circuit depth, independently of its duration. It disrupts the determinantal wave functions underlying classically tractable sampling and generates candidate tasks beyond known efficient classical methods, as supported by our numerical evidence. However, it preserves the classical computability of observables used for validation. We demonstrate eigenstate preparation and the quench protocol on state-of-the-art trapped-ion quantum computers. Measurements of energies, conserved charges, and emptiness-formation probabilities test both the preparation and the subsequent dynamics, while symmetry post-selection mitigates errors. We complement the hardware experiments with a trap-based accreditation protocol on calibrated device emulators, where matched test circuits bound the error in the target probability distribution without requiring classical simulation of the target circuit. Our results establish a platform that combines efficient preparation of eigenstates of interacting spin-1/2 chains, physically motivated dynamics and validation, and concrete sampling tasks for investigating quantum advantage in many-body systems.

T8.94 Compressing Quantum Trajectories on Neural Variational Manifolds

Dingzu Wang*, Dario Poletti* (Singapore University of Technology and Design)

2:55pm – 3:10pm

Neural quantum states (NQS) are a promising tool for dealing with many-body quantum dynamics, as they can allow one to describe states with volume-law entanglement. Given the differentiability of the wave-function stemming from the Schrödinger equation, here we impose a continuous and differentiable parametrization in time of the neural network, by expressing its parameters as the sum of temporal basis functions weighted by (trainable) time-independent coefficients. We show accurate time evolution using simply a restricted Boltzmann machine (RBM) as the instantaneous neural network and demonstrate that this smooth neural quantum state allows us to initialize and evaluate the wave function at times at which it was not trained, both in between the training interval and beyond.

T8.85 Quantum-compatible Riemannian conjugate gradient for ground state preparation

Andres Arcia Lopez*, Marek Gluza*, Cyrus Mostajeran*, Yudai Suzuki* (EPFL)

3:10pm – 3:25pm

Riemannian optimization provides a natural geometric framework for designing quantum algorithms for ground-state preparation, most notably through quantum imaginary-time evolution. However, existing geometry-aware approaches primarily employ steepest-descent updates, leaving more advanced methods from classical Riemannian optimization largely unexplored. In this work, we introduce quantum conjugate gradient descent (QCGD), a quantum-compatible implementation of Riemannian conjugate gradient that combines the steepest descent direction with information retained from previous search directions. Compared with the baseline double-bracket quantum imaginary-time evolution (DB-QITE) algorithm, the proposed approach achieves faster convergence per iteration. This improvement, however, comes at the cost of increased circuit depth for each update step, revealing a trade-off between convergence rate and implementation complexity. Nevertheless, since the circuit depth

for those algorithms grows exponentially with the number of iterations, the proposed method may offer practical advantages, particularly in the early fault-tolerant regime.

T9: Quantum Algorithms I

Time: Wednesday 28 Oct, 4:15pm; Venue: Think Tanks 2&3; Chair: (TBD)
Time allocated for invited talks is 15 min speaking time, plus 5 min Q&A, and time allocated for contributed talks is 12 min speaking time plus 3 minutes Q&A.

T9.111 (INVITED) Quantum-Inspired Algorithms beyond Unitary Circuits: the Laplace Transform

Noufal Jaseem*, Sergi Ramos-Calderer, Gauthameshwar S., Dingzu Wang, Jos'E Ignacio Latorre, Dario Poletti* (SUTD)
4:15pm – 4:35pm

Quantum-inspired algorithms can deliver substantial speedups over classical state-of-the-art methods by executing quantum algorithms with tensor networks on conventional hardware. Unlike circuit models restricted to unitary gates, tensor networks naturally accommodate non-unitary maps. This leads us to introduce a framework whereby one can design better performing algorithms with modular components inheriting a quantum algorithmic structure, yet going beyond unitarity thanks to the explicit use of non-unitary gates. As a concrete example, here we introduce a tensor-network approach to compute the discrete Laplace transform, a non-unitary, aperiodic transform (in contrast to the Fourier transform). We encode a length-N signal on two paired n-qubit registers and decompose the overall map into a non-unitary exponential Damping Transform followed by a Quantum Fourier Transform. We prove that this decomposition admits strong MPO compression to low bond dimension resulting in significant acceleration, even for input data that cannot be compressed efficiently into matrix product states. We demonstrate simulations up to $N = 2^{30}$ input data points, with up to 2^{60} output data points, and quantify how bond dimension controls runtime and accuracy, including precise and efficient inference of pole locations.

T9.95 Symmetric Tight-Frame Quantum Kernels in a Trapped-Ion Optical Qudit

Jia-Yang Gao*, Manas Mukherjee (Centre for Quantum Technologies, National University of Singapore)
4:35pm – 4:50pm

We study tight-frame quantum kernels for learning and investigate how their symmetric measurement geometry translates into performance across different classification tasks. We construct quantum feature representations from the nine-projector qutrit Hesse symmetric informationally complete (SIC) frame and the twelve-projector complete set of mutually unbiased bases (MUB). We benchmark these tight-frame kernels against several classical kernels on a broad set of qutrit learning problems, including independently rotated contextuality datasets, mixed-state contextuality, generalized C_5, C_7, and C_9 witness classification, and discrete-Wigner-negativity classification. Partial-frame studies further reveal how learning performance emerges as additional operator-space directions are resolved and how full-frame tightness recovers the complete qutrit Hilbert–Schmidt geometry. Finally, we implement the SIC and MUB kernel on a trapped 138Ba+ optical qudit and demonstrate proof-of-principle experimental quantum-kernel construction. These results establish symmetric tight-frame measurements as a practical and reusable route to quantum feature engineering in trapped-ion qudits, while emphasizing representation geometry and measurement-resource tradeoffs.

T9.17 Quantum Stochastic Processes with Kirkwood-Dirac Quasiprobabilities: Nonclassicality, Non-Markovianity, Simulation and Quantum Computing Advantage

Kelvin Onggadinata*, Arghya Maity, Zhian Jia, John Kam, Kavan Modi, Teck Seng Koh (Nanyang Technological University)
4:50pm – 5:05pm

Classical stochastic processes — multi-time joint probability distributions over outcomes — are powerful and ubiquitous tools for modelling owing to their ability to capture full statistics and temporal correlations. In this work, we look into an alternative description of a quantum stochastic processes obtained from a multi-time quantum process with measurements at each discrete time using Kirkwood-Dirac (KD) quasiprobabilities, which we refer to as the KD-process. We show that the KD-process can well characterize whether a stochastic process is classical/quantum and Markovian/non-Markovian. In particular, we demonstrate consistency with the classi-

fication of non-coherence-detecting-and-generating (NCGD) and non-discord-generating-and-detecting (NDGD) dynamics as classical processes. Moreover, we show through several examples that the KD-process returns the underlying classical stochastic process, whereas the standard approach characterized as quantum – thus drawing a tighter bound at the classical-quantum boundary. We discuss the classical simulability of the KD-process using a Monte Carlo sampling method, and identify space complexity and sampling complexity as the additional resources for the simulation. We find that sampling complexity grows with the non-classicality of the KD-process, and that Markov processes enable Markov chain sampling, which can significantly reduce the space complexity. Lastly, we demonstrate an application of the KD-process as a tool to examine the probabilistic evolutions of quantum computing. Using Grover's algorithm as a case study, the KD-process reveals a Markovian structure with striking resemblance to the classical unstructured search algorithm, and that sampling complexity grows sub-exponentially with the search size — signifying the hardness of classically simulating quantum computation even when the computational speedup is quadratic.

T9.89 Forecastability of quantum observable dynamics from partial local observations in closed many-body systems

Apimuk Sornsaeng*, Ninnat Dangniam, Supanut Thanasilp, Dario Poletti*, Thiparat Chotibut* (Chulalongkorn University)
5:05pm – 5:20pm

Forecasting quantum observable dynamics from restricted measurements requires inferring future many-body behavior from a finite history of local observables. We investigate the physical sources of forecasting difficulty in closed quantum spin chains by predicting spatially resolved local-magnetization dynamics using autoregressive predictors. We compare a partial-input protocol, in which the history of a single local observable is used to forecast the full vector of local magnetizations, with a many-input protocol in which all local observables are available to the predictor. To characterize the temporal structure of the dynamics, we quantify its finite-window effective dimensionality through the singular-value spectrum of a Hankel representation. We find that forecasting degradation arises through distinct mechanisms. Introducing interactions eventually distributes the observable dynamics over a substantially larger set of significant temporal modes, whereas exchange anisotropy can strongly reduce forecasting precision without a comparable increase in effective temporal dimensionality. Moreover, providing all local observables can substantially improve forecasting in relatively low-dimensional regimes, while offering limited improvement once the observable dynamics becomes high dimensional. The qualitative forecastability hierarchy also remains robust across different initial-state preparations. These results indicate that quantum observable forecastability is jointly determined by the temporal organization of the observable dynamics and by how completely the relevant dynamical information is exposed through the available measurements.

T9.35 Exact Tradeoff Between Quantum Error Correction and Quantum Darwinism: An Information-Theoretic No-Go Theorem

Arghya Maity*, Kelvin Onggadinata, Teck Seng Koh (SPMS, NTU Singapore)
5:20pm – 5:35pm

Quantum error correction (QEC) and Quantum Darwinism describe opposing consequences of system-environment interactions: QEC seeks to preserve logical quantum information, whereas Quantum Darwinism explains the emergence of objective classical information through its proliferation into the environment. Despite their common physical origin, no direct quantitative connection between these paradigms has previously been established. We introduce an exactly solvable block-environment model based on the logical GHZ block of the Shor [[9,1,3]] quantum error-correcting code, collectively coupled to N environment qubits. The logical fidelity, Holevo information, and Darwinistic redundancy are obtained systematically for arbitrary environment size and imperfect recovery efficiency. Eliminating the common decoherence parameter yields an exact tradeoff relating Darwinistic redundancy directly to the post-recovery logical fidelity, demonstrating that the emergence of redundant classical records occurs at the expense of logical quantum information. We further prove a model-independent no-go theorem showing that logical fidelity above a critical threshold precludes the emergence of Darwinistic redundancy, irrespective of the microscopic Hamiltonian or environment structure. The solvable model saturates this general bound, estab-

lishing the first quantitative information-theoretic connection between logical quantum information protection and the emergence of redundant classical records.

T9.15 Quantum Topological Data Encoding

Adam Wesołowski*, Dimitrios Thanos*, Daniel Leykam*, Lirandë Pira* (National University of Singapore)
5:35pm – 5:50pm

Many datasets encountered across a wide range of domains possess rich geometric and topological structure that is difficult to capture using conventional vector-based representations. Quantum machine learning offers the possibility of processing high-dimensional data in Hilbert spaces, but its practical success depends critically on how classical data is encoded into quantum states. We introduce quantum topological data encoding (QTDE), a general framework for encoding topological information into quantum states via topology-driven quantum evolution. Our method generalises an existing topology-driven quantum encoding framework to higher-dimensional data. We test the proposed method on clique-complexes classification tasks, and provide preliminary evidence that topology-driven quantum representations can capture discriminative information beyond that available through direct comparisons of classical topological descriptors. The proposed quantum representations consistently outperform a baseline based on direct comparisons of the combinatorial Laplacians describing the underlying topological structure. We indicate several areas of application where the framework can be used to provide a more efficient and reliable data representation.

T10: 2D materials

Time: Wednesday 28 Oct, 4:15pm; Venue: Think Tanks 4&5; Chair: (TBD)
Time allocated for invited talks is 15 min speaking time, plus 5 min Q&A, and time allocated for contributed talks is 12 min speaking time plus 3 minutes Q&A.

T10.82 (INVITED) Programmable Quantum Electronics

Peng Song* (Nanyang Technological University)
4:15pm – 4:35pm

n condensed matters, ferroelectricity and metallicity are conventionally incompatible, since free carriers screen the internal electric field. As a result, nonvolatile control of metallic device functionalities, including most quantum electronic properties, has been very difficult, although it's not only naturally appealing, but also technologically important. For example, ferroelectrically controlled magnetism represents one of the most energy-efficient magnetization switching schemes and is actively pursued in the spintronic community. In this talk, I will introduce our recent research that breaks this barrier using metallic ferroelectricity in WTe2. Within the material itself, the coupling between ferroelectricity and quantum geometry allows us to achieve nonvolatile electrical switching of nonreciprocal transport (Nat. Commun. 2025) and nonvolatile programmable nonlinear Hall effects (Nat. Commun. 2026). When stacked together with a magnetic layer, the metallic ferroelectricity leads to field-free detection of antiferromagnetic ground states (submitted) and anomalous Hall effect under in-plane magnetic field (submitted), both with robust electrical programmability. Together, these establish metallic ferroelectricity as a general route to programmable quantum electronics.

T10.125 (INVITED) Turning extreme in-plane anisotropy into optical chirality

Davit A. Ghazaryan*, Kostya S. Novoselov (Institute for Functional Intelligent Materials, National University of Singapore, Singapore)
4:35pm – 4:55pm

Chirality is a fundamental property describing entities exhibiting broken mirror symmetry, ranging from quasiparticle states to shapes of galaxies. It defines the selective geometric handedness inherent to (or induced in) natural systems. In light-matter interaction phenomena, optical chirality, quantified by circular dichroism, plays a foundational role with a longstanding goal of local enhancement and light's handedness control. At subwavelength scales, it traditionally relies on extensively multifaceted nanostructuring of planar metasurface arrays built on achiral media1. In a recent work, we showed an alternative, one may say, basic route towards achieving strong optical chirality of light based on mere helical stacking of ¡ lambda/7 scale bilayers of biaxial van der Waals (vdW) crystal possessing extreme in-plane optical anisotropy. Our findings demonstrate that a thin layer of an achiral biaxial van der Waals crystal with extreme in-plane optical anisotropy can do more than confine and direct light without losses at deep subwavelength scales — it can further distinguish between its handedness when twisted into a helical bilayer.

T10.78 (INVITED) A Wafer-Scale Two-Probe Graphene Platform for Ultra-Trace Biomarker Detection

Sergey Tkachev*, Gavin Kok Wai Koon, Glendon Chu Feng Sim, Alexandre Pimenta Lima, Antonio Helio Castro Neto (Institute for Functional Intelligent Materials, National University of Singapore)
4:55pm – 5:15pm

Single-layer graphene is exceptionally sensitive to its local electrostatic environment, since every carbon atom in the lattice is exposed at the surface. This property makes graphene an attractive transducer for detecting minute changes in surface charge arising from molecular recognition events, but translating this sensitivity into a manufacturable device remains a significant challenge. Here we present a wafer-scale approach to fabricating and testing two-probe graphene devices designed for ultra-trace detection of biologically relevant molecules.

Each device consists of a compact chip, a few millimeters on a side, patterned with gold electrodes defining multiple single-layer graphene channels a few hundred micrometers wide. Chemical-vapour-deposited graphene is transferred onto silicon wafers and patterned to produce more than 1,000 individual chips per wafer. A multi-

stage quality-control workflow combining optical microscopy, Raman spectroscopy, surface imaging and electrical characterisation identifies defective devices before functionalisation. Using predefined structural and electrical acceptance criteria, the process achieves an overall device yield of approximately 70-90%. The high uniformity of the graphene channels and their electrical contacts produces consistent device resistance across the wafer, enabling sensing through a simple two-terminal current measurement at zero gate bias.

Functional surface layers, comprising catalytic nanoparticle films and biomolecule-based recognition coatings, are deposited onto the graphene channels using a non-contact, picoliter-scale dispensing technique capable of addressing the micrometer-scale active areas with high spatial precision, something unachievable through conventional liquid-handling methods. Automated, wafer-integrated electrical probing is subsequently used to validate device performance directly on-wafer, without removing individual chips.

The resulting devices respond to target molecules through a simple two-terminal current measurement at fixed bias, without requiring gate modulation or complex electrochemical control. Sensing responses are observed extending from the picomolar into the micromolar concentration range, with fast signal stabilization and good selectivity against common interfering species. This work demonstrates a scalable, semi-automated route toward manufacturable graphene-based sensing platforms and highlights the broader potential of two-dimensional materials for high-throughput device fabrication relevant to future point-of-care and wearable diagnostic technologies.

T10.193 Computational Discovery of Inverted Resistive Switching in Two-Dimensional Materials

Sanchali Mitra*, Arnab Kabiraj, Yee Sin Ang* (Singapore University of Technology and Design (SUTD))
5:15pm – 5:30pm

Resistive switching devices based on two-dimensional (2D) monolayers, termed atomristors, offers a promising platform for highly scaled memory and neuromorphic devices. In conventional atomristors, a native vacancy initially defines a high-resistance state (HRS), while adsorption of a metal atom at the vacancy introduces conducting states and switches the device to a low-resistance state (LRS). Despite growing interest in 2D atomristors, systematic control over switching polarity and the atomic migration underlying these transitions remains largely unexplored. Here, we develop a materials-to-device computational workflow that combines high-throughput density functional theory (DFT), machine-learning molecular dynamics (ML-MD), nudged elastic band (NEB) calculations, and quantum transport simulations to uncover new switching materials and elucidate their atomic switching mechanisms. Screening approximately 2,900 exfoliable monolayers identifies 17 thermally stable candidates for atomristor functionality, including 9 materials exhibiting previously unreported inverted switching. In these materials, vacancy-released electrons delocalize and push the Fermi level into the conduction band, placing the device natively in the LRS. Au adsorption subsequently re-localizes these carriers and returns the Fermi level to the gap, driving LRS-to-HRS switching. Beyond material discovery, our workflow explicitly investigates the kinetics of Au adsorption and desorption between the electrode and vacancy, revealing a strong dependence of the migration barrier on the electrode-2D interlayer distance. At equilibrium separation, spontaneous Au adsorption occurs in several materials, whereas increasing the separation raises the migration barrier and suppresses spontaneous adsorption, providing a route toward voltage-controlled switching. The interlayer distance also modifies the resistance window through metal-induced gap states, linking interface geometry with both atomic kinetics and electronic transport. These findings expand the atomristor materials landscape and establish inverted switching as a distinct design paradigm for multifunctional memory and neuromorphic hardware. The proposed framework can be extended to different metal electrodes and few-layer systems, thus providing a computational design basis for the rapid prediction of switching kinetics and electronic modulation across diverse 2D-metal interfaces.

T10.187 Electric-Field Control of Terahertz Response via Spin-Corner-Layer Coupling in Altermagnetic Bilayers

Jianhua Wang*, Yee Sin Ang* (Singapore University of Technology and Design)
5:30pm – 5:45pm

Electric field control of electron charge and spin degrees of freedom is fundamental to modern semiconductor and spintronic devices. Yet controlling electromagnetic waves with an electric field, particularly in the terahertz

(THz) band, remains a challenge. Here, we propose a spin-corner-layer coupling (SCLC) mechanism in second-order topological altermagnetic bilayers. By using an electric field to influence electrons between different layers, the SCLC mechanism enables simultaneous control over corner and spin degrees of freedom, thereby allowing electric-field tuning of the absorption, emission intensity, and even polarization of THz waves. Taking bilayer $NiZrI_6$ nanodisks as a prototype, we demonstrate that an ultralow electrostatic field can switch both the spin and the layer polarizations of corner states. This dual switching modulates transition dipole moments and oscillator strengths between different corner states, thereby enabling the manipulation of THz waves. This study establishes a mechanism for the electric-field control of spin and THz waves through SCLC, yielding important implications for the advancement of THz spintronics.

T11: Solid State Devices

Time: Wednesday 28 Oct, 4:15pm; Venue: Think Tanks 9&10; Chair: (TBD)
Time allocated for invited talks is 15 min speaking time, plus 5 min Q&A, and time allocated for contributed talks is 12 min speaking time plus 3 minutes Q&A.

T11.75 (INVITED) Probing the Bistable Switching in a Black Phosphorus Tunnel Transistor

Subhajit Jana*, Mikhail Kravtsov, Alexey Ermakov, Xin Zhou, Andrei Kudriashov, Leonid Elesin, Xiangyu Zhou, Artur Shilov, Dmitry Svintsov, Takashi Taniguchi, Kenji Watanabe, Kostya Novoselov, Ahmet Avsar, Alessandro Principi, Denis Bandurin* (National University of Singapore)
4:15pm – 4:35pm

Two-dimensional black phosphorus (BP) is an exceptional platform for engineering quantum transport through electrostatic control, owing to its tunable narrow bandgap and high carrier mobility. Herein, we report the observation of a BP tunnel field-effect transistor (TFET) hosting two mechanistically distinct and coexisting tunnel junctions – one arising from contact doping at the Au/BP interface and another induced electrostatically by dual-gate fields within the channel. Their interplay produces two well-separated negative differential conductance (NDC) transitions and hysteretic bistability in the transfer characteristics, with thresholds independently programmable through gate voltage and bias. Our measurements establish the origin of both transitions and delineate the conditions under which NDC and bistability persist, providing a controlled experimental window into tunneling-driven transport instabilities in a van der Waals semiconductor. The resulting transport landscape is highly nonlinear and fully gate-reconfigurable, positioning BP TFETs as a model system for studying bistable quantum transport.

T11.86 (INVITED) Suppressing Random Native-Oxide Disorder with Ruthenium Capping Enables Uniform Superconducting Resonator Performance

Senthil Kumar Karuppannan*, Naga Manikanta Kommanaboina, Hui Hui Kim, Nelson Lim Chee Beng, Febiana Tjiptoharsono (NQFF, Institute of Materials Research and Engineering, Technology and Research, A*STAR)
4:35pm – 4:55pm

Superconducting thin films are a promising platform for quantum devices and are compatible with established microfabrication processes. However, scaling superconducting devices remains challenging because fabrication-induced surface defects and native surface oxides strongly affect devices' internal quality factors.1–4 These defects create intrinsic losses in the film, which are two-level system losses, leading to variations within the chip and across different wafers. Therefore, suppressing surface oxide defects is essential for improving device uniformity by minimizing intrinsic loss and improving reproducibility. We investigate a 5 nm thick ruthenium (Ru) capping layer as a self-limiting oxide barrier for tantalum superconducting thin films. We characterized the films' structural and morphological properties using atomic force microscopy, X-ray diffraction, and transmission electron microscopy. Microwave measurements show that the Ru capping layer significantly reduces variations in the internal quality factor across individual chips and between fabrication batches. This indicates that minimizing random surface oxide-induced loss improves film uniformity and reduces quality-factor variation. These results demonstrate that Ru is an effective self-limiting oxide capping material for enhancing the stability, uniformity, and reproducibility of superconducting thin films, making it a promising approach for scalable superconducting quantum technologies.

T11.126 Engineering NbN Thin Films for Coupling with Perpendicular Magnetic Multilayers

Mukhammad Ali Obidov*, Gunasheel Kautilyaa Krishnaswami*, Anjan Soumyanarayanan* (National University of Singapore)
4:55pm – 5:10pm

Niobium nitride (NbN) is a widely used superconductor for single-photon detectors, superconducting qubits, and microwave resonators. Its high critical temperature (Tc) and upper critical field make it more robust than conventional superconductors (e.g., Al, Nb), while ensuring foundry-compatible growth processes. Coupling NbN with a magnetic multilayer could add magnetic tunability to these established platforms. However, growing high-quality NbN with an interface suited to a perpendicular anisotropy (PMA) multilayer is nontrivial. Its Tc is highly sensi-

tive to nitrogen stoichiometry, crystallinity, and interface roughness. Here, we optimize NbN growth by reactive sputtering and engineer its interface for a PMA multilayer. Notably, films grown on Si/SiO_2 reach a Tc of 14.1 K without epitaxial growth. Seed layers such as MgO and TaN/W further improve Tc, RRR, and roughness on thin NbN films. Finally, a metallic buffer layer enables a chiral [Ir/Fe/Co/Pt] multilayer on NbN with high PMA and controllable magnetic properties. Together, these results establish a scalable route to couple NbN's high-Tc, high-field superconductivity with PMA magnetism. This platform builds on NbN's established role in photon detection, qubits, and resonators. It opens a path toward magnetically tunable superconducting devices.

T11.177 (INVITED) Toward Spin-Texture–Vortex Coupling: Chiral Magnetism on Wafer-Scale Superconducting Platforms

Gunasheel Kauwtilyaa Krishnaswamy* (National University of Singapore)
5:10pm – 5:30pm

Interfacial coupling between chiral ferromagnets (FM) and superconductors (SC) can host novel physics, including spin-triplet superconductivity [1]. Moreover, vortex-spin-texture pairs are predicted to host Majorana bound states, offering a route to non-Abelian braiding for topological quantum computing [2]. Realizing such pairs requires balancing superconducting length scales, proximitized superconductivity, and controllable chiral magnetism. Preliminary demonstrations have relied on insulating or thick metallic buffers, or amorphous SCs, to sustain interfacial chiral coupling [3-5]. Growing ultrathin chiral FMs directly on textured SCs such as Nb, as required for practical devices, is comparatively difficult, as magnetic properties degrade sharply [4]. This is compounded by a strong exchange interaction and large FM thickness, both of which suppress Cooper-pair coherence in proximitized FMs [1]. High-quality perpendicular FM-SC junctions require ultrathin chiral FMs that host controllable spin textures while remaining compatible with proximity coupling. Here, we design spin-texture-hosting [Ir/Fe/Co/Pt] multilayers on textured superconducting Nb and NbN. Using magnetometry and GHz spectroscopy, we identify the origin of this degradation [6]. Strain transfer from the crystalline SC underlayer weakens the interfacial DMI, reduces magnetic anisotropy, and introduces magnetic inhomogeneity in the chiral layer. Interlayer engineering relieves this strain and recovers these properties toward their unstrained reference values, meeting the proximity-compatibility requirement for high-quality FM-SC junctions. Building on this platform, we realize ferromagnetic Josephson junctions that host spin textures within the Cooper-pair proximity regime. Crucially, these junctions are realized on a 200 mm wafer-scale platform compatible with CMOS foundry processes. This establishes a scalable route to study unconventional superconductivity and opens a path toward wafer-scale, topological quantum technology platforms. [1] Linder, J., Robinson, J., Nature Phys 11, 307-315 (2015). [2] G. Yang, et al., Physical Review B 93, 224505 (2016) [3] X. Palermo, et al., Physical Review Applied 13, 014043 (2020) [4] A.P. Petrovic, et al., Physical Review Letters 126, 117205 (2021) [5] Y-J. Xie et al., Physical Review Letters 133, 166706 (2024) [6] G.K.Krishnaswamy et al., In Preparation (2026)

T11.188 2D Janus Niobium Oxydihalide NbOXY : Multifunctional Piezoelectric Semiconductor for Electronics, Photonics, Sensing and Sustainable Energy Applications

Su Tong*, Yee Sin Ang* (SUTD)
5:30pm – 5:45pm

Two-dimensional (2D) niobium oxydihalide NbOI2 has recently been demonstrated as an excellent in-plane piezoelectric and nonlinear optical material. Here, we show that Janus niobium oxydihalide, NbOXY (X, Y = Cl, Br, I and $X \neq Y$), is a family of multifunctional anisotropic semiconductors with exceptional piezoelectric, electronic, photocatalytic, and optical properties. NbOXY monolayers are stable and flexible, with band gaps around the visible-light regime of $\approx$1.9 eV. The carrier mobility of NbOXY exhibits an exceptionally strong anisotropy ratio of 400, which is larger than that of most anisotropic 2D semiconductors. The exceptionally large deformation potential of NbOXY monolayers leads to a strong piezoresistive effect, making them useful for strain-sensing applications. Inversion symmetry breaking in Janus NbOXY generates a sizable out-of-plane d31 piezoelectric response while retaining strong in-plane piezoelectricity. Remarkably, NbOXY exhibits an additional out-of-plane piezoelectric response, d32, as large as 0.55 pm/V. G0W0-BSE calculations further reveal strong linear optical dichroism of NbOXY in the visible-to-ultraviolet regime. The optical absorption peaks of 14-18% in the deep-UV

regime (5-6 eV) outperform those of the vast majority of other 2D materials. The high carrier mobility, strong optical absorption, sizable built-in electric field, and band alignment compatible with overall water splitting further suggest the potential of NbOXY for solar-to-hydrogen conversion. We further propose a directional stress-sensing device to demonstrate how the out-of-plane piezoelectricity can be harnessed for functional device applications. Our findings unveil NbOXY as an exceptional multifunctional 2D semiconductor for flexible electronics, optoelectronics, UV photonics, piezoelectronics, and sustainable energy applications.

T12: Metamaterials and Photonics

Time: Wednesday 28 Oct, 4:15pm; Venue: Think Tanks 11&12; Chair: (TBD)
Time allocated for invited talks is 15 min speaking time, plus 5 min Q&A, and time allocated for contributed talks is 12 min speaking time plus 3 minutes Q&A.

T12.70 (INVITED) A Photonic Tautochrone: Spatiotemporal Beam Focusing for Enhanced Nonlinear Response

Kevin Dini* (Nanyang Technological University)
4:15pm – 4:35pm

We propose to implement an optical analogue of the tautochrone property, which enables isochronous oscillations in mechanical systems, to allow the focusing both in space and in time of ultrashort pulses inside photonic systems. This allows to enhance nonlinear effects, resulting in orders of magnitude increase of nonlinearity-induced phase shifts, while employing low irradiances. Building upon the optical-mechanical analogy, we show that our photonic tautochrone operates as an optical limiter for temporal light pulses, implements temporal bistability and even multistability with large numbers of states, going beyond current bistable optical systems. Finally, we extend this concept to the quantum domain and predict a tautochrone quantum blockade regime exhibiting stronger antibunching.

T12.76 Coexistence of polariton bound states in the continuum and 2D radiative excitons

Simone Zanotti*, Marco Liscidini, Dario Gerace, Lucio C. Andreani (Nanyang Technological University)
4:35pm – 4:50pm

Bound states in the continuum (BICs) enable optical modes with ideally infinite radiative lifetimes despite lying within the radiation continuum. Radiation-matter interaction in periodically patterned planar waveguides embedding two-dimensional (2D) optically active excitations can be described quantum mechanically by diagonalizing a non-Hermitian operator, known as the Hopfield matrix, which can be generalized to incorporate independent photonic and excitonic losses into the polaritonic states. However, since 2D excitons undergo intrinsic wavevector-dependent radiative decay within the light cone, whether the Hopfield formalism can consistently account for this process while preserving polariton BICs has remained an open question. Here we show that a non-Hermitian Hopfield formalism incorporating excitonic radiative losses correctly captures the existence of genuine k=0 polariton BICs with diverging radiative lifetimes. The theory provides a unified microscopic framework for radiative excitons and polariton BICs, and an efficient predictive tool for designing photonic-crystal platforms coupled to quantum wells, transition-metal dichalcogenides, and other 2D excitonic materials.

T12.153 Reconfigurable halide perovskites polaritonic integrated circuits

Andrea Zacheo*, Marco Marangi, Tim Collin Meiller, Filippo Martinelli, Cesare Soci (Nanyang Technological University)
4:50pm – 5:05pm

Integrated photonic technologies require active materials capable of providing large optical modulation within compact footprints while also sustaining long-distance propagation. Exciton-polaritons offer a promising route towards meeting these requirements through their strong light-matter interactions and enhanced optical nonlinearities, yet integrated polariton circuits remain challenging to realize because long-range propagation and strong, locally controlled optical modulation are difficult to achieve simultaneously. Here, we demonstrate actively reconfigurable polariton circuits in polycrystalline halide perovskites by integrating polariton waveguides with electrical microheaters. Local electrothermal actuation drives a structural phase transition in the perovskite crystal lattice, accompanied by an excitonic spectral shift of approximately 60 meV that enables active control of polariton propagation. Over a modulation length of only $10\,\mu$m, the device can operate either as a π phase shifter or as an intensity switch, depending on the excitonic fraction of the propagating mode. Our work establishes on-demand excitonic reconfiguration as a route towards compact and multifunctional polariton circuitry in polycrystalline halide perovskites, and opens a pathway towards the heterogeneous integration of active polaritonic modulators with established photonic platforms.

T12.67 Axionic Surface Waves

Manjima Sudheer*, Jianwei Liu*, Hau Tian Teo*, Baile Zhang* (Nanyang Technological University, Singapore)
5:05pm – 5:20pm

Axion electrodynamics describes electromagnetic responses arising from the coupling between axion field and electromagnetic fields. At an interface where the axion field changes, such as the boundary of an axion insulator or a Tellegen medium, this coupling induces surface charges and Hall-like surface currents, conventionally viewed as local responses to externally applied static fields. Understanding whether these boundary responses can themselves form propagating excitations offers a new perspective on axion electrodynamics. Here, we show that a dielectric-axion interface supports an electromagnetic surface wave that self-consistently drives and transports these boundary responses. The resulting axionic surface wave carries a propagating charge-current texture, comprising a longitudinal surface-charge wave and a rotating in-plane surface current, even for a time-independent axion field. Remarkably, this dynamical texture is accompanied by a dual-transverse-spin structure, combining the familiar in-plane transverse spin with an intrinsic out-of-plane component arising from the magnetoelectric coupling. Our results establish axionic surface waves as a route to dynamical axion boundary electrodynamics and identify intrinsic dual-transverse spin as an electromagnetic signature of the coupled boundary response.

T12.68 Transition from Continuous to Discrete Time Crystal in Nano-opto-mechanical Metamaterials

Peter Paul*, Jinxiang Li*, Eric Plum*, Giorgio Adamo* (University of Southampton)
5:20pm – 5:35pm

Time crystals are a nonequilibrium many-body phase of matter characterised by spontaneous time-translation symmetry breaking. While classical continuous time crystals have been demonstrated in nano-opto-mechanical metamaterials, their discrete counterpart remain comparatively less explored. Studying continuous and discrete time-crystals, and the transitions between the two states, on technologically relevant platforms like micro and nano electro/opto-mechanical systems (MEMS and NEMS), is important for applications in precision sensing, timing, and information processing. Here, by using nano-opto-mechanical metamaterials consisting of silicon nitride nanowire arrays decorated with plasmonic resonators, we experimentally observe the appearance of a continuous time-crystal (CTC) response from a thermal state, and investigate both numerically and experimentally the transition to a discrete time-crystal (DTC) state. Under continuous-wave laser illumination, the nanowires oscillations transition from incoherent thermo-mechanical motion to a collective state characterized by large oscillation amplitude, common frequency, and phase spontaneously selected over the $0-2\pi)$ range. Although individual nanowires possess slightly different natural frequencies due to imperfect fabrication, light-induced non-reciprocal coupling drives them into a synchronized state exhibiting coherent many-body dynamics. The metamaterial enters a nonlinear regime that self-limits the nanowires oscillations to amplitudes comparable to their thickness. Upon introducing a periodic drive near twice the intrinsic oscillation frequency, the system undergoes subharmonic locking and develops two symmetry-related states, with phases separated by π, characteristic of discrete time-crystalline order. By modelling the nanowire metamaterial as pairs of non-reciprocally coupled nonlinear Langevin oscillators, we accurately describe the DTC-CTC transition when the drive is changed from continuous to periodic.

T12.104 Beyond the Dicke limit: Superradiant J-exciton-polaritons in BIC metasurfaces

Marco Marangi*, Alexander M. Dubrovkin, Anton N. Vetlugin, Giorgio Adamo, Cesare Soci (Nanyang Technological University)
5:35pm – 5:50pm

Highly correlated photon sources can be realized through cooperative coupling among quantum emitters, giving rise to superradiant collective emission. In solid-state ensembles, however, such collective behaviour is confined to subwavelength scales and is strongly suppressed at room temperature by inhomogeneous broadening and rapid dephasing, limiting practical implementations. Here, we use dielectric metasurfaces supporting a bound-state-in-the-continuum resonance to mediate interactions between spatially separated J-aggregates. Spatial coherence measurements reveal a complex emission topology whose amplitude and phase distributions evolve strongly with excitation fluence. Analysis of the domain number and size shows that initially separate inter-aggregate domains

coalesce into fewer, larger locally synchronized regions, accompanied by fluence-dependent photon superbunching reaching $g^{(2)}(0) = 3.77$. These results establish dielectric metasurfaces as a platform for extending superradiant cooperativity from subwavelength to micrometre scales through common-mode coupling.

T13: Topologigal States

Time: Thursday 29 Oct, 11:15am; Venue: Think Tanks 2&3; Chair: (TBD)
Time allocated for invited talks is 15 min speaking time, plus 5 min Q&A, and time allocated for contributed talks is 12 min speaking time plus 3 minutes Q&A.

T13.127 (INVITED) Meta-photonic topologies: from concept to applications

Yijie Shen* (NTU)
11:15am – 11:35am

Abstract: Topological complex electromagnetic waves give access to nontrivial light-matter interactions and provide additional degrees of freedom for information transfer. For instance, topologically stable quasiparticles or skyrmions have been demonstrated in quantum fields, solid-state physics, and magnetic materials, but only recently observed in photonic fields, triggering fast expanding research across different spectral ranges and applications. Here I introduce an extended family of photonic skyrmions within a unified framework, starting from fundamental theories to experimental generation and topological control in spatiotemporally structured light. I will further highlight generalized classes of structured wave topological quasiparticles beyond optical skyrmions and outline their exotic topological robust properties, emerging applications of topologically protected information networks and light-matter interactions.

Refs: Nature 638, 394-400 (2025); Adv. Opt. Photonics 17(2) 295-374 (2025); Optics & Photonics News 36, 26-33 (2025); Nat. Photonics 18, 15-25 (2024); Nat. Electron. 9, 479–488 (2026).

T13.69 (INVITED) Braiding Lasers on a Chip

Bofeng Zhu* (Nanyang Technological University, CDPT)
11:35am – 11:55am

Topology is revolutionizing our understanding of physics, revealing intriguing phenomena by governing how systems evolve under continuous manipulation. Non-Hermitian physics, where energy dissipation and gain reshape wave dynamics, introduces unique topological properties: eigenvalues can braid around exceptional points, forming nontrivial links and knots in complex energy surfaces. However, such topologies have remained elusive to direct visualization. Here, we demonstrate non-Hermitian braiding of laser modes on a photonic chip. By controlling their trajectories in parameter space, we directly visualize the resulting braiding through the evolution of laser quantities, showing rich topological structures like Hopf links, trefoil knots, and Solomon links. Our chip-based platform offers scalable and programmable control over non-Hermitian dynamics, enabling robust light manipulation, reconfigurable lasing behavior, and a versatile testbed for exploring topological photonics.

Related papers: (1) Nat. Phys. 22, 1344 (2026). (2) Phys. Rev. B 110, 134317 (2024).

T13.79 Optical skyrmions: from classical to quantum

Zhenyu Guo*, Nilo Mata-Cervera, Yijie Shen* (NTU)
11:55am – 12:10pm

Optical skyrmions are topologically nontrivial structures formed by continuous mappings from real space to an optical state space. The rich degrees of freedom of structured light enable their controlled generation, propagation, transformation, and light–matter interactions. More recently, optical skyrmions have been extended into the quantum regime, where topological textures can be encoded either in multiple degrees of freedom of a single photon or in the nonlocal correlations between entangled photons. This talk will review the fundamental principles and recent developments of optical skyrmions, from their construction in classical light to quantum skyrmions in single-photon and biphoton systems, with particular emphasis on the interplay among topology, entanglement, and robustness against optical perturbations.

T13.6 Beyond predicting existence: Unified winding numbers for topological edge states in non-Hermitian quadripartite lattices

Yating Wei* (Southeast University)
12:10pm – 12:25pm

Non-Hermitian topological systems have drawn great interest in condensed matter physics and optics. The non-Hermitian skin effect has overturned the conventional bulk-boundary correspondence. While abundant phenomena and topological theories have been developed, interactions between topological edge states and the skin effect remain underexplored. Based on a one-dimensional extended non-Hermitian SSH4 model, we systematically investigate the interplay between topological edge states and the skin effect. The skin effect strongly modulates the localization of edge states and may reverse their localization direction. In certain parameter ranges, edge states can also decouple from the skin effect and persist inside the band gap. These findings advance the topological theory of the SSH model and support experimental implementations in circuits and acoustics. We also provide new routes to designing robust devices for energy storage and conversion, such as directional energy harvesters, non-reciprocal amplifiers and anti-noise sensors.

T13.25 Engineering and controlling exceptional point topologies in nanophotonic systems

Kaiyuan Wang, Matthew Foreman* (Nanyang Technological University)
12:25pm – 12:40pm

Exceptional points are non-Hermitian spectral and scattering singularities where complex eigenvalues and their corresponding eigenstates coalesce. These singular parameter points give rise to exotic physical phenomena, enabling enhanced optical sensing, chiral light-matter interactions, and non-reciprocal wave manipulation. Achieving precise control over higher-order exceptional points and tailoring the topology of the associated Riemann surfaces in physical systems remains challenging due to intricate multi-parameter tuning requirements and environmental noise sensitivity.

In this talk, we discuss strategies for engineering and controlling exceptional point topologies across a range of micro and nanophotonic platforms, including plasmonic nanoparticles and multi-port passive networks. We demonstrate how physical parameters can be mapped directly to complex mathematical singularities, providing clear design rules for higher-order degeneracies without relying on strict parity-time symmetries. We also explore phase-only control mechanisms and boundary projections that induce effective non-Hermiticity, allowing programmatic reshaping of Riemann sheet topologies. These approaches facilitate the realisation of anisotropic exceptional points, linear eigenvalue splitting along designated parametric directions, and noise-robust sensing configurations that suppress systemic drift while preserving high signal sensitivity. Our findings provide practical guidelines for controlling non-Hermitian phenomena across nanophotonic, plasmonic, and integrated optical systems.

T13.74 On-chip terahertz isolator based on topological photonic integrated circuits

Ridong Jia* (National University of Singapore)
12:40pm – 12:55pm

Chip-scale non-reciprocity is essential for advancing integrated photonics, particularly in realizing photonic circulators and isolators for data communication, signal modulation, and quantum computing. However, achieving a non-reciprocal silicon chip with a small footprint, high isolation ratio, low loss, and active control remains a challenge. We present a terahertz on-chip isolator based on topological photonic integrated circuits that provides a promising solution. Experimentally, we have achieved a maximum isolation ratio of 64.3,dB and a low chip loss of 2.6,dB by fine-tuning the non-reciprocal critical coupling points of a topological cavity with a small footprint of $6.4 \times 2.5\lambda^2$. An all-optical method is also applied to actively modulate the isolation ratio from 0 to 48,dB. The development of a non-reciprocal topological silicon chip marks a pivotal advancements, especially for terahertz communication technologies.

T14: Nano-Optics

Time: Thursday 29 Oct, 11:15am; Venue: Think Tanks 4&5; Chair: (TBD)
Time allocated for invited talks is 15 min speaking time, plus 5 min Q&A, and time allocated for contributed talks is 12 min speaking time plus 3 minutes Q&A.

T14.142 (INVITED) Nanoscale Light Confinement and Scattering: From Classical to Quantum On-Chip Meta-Devices

Zhaogang Dong* (Singapore University of Technology and Design & Q.InC, A*STAR)
11:15am – 11:35am

Controlling light confinement and scattering at the nanoscale provides a powerful route to a new generation of functional on-chip meta-devices spanning classical and quantum photonics. By engineering optical resonances in metallic and dielectric nanostructures, key degrees of freedom of light, including spectrum, polarization, phase, and momentum, can be precisely controlled within compact integrated platforms. In this talk, we will present cavity-enhanced meta-structures that exploit local density of optical states (LDOS) engineering, high-Q/V resonances, and multipolar hybridization to bridge classical light manipulation with emerging quantum functionalities. On the source side, we demonstrate tunable nanoscale emitters, linearly polarized single-photon sources, and chiral bilayer metasurfaces enabling spin-selective emission. On the detection side, resonant optical confinement is employed to realize wavelength-selective photodetector pixels, near-infrared silicon photodetectors based on disordered nanophotonic structures integrated with upconversion nanoparticles, and ultrabroadband Sb_2Te_3 thermoelectric detectors spanning the visible to mid-infrared. Together, these advances establish a scalable pathway toward integrated meta-sources and meta-detectors, illustrating how nanoscale control of light can advance on-chip photonic systems from classical optical functionality toward quantum-enabled operation.

T14.92 Resolution and Robustness Bounds for Reconstructive Spectrometers

Changyan Zhu* (Nanyang Technological University)
11:35am – 11:50am

Reconstructive spectrometers are a promising emerging class of devices that combine complex light scattering with inference to enable compact, high-resolution spectrometry. Thus far, the physical determinants of these devices' performance remain under-explored. We show that under a broad range of conditions, the noise-induced error for spectral reconstruction is governed by the Fisher information. We then use random matrix theory to derive a closed-form relation linking the variance bound to a set of key physical parameters: the spectral correlation length, the mean transmittance, and the number of frequency and measurement channels. The analysis reveals certain fundamental trade-offs between these physical parameters, and establishes the conditions for a spectrometer to achieve "super-resolution" below the limit set by the spectral correlation length. Our theory is confirmed using numerical validations with a random matrix model as well as full-wave simulations. These results establish a physically-grounded framework for designing and analyzing performant and noise-robust reconstructive spectrometers.

T14.22 Millisecond optical coherence and strong collective coupling in an integrated telecom rare-earth photonic platform

Kah Jen Wo*, Pavel A. Dmitriev, Karthik Dasigi, Fumiya Hanamura, Steven Touzard (CQT, NUS)
11:50am – 12:05pm

Long-range quantum network nodes require the combination of strong light-matter coupling, long coherence times and in situ spectral control at telecom wavelengths. The coherence of erbium in integrated devices is held back by its hosts, which do not simultaneously provide the weakly magnetic nuclear-spin environment and the well-defined substitutional sites found in coherence-optimised bulk crystals. Here we bring such an optimised crystal onto a photonic chip, by bonding an Er^{3+}:$CaWO_4$ host without an adhesive interlayer to a high-Q electro-optically tuneable thin-film lithium niobate microring resonator. At an effective temperature of 75mK and a field of only 0.2T, the bonded ensemble retains an effective homogeneous linewidth of 289±34Hz (T_M=1.10±0.13ms), with spectral diffusion proceeding at 86±18Hz and saturating at 1.5±0.2kHz. Electro-optically tuning the resonator through the erbium optical transition resolves an avoided crossing with a collective cooperativity of C=6.7±0.4. Exploiting

superhyperfine coupling to the host's 183W nuclear spins, we store and retrieve optical phase information over 5s with a visibility of 0.935±0.015. Strong collective coupling, millisecond coherence and in situ spectral tuning in a single device thus establish heterogeneous integration leveraging coherence-optimised hosts as a route to scalable telecom quantum networks.

T14.184 Progress on a Reconfigurable Cesium Optical Tweezer Array Platform

Jinyu Zhou*, Nandan Patel, Tong-Yan Xia, Boon Long Ng, David Wilkowski* (Centre for Quantum Technologies)

12:05pm – 12:20pm

Neutral atoms in optical tweezers are a leading platform for scalable quantum computing, offering long coherence times, high-fidelity Rydberg gates, and reconfigurable connectivity. We report progress on a cesium-133 atom-array quantum processor. Single atoms are loaded into a static 1064 nm tweezer array generated by a spatial light modulator and imaged site-resolved at 852 nm. A mobile array driven by crossed acousto-optic deflectors transports atoms between sites and rearrange stochastically loaded atoms into defect-free configurations.We discuss trap uniformity, single-atom survival under imaging and transport, and the path towards an operational quantum processor.

T14.53 A Family of Concentric, Circular Reflection Patterns in Nested Herriott cells for Free-Space Delay Line

Arya Chowdhury*, Emilien Lavie*, Pranay Tiwari*, Yu Guo*, Anindya Banerji*, Alexander Ling* (Centre for Quantum Technologies, National University of Singapore)
12:20pm – 12:35pm

Multipass cells enable long, stable optical path lengths (OPLs) in compact free-space systems. This makes them well-suited to laser spectroscopy and delay-line based optical memory, where storage time scales directly with OPL. The standard multipass cell, the Herriott cell, comprises two coaxial spherical mirrors. The beam traverses the cell, forming an elliptical reflection pattern on the mirror surfaces and fulfilling the re-entrant condition as it exits through the entry pupil. A family of re-entrant solutions exists for Herriott cells, spanning a wide range of achievable reflection numbers for a fixed mirror radius of curvature. However, the Herriott cell's OPL is limited by the single elliptical reflection path, leaving most of the mirror surface unused.

Nested Herriott cells embed a smaller spherical mirror within a larger one, rotating the singular elliptical beam path on each inner mirror reflection. This produces longer OPL within the same cell volume through concentric, circular reflection patterns that better utilise the mirror surface. A family of solutions to these concentric, circular patterns, similar to those in Herriott cells, will provide a broad set of achievable OPLs for a fixed mirror geometry. Existing methods yield only a single re-entrant solution for a given mirror curvature and ring count, and a full experimental sweep of the parameter space is impractical.

This work identifies a family of concentric, circular reflection patterns for given mirror radii of curvature by exploiting the spatial and rotational geometry of the reflection spots. For a given mirror design, this model identifies 179 practically feasible concentric solutions across 2-, 3-, and 4-ringed configurations. Three of these solutions were experimentally realised, yielding stable reflection patterns with OPLs of 208 m, 195 m, and 78 m, respectively. This family of solutions maps the relationships between reflection number, ring count, mirror separation, and OPL, providing a design framework for optimising nested Herriott cells for compact delay lines with long OPL.

T14.5 Optical Asymmetric Transmission in Dielectric Nanopillar Structures

Shuai Gao* (Southeast University)
12:35pm – 12:50pm

Optical asymmetric transmission holds significant importance for optical applications. Periodic dielectric gratings are attractive for asymmetric transmission owing to their fabrication simplicity. In this work, we study the asymmetric transmission properties of a periodic all-dielectric grating structure fabricated on a semi-infinite silica substrate. When considering the visible-to-near-infrared wavelength range, the period and substrate refractive in-

dex are closely related with asymmetric transmission. These parameters can collectively control the wavelength range over which asymmetric transmission occurs. The asymmetric transmission is attributed to the difference in intensity between higher-order diffraction orders with forward and backward incident light. For macroscopic periodic structures, no optical asymmetric transmission was observed.

T15: Physics and AI

Time: Thursday 29 Oct, 11:15am; Venue: Think Tanks 9&10; Chair: Adolphus Lye
Time allocated for invited talks is 15 min speaking time, plus 5 min Q&A, and time allocated for contributed talks is 12 min speaking time plus 3 minutes Q&A.

T15.19 (INVITED) Topology-aware Neural Network for Protein–Nucleic Acid Dissociation Constant Prediction

Hon Lin Too* (Nanyang Technological University)
11:15am – 11:35am

Protein–nucleic acid interactions drive essential biological functions, and accurately predicting the binding affinity of protein–nucleic acid complexes is crucial for understanding the molecular mechanisms underlying these interactions. Here, we present a structure-based, multi-graph ensemble graph neural network (GNN) framework for predicting protein-nucleic acid dissociation constants (Kd) directly from complex structures. To our knowledge, this is the first graph-based approach that jointly models protein-DNA and protein-RNA binding within a single, unified architecture. We introduce a three-level graph-based molecular representation, namely atom-level, edge-level, and simplex-level graphs, the latter constructed via a chemically inspired weighted Vietoris-Rips complex, to jointly capture pairwise atomic interactions and higher-order structural motifs within protein-nucleic acid complexes. Evaluated on the PDBbind 2020 general set, our ensemble model achieves an R-score of 0.627 ± 0.065 and MAE of 0.991 ± 0.100 on held-out test data, with incorporation of higher-order graph representations yielding a statistically significant improvement over the atom-level model alone (p ¡ 0.05). While our model does not yet match the performance of existing structure-based methods specialized for a single nucleic acid type and binding free energy prediction, it retains reasonable predictive accuracy across both protein-DNA and protein-RNA complexes despite substantial imbalance in available training data, suggesting that joint training enables the model to learn shared, nucleic-acid-agnostic determinants of binding. These results demonstrate the value of higher-order, structure-aware graph representations for generalizable protein-nucleic acid binding affinity prediction

T15.2 (INVITED) Physics-enhanced Machine Learning for Probabilistic Risk Assessment in Nuclear Safety

Adolphus Lye*, Theodore Kay Chen Ong, Sicong Xiao (Singapore Nuclear Research and Safety Institute, National University of Singapore)
11:35am – 11:55am

With the dawn of Industry 5.0, the nuclear industry has seen the increased implementation of data-driven Artificial Intelligence approaches to assist the risk analysts in performing the various tasks such as: (1) reliability analysis; (2) accident modelling; (3) fault-diagnostics; (4) digital-twin; (5) prognostics; and (6) reactor performance monitoring, as part of the wider probabilistic risk assessment for nuclear safety.

However, such data-driven strategies can fall short in providing generalised and physically-consistent predictions due to: (1) poor data quality; (2) limited data availability; (3) accurate-but-wrong model predictions; (4) presence of uncertainties; and (5) non-interpretable models and inexplainable predictions. To address such issue, physics-enhanced machine learning approaches have been implemented to provide for interpretable surrogate models by accounting for the governing physics-based equations of the system of interest, and to provide for explainable model prediction results for risk-informed decision-making. Such strategy has garnered increasing attention in recent years.

Henceforth, the talk shall provide an overview of the implementation of physics-enhanced machine learning strategies in recent years by covering the following aspects: (1) the concept of physics-enhanced machine learning, and why it is needed for probabilistic risk assessment; (2) the challenges faced in performing probabilistic risk assessment which physics-enhanced machine learning seeks to address; (3) reviewing the physics-enhanced machine learning strategies implemented in the recent literature in the context of probabilistic risk assessment in nuclear safety; and (4) providing perspectives on the open research challenges, and outlining the opportunities for future research.

T15.56 Reinforcement learning for quantum environments with memory

Josep Lumbreras*, Ruo Cheng Huang*, Yanglin Hu, Marco Fanizza, Mile Gu* (Nanyang Technological University)

11:55am – 12:10pm

In reinforcement learning, an agent interacts sequentially with an environment to maximize a reward, receiving only partial, probabilistic feedback. This creates a fundamental exploration-exploitation trade-off: the agent must explore to learn the hidden dynamics while exploiting this knowledge to maximize its target objective. While this framework has been extensively studied classically, applying it to quantum systems requires dealing with hidden quantum states that evolve under unknown dynamics. We formalize this problem via a framework in which the environment maintains a hidden quantum memory that evolves via unknown quantum channels, and the agent intervenes sequentially via quantum instruments. For this setting, we adapt an optimistic maximum-likelihood estimation algorithm. We extend the analysis to continuous action spaces, enabling us to model general positive-operator-valued measures (POVMs). By controlling the propagation of estimation errors through quantum channels and instruments, we prove that the cumulative regret of our strategy scales as $\widetilde{\mathcal{O}}(\sqrt{K})$ over K episodes. Furthermore, via a reduction to the multi-armed quantum bandit problem, we establish information-theoretic lower bounds demonstrating that this sublinear scaling is strictly optimal up to polylogarithmic factors. As a physical application, we consider consider the fundamental cost of learning a quantum process, any lack of knowledge about the source leads to additional thermodynamic dissipation.

T15.55 Time-ordered free energy in correlated quantum systems: An agentic approach

Ruo Cheng Huang*, Isha Le Xue Singh*, Yuxuan Qu*, Paul Riechers, Varun Narasimhachar, Mile Gu (Nanyang Technological University)

12:10pm – 12:25pm

How much work can an agent extract from a temporal sequence of quantum states when it can only operate online under causal constraints—deciding which energy extraction method to use with knowledge of what it has observed before? Here, we study this problem in the context of quantum state sequences that are potentially non-Markovian—generated by some underlying hidden Markov machine that the agent cannot observe. Using techniques from dynamic programming and computational mechanics, we present a method to identify the provably optimal agent strategy, with time complexity that scales linearly with sequence length. This motivates us to introduce the maximum work such agents can extract—*time-ordered free energy* (TOFE)—as a fundamental measure of free energy available in a temporally correlated quantum system subject to causal considerations.

T15.28 Towards Critical Branching Mechanism in Recurrent Neural Networks

Feixiang Ren*, Ling Feng* (ASTAR, Institute of Advanced Intelligence and Computing)

12:25pm – 12:40pm

Criticality has been proposed as a key organizing principle in biological neural systems, yet its origin and relevance in artificial neural networks remain unclear. We analyze hidden-state dynamics in trained long short-term memory (LSTM) networks and show that small networks near their optimal training epochs (steps) exhibit scale-free avalanche statistics and branching parameters close to unity, indicative of near-critical dynamics, while larger models remain subcritical. To explain the coexistence of subcritical branching with robust 1/f noise, we introduce a mixture branching process framework that links heterogeneous branching dynamics to long-range temporal correlations. These results identify critical-like behavior in LSTMs as an emergent, capacity-dependent dynamical regime.

T16: Quantum Algorithms II

Time: Thursday 29 Oct, 11:15am; Venue: Think Tanks 11&12; Chair: (TBD)
Time allocated for invited talks is 15 min speaking time, plus 5 min Q&A, and time allocated for contributed talks is 12 min speaking time plus 3 minutes Q&A.

T16.84 Autonomous quantum machine learning via Riemannian gradient-based optimization

Kasidit Srimahajariyapong*, Marek Gluza*, Supanut Thanasilp, Thiparat Chotibut, Zoe Holmes, Yudai Suzuki, Suwannachad Suwannachit, Ricard Puig, Tithivich Paka (Nanyang Technological University)
11:15am – 11:30am

Quantum machine learning typically relies on a classical-quantum feedback loop, creating a fundamental bottleneck for scalability. Here, we propose a framework for autonomous quantum machine learning based on Riemannian gradient optimization, achieving learning without intermediate measurement or classical feedback. We derive the Riemannian gradient update rules for a broad class of learning objectives and identify sufficient conditions under which the resulting training dynamics become fully autonomous. In the self-training regime, we characterize two properties of the proposed model: (1) an exponential convergence guarantee with respect to the training iterations given sufficiently small step sizes and (2) the automatic extraction of hidden symmetries through the training process. While we show that the circuit depth grows exponentially with the number of training iterations, we demonstrate that efficient learning can still be achieved at low circuit depths with only a few training samples. Our results establish autonomous quantum machine learning as a learning paradigm that removes the classical optimization loop while retaining strong theoretical guarantees and strong practical performance.

T16.162 Near-Optimal Parameter Tuning of Level-1 QAOA for Ising Models

V Vijendran*, Dax Enshan Koh, Eunok Bae, Hyukjoon Kwon, Ping Koy Lam, Syed M Assad (Centre for Quantum Technologies & A*STAR Quantum Innovation Centre)
11:30am – 11:45am

The Quantum Approximate Optimisation Algorithm (QAOA) tackles combinatorial optimisation problems by encoding their solutions into the ground state of an Ising Hamiltonian prepared by a p-level parameterised circuit, with the angles tuned classically. Parameter optimisation is widely regarded as a central bottleneck, even for the shallowest circuits. Focusing on QAOA at p = 1 (QAOA1), we show that tuning the two angles (γ, β) for weighted Ising models is not a black-box search but a structured signal-processing problem. We prove that the QAOA1 expectation value is a partial Fourier series in γ whose frequencies are determined explicitly by the problem's couplings and fields, giving instance-wise bandwidth bounds and, via the Nyquist–Shannon theorem, the sampling resolution needed to avoid the aliasing that causes coarse-grid searches to return spurious optima. We then eliminate the mixer angle analytically, computing $\beta^*(\gamma)$ in closed form to reduce the search to one dimension, and apply a subdivision algorithm that locates the globally optimal γ in polynomial time with a certificate of optimality when the weights are commensurable and bounded. For regular weighted graphs, we further prove the conventional wisdom that the globally optimal $\gamma^* \in \mathcal{R}^+$ concentrates near zero and coincides with the first local optimum, giving a rigorous account of the empirical success of small-angle initialisation and allowing gradient descent to replace exhaustive line searches. Validated within Recursive QAOA (RQAOA) on weighted instances of 128 and 256 qubits, our method consistently outperforms both coarsely optimised RQAOA and semidefinite programming.

T16.163 Optimizing quantum-classical algorithmic resources for accuracy in VQE

Harshit Verma* (Majulab, Center for Quantum Technologies)
11:45am – 12:00pm

Variational Quantum Eigensolver (VQE) is a hybrid quantum-classical algorithm that works by refining the tunable parameters (through classical optimizer) in a variational quantum circuit, in order to minimize the measured energy of the prepared state [**?**, **?**]. This work [**?**] aims at characterizing and minimizing the algorithmic resources – quantum and classical – that control the achievable accuracy of VQE algorithm.

We consider the number of gates as an algorithmic quantum resource. In the absence of noise, increasing the

number of gates – through adding ansatz layers – enhances the expressibility, and thereby improves the achievable accuracy of the algorithm. On the classical side, we consider the number of iterations of the classical optimizer as an algorithmic resource. For a fixed circuit size, the accuracy eventually saturates with iterations as the optimization converges.

Noise – a characteristic of current quantum computers – upends the above simple relationship of algorithmic resources with accuracy. First, noise limits the circuit depth that can produce meaningful results, as errors accumulate with increasing depth [**?**, **?**, **?**], inducing bias in the estimated energy. Moreover, the scenario is further nuanced when the number of iterations is also taken into account. A key question then arises: does increasing the computational effort through additional iterations continue to improve accuracy, or does the accumulation of noise ultimately offset the marginal benefits gained from further optimization? This question also feeds into the overarching resource optimization objective: What is required to minimize resources for a given (desired) accuracy of the algorithm?

In this work (https://arxiv.org/pdf/2606.20153, attached), we develop phenomenological scaling relations that captures the trade-offs between accuracy, circuit size, and iteration count in VQE algorithm; that enables us to either minimize the resource for a target accuracy or maximize the accuracy for a given resource cost. The scaling relations approach parallels recent developments in classical machine learning, where scaling laws relate model performance to compute, data, and parameters, albeit the element of noise is generally absent in this case and forms a distinguishing feature of quantum algorithms.

T16.72 Quantum Determinantal Point Process for Anomaly Detection in Financial Data

Bella Santosa*, Hallie Shiotsu, Bryan Teo, Zheng Da Wang, Daniel Leykam (SUTD)
12:00pm – 12:15pm

Determinantal point processes (DPPs) sample subsets with a bias towards diversity by defining the probability of subsets as the determinant of its matrix. The intrinsic diversity in DPP sampling makes it appealing for training data sampling for anomaly detection models, where random sampling may fail to select the small proportion of outliers. Considering this clear advantage, however, classical DPP sampling bears a significant computational overhead of a cubic function to the feature space dimension ($\mathcal{O}[d^3]$). To leverage on the similarity of DPP correlations to that of non-interacting fermions, we implement a quantum analogue of the DPP sampler in a near-term quantum circuit simulation using an iterative Clifford loader as a d-dimensional subspace encoder, thus introducing a quantum speedup to $\mathcal{O}[d \log n]$ where n is the size of the subsamples. We embed this sampler in a single-stage and two-stage unsupervised isolation forest workflows for anomaly detection, and benchmark against classical DPP sampling and purely random sampling across datasets of various contamination rates, anomaly structures, and feature space dimensions. We find that datasets with cluster-like anomaly structure show a significant DPP advantage as compared to dependency and local anomaly types. Though limited by the simulation qubit count, we show that quantum DPP is a viable speed-up of classical DPP for smaller dimensionalities. We also compare quantum and classical DPP performance against random sampling in semi-supervised models, where DPP advantage is not observed for these partially labelled datasets. These DPP workflows are then applied to real credit card transaction data for fraudulent transaction detection with 0.172% contamination rate. Our findings show that DPP improves the precision, recall and F1 score of the model by 19% against random uniform sampling in the single-stage workflow, and up to 18% in the two-stage workflow. A similar performance is seen in workflows for smaller DPP sampling batches adapted for quantum implementation. Our study therefore provides insight in the potential quantum computational speed-up to anomaly detection for quantitative finance applications on near-term devices.

T16.31 Entanglement and Coherence Hierarchy in Post-Selected Quantum Metrology with Kirkwood-Dirac Quasiprobabilities

Kuan-Fu Chiu*, Kelvin Onggadinata, Arghya Maity, Teck Seng Koh (NTU SPMS)
12:15pm – 12:30pm

Expressions of post-selected Quantum Fisher information (QFI) are commonly presented from a global perspective, leaving the final detection stage implicit. Consequently, it is not straightforward to conditionally identify the

contributions of each detection outcome to parameter sensitivity and the underlying quantum resources. Here, we retain the final detection stage and derive a decomposition of post-selected Quantum Fisher information in terms of conditional Kirkwood-Dirac (KD) quasiprobabilities, which identifies the real and imaginary quantum modification terms separately, using geometrical metrics. We introduce KD coherence densities and KD entanglement densities to show that the imaginary-KDQ-driven classical Fisher-information component of the post-selected QFI is upper-bounded by these detection-dependent quantities. In addition, we demonstrate the hierarchy between them: KD coherence densities are greater than or equal to KD entanglement densities. In a single qutrit model, we illustrate a detection-controlled trade-off between the probability-dependent and phase-dependent contributions. Finally, we extend the framework to a multipartite system and show that balanced and unbalanced bipartitions generally yield different KD entanglement densities.

T17: Quantum Communication

Time: Friday 30 Oct, 11:15am; Venue: Think Tanks 2&3; Chair: (TBD)
Time allocated for invited talks is 15 min speaking time, plus 5 min Q&A, and time allocated for contributed talks is 12 min speaking time plus 3 minutes Q&A.

T17.137 (INVITED) Short-Reach Optical Systems: Technology Trends and Implications for Quantum Key Distribution over WDM

Sunghyun Bae* (Sejong University)
11:15am – 11:35am

The recent growth of AI workloads and the requirements of 6G have driven a sharp rise in data center and user internet traffic. Short-reach optical systems, including mobile fronthaul, data center networks, and passive optical networks, are therefore required to support higher capacity. Moreover, since these systems are constrained by cost as well as by speed, intensity-modulation direct-detection remains preferred. These trends in fiber-optic communication indicate what must be considered when quantum key distribution is to be integrated using WDM. This talk reviews the technology trends of short-reach optical systems to date, and presents our recent work on transmitting signals beyond 100 Gb/s per wavelength.

T17.24 (INVITED) The Singapore Optical Ground Station: An Urban Platform for Satellite Quantum Communications

Shaik Abdillah*, Moritz Mihm, Muskan Varshney, Matthew Wee, Soe Moe Thar, Darius Lee, Euk Jin Alexander Ling* (Centre for Quantum Technologies, National University of Singapore)
11:35am – 11:55am

Satellite quantum networks offer a path towards global-scale quantum communication, owing to the quadratic loss scaling of space–Earth optical links, in contrast to the exponential attenuation of optical fibre. To support this, a network of high-precision optical ground stations (OGSs) is required to sustain the line-of-sight optical link between space and ground segments. To date, most OGSs are situated in remote locations away from population centres to mitigate the effect of anthropogenic light pollution on QBER. However, this approach limits access to the infrastructure and connectivity necessary for practical OGS deployment, creating a fundamental trade-off between low-background operation and urban accessibility. The Singapore Optical Ground Station (SOGS) was commissioned in 2024 as a quantum-capable facility located on a metropolitan site. We present experimental characterisations of SOGS against link-loss models to validate its feasibility for sustaining a space–Earth quantum link. This includes passive tracking of low-Earth-orbit satellites with tracking precision ranging from tracking precision ranging from 1.04” to 3.64”, approaching Singapore’s atmospheric seeing limit of approximately 2”-3”. Sky background measurements yielded noise levels of 200–1200 cps, varying primarily with lunar phase and angular separation from the Moon, and remaining within operational bounds even under high lunar illumination. SOGS’s tracking precision, background levels, and detector performance compare favourably against a reference link budget shown to yield secure key rates of 19.2 kbit per pass. In tandem with its quantum networking capabilities, SOGS’s equatorial location provides frequent access to a broad range of orbital inclinations, making it an attractive testbed for optical space situational awareness, including passive satellite monitoring and orbit refinement. To date, the SOGS has successfully optically tracked various space assets including equatorial and MEO CubeSats. Taken together, these capabilities position SOGS as an experimental hub for both quantum networking and the growing space ecosystem in Singapore. This represents a key step towards the deployment of satellite quantum links in the region.

T17.41 Exponential speedup of polarization stabilization for long distance DWDM quantum networks

Jinyi Du*, En Teng Lim*, Xingjian Zhang*, Hongwei Gao*, George Chen*, Dawn Tan*, Alexander Ling* (Centre for Quantum Technologies, NUS; Department of Physics, NUS)
11:55am – 12:10pm

Stable polarization control is essential for fibre based entanglement distribution. Conventional stabilization com-

monly uses bright classical reference light, but photon leakage and Raman noise can saturate single photon detectors. Entangled photon based polarization feedback provides a natural alternative that avoids introducing bright classical reference light. However, it faces two fundamental limitations in long distance entanglement distribution. First, calibration typically occupies the same quantum channels used for entanglement transmission, introducing unavoidable transmission downtime. Second, conventional two-link feedback relies on coincidence events in which both photons must traverse their respective lossy network fibres. The data integration time for each feedback measurement scales inversely with the loss, leading to an exponentially increasing acquisition cost with fibre distance. Here, we overcome both limitations through two successive forms of decoupling. First, spectrally adjacent entangled photon sidebands probe the polarization transformation of a central entanglement channel, decoupling polarization feedback from entanglement distribution and eliminating calibration induced downtime. Second, optical switching and local reference fibres decompose the two-link feedback measurement into two independent single-link measurements, changing the acquisition time scaling from the product-of-losses to the sum-of-losses. We demonstrate the method over 87 km and 46 km fibre links with losses of 18.5,dB and 10.5,dB, respectively, achieving a tenfold reduction in feedback acquisition time while maintaining continuous high fidelity entanglement distribution for more than 24 hours. This approach provides a scalable route toward continuous polarization stabilization in long distance DWDM quantum networks.

T17.26 Quantifying 1st & 2nd Order Polarization Mode Dispersion Induced-Errors for Broadband Polarization-Encoded Quantum Communications

Rui Ming Chua* (CENTRE FOR QUANTUM TECHNOLOGIES, TECHNOLOGY INNOVATION INSTITUTE)

12:10pm – 12:25pm

We studied the effect of polarization mode dispersion on measurement errors in polarization-encoded quantum communications up to the second order. We show that when expanded up to the second order, the Band-Averaged Mueller Matrix describing broadband polarization state transmission can be described by a general rotation and contraction where its Singular Value Decomposition returns the key features of the channel: the optimal and worst states for transmission, and their corresponding errors. We propose new metrics to define specifications for optical fiber performance for quantum communications. Finally, we present some results in compensating polarization mode dispersion.

T18: Quantum Devices

Time: Friday 30 Oct, 11:15am; Venue: Think Tanks 4&5; Chair: (TBD)
Time allocated for invited talks is 15 min speaking time, plus 5 min Q&A, and time allocated for contributed talks is 12 min speaking time plus 3 minutes Q&A.

T18.148 (INVITED) Photon-pair generation in thin-film lithium tantalate racetrack resonators

Sakthi Sanjeev Mohanraj*, Xiaodong Shi, Lin Zhou, Ran Yang, Di Zhu* (National University of Singapore,)
11:15am – 11:35am

We demonstrate a cavity-enhanced photon-pair source based on a periodically poled thin-film lithium tantalate racetrack resonator. It produces broadband, bright biphoton frequency combs, showcasing the potential of this material platform for quantum photonics.

T18.155 Tunable frequency-domain quantum interference in a nonlinear microresonator

Lin Zhou* (National University of Singapore)
11:35am – 11:50am

Scalable generation and control of high-dimensional quantum states remain central challenges in the development of photonic quantum processors. Nonlinear microresonators offer a compact platform for generating photon pairs, while control of their correlations across frequency modes typically relies on downstream filters and modulators. Here, we realize photon-pair generation and coherent electro-optic control within a single thin-film lithium niobate (TFLN) microresonator. This integration enables us to shape the spectral–temporal structure of biphoton correlations during photon-pair generation, making the source itself an active element for coherent quantum-state preparation.

T18.139 Toward mid-infrared imaging and ranging with superconducting nanowire single-photon detectors

Xitong Duan*, Taeyong Chang, Ruixiang Guo, Pierre Brosseau, Christian Kurtsiefer, Cesare Soci* (Nanyang Technological University)
11:50am – 12:05pm

Mid-infrared (MIR) light detection and ranging (LiDAR) combines depth-resolved sensing with wavelength-specific contrast arising from molecular vibrational absorption, providing chemical and material information beyond that typically accessible with visible and near-infrared (NIR) LiDAR. However, the lower photon energy at MIR wavelengths makes efficient single-photon detection increasingly demanding, particularly in photon-starved scenarios such as long-range, low-reflectivity, or low-illumination measurements, where weak return signals place stringent requirements on detector sensitivity and timing performance. Superconducting nanowire single-photon detectors (SNSPDs), combining single-photon sensitivity, low dark-count rates, excellent timing resolution, and broadband spectral coverage extending into the MIR, therefore provide an attractive route toward photon-efficient MIR time-of-flight (ToF) LiDAR. Here, we report progress toward an integrated MIR LiDAR platform based on SNSPD detection. Experimentally, we first established a NIR proof-of-concept ToF LiDAR system, achieving cm-scale depth resolution. We subsequently implemented free-space single-pixel imaging using SNSPD detection. In parallel, our SNSPD development has extended the detector response into the MIR, with a measurable photoresponse currently verified at 3.7 μm. These developments are now being integrated into a unified free-space MIR single-photon LiDAR system, initially with the aim of achieving photon-efficient imaging and ranging within the 3.5-4 μm atmospheric transmission window.

T18.100 Monolithic metal-superconductor nanowire detector array for polarization state tomography without external optics

Pierre Brosseau*, Jiawei Wang, Giorgio Adamo, Anton N. Vetlugin, Cesare Soci* (Nanyang Technological University)
12:05pm – 12:20pm

Polarization state tomography of single photons and photon pairs is usually performed by rotating waveplates and

polarizers in front of a detector, an approach that is slow and difficult to scale or integrate. Following our previous work on fiber-based and multi-pixel polarimetry, we now demonstrate a monolithic superconducting nanowire single-photon detector in which polarization selectivity is built directly into the photon-absorbing nanowire. Gold nanowires are patterned on top of NbTiN nanowires in the same lithographic step, forming plasmonic metamaterial pixels: U-shaped wires respond preferentially to a chosen linear polarization, while chiral S-shaped meanders respond to one handedness of circular polarization. Combining four such pixels into an array provides a complete polarization measurement basis with no moving optical components. Using this approach, we demonstrate quantum state tomography of single photons with an ensemble average fidelity above 98%, and individual state reconstructions reaching 99.6% fidelity within milliseconds of integration. We discuss the scalability of this monolithic approach and its prospects for quantum communication, imaging and other applications requiring fast, on-chip polarization measurement. Based on: arXiv:2607.06047

T18.91 Tantalum Nano-constriction Josephson Junctions for Low-Loss Superconducting Quantum Circuits

Ding Huang* (Institute of Materials Research and Engineering, A*STAR)
12:20pm – 12:35pm

Superconducting constriction-based Josephson junctions offer a simple single-layer geometry, direct compatibility with the thin-film processes used for superconducting quantum circuits, and access to critical currents beyond those achievable with oxide tunnel junctions. However, integrating such junctions into low-loss superconducting microwave circuits has remained challenging. To date, superconducting resonators incorporating constriction-based junctions have exhibited internal quality factors below 1×10^4, far below those routinely achieved in state-of-the-art low-loss resonators. Here, we demonstrate constriction-based junctions and nanoSQUIDs in tantalum, the material platform underlying some of today's highest-coherence superconducting qubits, and improve the single-photon internal quality factor by more than an order of magnitude over previous constriction-integrated resonators. Tantalum constriction-based nanoSQUIDs exhibit well-behaved weak-link characteristics and clear flux-periodic voltage modulation. These results establish tantalum constriction junctions as low-loss, process-robust Josephson elements, enabling flux-tunable tantalum resonators and opening a path toward integrated nanoSQUID thermometry and magnetometry on a platform compatible with state-of-the-art coherent superconducting quantum circuits.

T18.130 Towards Scalable Integrated SNSPDs: Photon-Number Resolution, Foundry Integration, and New Material Platforms

Filippo Martinelli*, Vagif Aliyev, Anton Vetlugin, Cesare Soci* (Nanyang Technological University)
12:35pm – 12:50pm

Integrated superconducting nanowire single-photon detectors (SNSPDs) are a critical component in the development of large-scale photonic quantum computers. Although SNSPDs have been successfully integrated onto standard silicon photonic circuits with promising performance, this has mostly been limited to ad-hoc PIC platforms. Three challenges remain open: compatibility of SNSPD integration with standard foundry photonic circuit manufacturing, the demonstration of integrated schemes capable of resolving one- from multi-photon states, and the demonstration of high-performing detectors on emerging material platforms such as thin-film lithium niobate. In this talk, we present our results and strategies for addressing each of these. We report the design and realization of a compact integrated photon-number-resolving detector based on coherent perfect absorption, with the potential to resolve photon numbers beyond 30. We demonstrate a post-processing method for integrating detectors on PICs fabricated in commercial foundries, fully compatible with standard foundry and CMOS workflows. Finally, we present preliminary results on high-efficiency devices realized on thin-film lithium niobate.

T19: Quantum Algorithms III

Time: Friday 30 Oct, 11:15am; Venue: Think Tanks 9&10; Chair: (TBD)
Time allocated for invited talks is 15 min speaking time, plus 5 min Q&A, and time allocated for contributed talks is 12 min speaking time plus 3 minutes Q&A.

T19.16 Forecasting-Accelerated Variational Quantum Circuit Optimization

Tianqi Chen*, Jiabin You*, Jian Feng Kong* (IAIC, ARES)
11:15am – 11:30am

Variational quantum algorithms are promising candidates for near-term quantum computation, but their practical performance is often limited by the large number of circuit evaluations required during classical optimization. Here we propose a forecasting-accelerated framework for variational quantum optimization in which the parameter trajectory generated by a quantum algorithm is treated as a multivariate time series. Using a PatchTST-based Transformer forecaster, short segments of previously validated optimization trajectories are used to propose look-ahead candidate parameters. These candidates are not accepted directly; instead, they are screened by explicit evaluation of the variational objective, and the current and historically best parameters are retained as fallback options. This conservative validation rule allows the forecaster to act as a classical proposal mechanism while preserving the reliability of variational energy selection. We formulate the method for the variational quantum eigensolver and benchmark it on lithium hydride, where the goal is to reduce the number of expensive gradient-evaluated iterations needed to reach a target accuracy. We further extend the same forecasting princi- ple to quantum circuit Born machine training for short biological sequence distributions, using DNA or RNA motif distributions as biologically interpretable targets. Our framework provides a general route for combining time-series forecasting with hybrid quantum-classical optimization, with potential applications to both quantum many-body Hamiltonian simulations and quantum generative modeling.

T19.174 Energetic Efficiency of Resource State Generation for Fusion-Based Quantum Computation

Nathan Shettell*, Harshit Verma, Alexia Auffeves, Ariane Soret, Katia Hakem, Gregoire de Gliniasty, Pierre-Emmanuel Emeriau (MajuLab, CNRS, CQT)
11:30am – 11:45am

Fusion-based quantum computation enables fault-tolerant quantum computing by connecting networks of small entangled resource states through fusion measurements. Multiple strategies can be used to achieve fault tolerance, including increasing resource-state quality, multiplexing probabilistic operations, exploiting nonlinear interfaces, or increasing the size of the error-correcting network. However, these approaches trade physical resources, noise suppression, and computational overhead in fundamentally different ways, making it unclear which is energetically favourable.

Here, we develop a physically grounded full-stack benchmarking framework that connects hardware-level constraints (photon loss, distinguishability, cryogenic power, and optical resources) to computational performance and energetic cost. By propagating resource-dependent noise through resource-state generation, fusion, and fault-tolerant encoding, we quantify how different physical strategies translate into network overhead and energy consumption. This reveals a fundamental trade-off between investing energy to suppress physical noise and investing physical resources to tolerate it: operating further below threshold can substantially reduce the required computational architecture, but may demand greater energetic investment, while operation closer to threshold shifts the cost toward larger fault-tolerant networks. Our framework provides a common basis for identifying energetically favourable routes to scalable photonic quantum computing.

T19.81 Tailoring polynomials for quantum signal processing using methods of Riemannian geometry

Andrew Wright* (NTU)
11:45am – 12:00pm

Gradient descent is foundational to optimization but its performance depends on the strategy for assigning an

effective learning rate. In this work we provide analytical formulas expressing the optimal solutions to such line-search in the generalization of the gradient descent to Riemannian geometry of the unitary group which allows for quantum algorithmic applications to finding ground-state of quantum many-body systems. Our formulas are expressed through surprisingly simple functions of the first moments of the cost-function Hamiltonian and we propose an iterative procedure which builds polynomials that can be used for quantum signal processing based on measurements of the mean, variance and skewness of the energy distribution. This allows to shed light on the structure of polynomials used in quantum signal processing through the lens of Riemannian geometry where the polynomial roots can be interpreted through the associated approximation to the line-search minimizer. We study numerical compilation and gate-counts of the implementation using block-encodings in Qrisp and we provide tensor network results for homogeneous systems involving a large number of qubits.

T19.38 Towards fault-tolerance with universal phase-error-transparent gates for high-spin cat codes

Kelvin Onggadinata*, Si Yan Koh, Arghya Maity, Kuan Eng Johnson Goh, Bent Weber, Kay Jin Lim, Hui Khoon Ng, Teck Seng Koh (Nanyang Technological University)
12:00pm – 12:15pm

High-dimensional nuclear spins offer a hardware-efficient route to quantum error correction (QEC), with the spin-cat code providing intrinsic robustness against phase errors – the dominant noise channel in donor-in-silicon architectures. However, realizing the full potential of this encoding requires gate operations that preserve its error-correcting properties. In this work, we construct a universal logical gate set satisfying the error-transparent (ET) criterion, which ensures that phase errors occurring stochastically during gate operation are propagated in a controlled and systematically traceable manner and remain correctable in a subsequent QEC step. We discuss practical implementations for the donor-in-silicon architecture. In simulations of fidelity performance with error correction requiring only a single ancilla qubit, we find that ET gates significantly outperform non-ET gates and may be necessary to surpass the break-even point. Among the gates in the universal gate set constructed, we identify the logical X gate as the primary challenge and discuss potential realization schemes. We further demonstrate that ET measurement in the computational basis is achievable via spin parity measurement, and that error correction circuits constructed from ET operations achieve optimal error correction capacity. Our work charts a concrete path towards full fault-tolerant quantum computation with high-dimensional nuclear spin systems.

T19.120 Broken-symmetry phenomena enhanced by quasi-bound states in the continuum

Jan David Fischbach* (Nanyang Technological University)
12:15pm – 12:30pm

Many of the most powerful and elegant models in physics are grounded in symmetries. In electrodynamics, for example, geometric symmetries govern the observable effects of light-matter interactions. However, for man-made objects, exact symmetries are rarely met and tiny deviations are common. Nonetheless, even approximate symmetries keep many symmetry-derived rules effectively intact. However, as we will show here, this is not universally true. We demonstrate that an incremental violation of the symmetry of a carefully designed system can produce an optical response maximally different from the unbroken symmetry case. To do so, we exploit symmetry-protected quasi-bound states in the continuum (qBICs). Specifically, we design a four-fold rotationally symmetric meta-surface composed of nearly dual-symmetric meta-atoms that supports a pair of spectrally aligned electric and magnetic qBICs. At normal incidence, symmetry forbids helicity-preserving reflection. However, for arbitrarily small deviations from normal incidence, the strong resonant enhancement associated with the qBICs overcomes the near-symmetry suppression and enables perfect helicity-preserving reflection. This rapidly emerging violation of symmetry-rules reveals a fundamental intricacy when it comes to treating near-symmetric systems. At the same time, our work opens the door to novel applications in metrology and sensing.

T20: Instrumentation and Processes

Time: Friday 30 Oct, 11:15am; Venue: Think Tanks 11&12; Chair: (TBD)
Time allocated for invited talks is 15 min speaking time, plus 5 min Q&A, and time allocated for contributed talks is 12 min speaking time plus 3 minutes Q&A.

T20.108 (INVITED) Accelerating cryogenic characterization of quantum devices with novel ADR cryostats

Pau Jorba*, Oleh Ivashko*, Jan Spallek, Felix Rucker, Alexander Regnat (kiutra GmbH)
11:15am – 11:35am

To enable the wide range application of quantum computing, the performance of qubits and associated devices must be improved to minimize error rates and improve coherence times. This requires comprehensive testing and characterization of new materials, innovative designs, and novel fabrication methods. The development cycles to improve these various aspects are slow due to classic cryogenic solutions having long cooldown times. We present a novel cryostat [1] developed for the characterization of quantum devices at sub-Kelvin temperatures, based on magnetic cooling. We describe how continuous sub-Kelvin cooling and wide-range temperature control can be achieved by combining multiple ADR units and mechanical thermal switches. We also present a novel sample loader mechanism [2]that allows to automatically cool and test devices from room temperature to below 50 mK in less than 4 hours. Finally, we show how it can be used to study low-temperature characteristics of various quantum devices.

[1] Regnat et al. (2018) Cryogen-free cooling apparatus (EP 3163222). European Patent Office. [2] Spallek et al. (2022) System and method for inserting a sample into a chamber (EP 3632560). European Patent Office.

We acknowledge funding from the German Federal Ministry of Education and Research (BMBF) within the MUNIQC-SC project.

T20.88 Towards the Development of a Light-field Quantum Diamond Microscope(LFQDM)

Priyanshu Bhattacharya*, Niko Reed*, Connor Roncaioli*, Daniel G. Ang*, Ronald Walsworth* (Department of Electrical and Computer Engineering, University of Maryland, College Park, Maryland, USA)
11:35am – 11:50am

NV centers in diamond are solid-state quantum sensors with applications ranging from magnetic-field sensing and navigation to nanoscale thermometry and searches for new physics such as dark matter. The performance of an NV-based quantum sensor depends strongly on material properties such as strain. As NV-sensors move toward larger-scale deployment, rapid and repeatable characterization of these properties throughout the diamond volume becomes increasingly important. Conventional volumetric characterization relies on axial scanning which increases the acquisition time. Light-field imaging provides a route to acquiring depth information with reduced axial scanning.

We built LFQDM by placing a microlens array at the intermediate imaging plane of a conventional widefield quantum diamond microscope. The conventional widefield arm was first validated by performing zero-field and bias-field ODMR measurements, including pixel-by-pixel measurements showing all eight resonances. We then characterised the light-field arm by following the general experimental approach by Levoy et al. with a Thorlabs test grid. We performed optical sectioning and synthetic refocusing measurements by translating the target along the optical axis and computationally refocusing the recorded lightfields. We successfully demonstrated synthetic refocusing over axial target displacements approaching 900 μm. These results provide a first step toward rapid volumetric characterization of NV-diamond material for future strain and magnetic-field imaging.

T20.198 Nanometric Localization with Structured Light

Yu Wang*, Benquan Wang, Eng Aik Chan, Jun-Yu Ou*, Songze Li, Zhenyu Guo, Xi Xie, Masako Kishida, Che-Chin Chen, Yijie Shen* (Nanyang Technological University)
11:50am – 12:05pm

Advancements in the semiconductor industry are driven by the development of increasingly compact devices with complex raised and etched geometries. For effective characterization and quality control of these structures in

both scientific research and industry, precise and real-time metrology is essential. However, achieving location of sub-wavelength structures with nanometer precision remains a significant challenge. In this work, we introduce a single-shot and label-free optical metrology technique for determining the 1D displacement of sub-wavelength nanostructures with an impressive precision of 7.2 nm (λ/110). Such high precision benefits from utilizing Laguerre–Gaussian (LG) and Hermite–Gaussian (HG) beams with phase jumps as structured illumination and AI analysing method can retrieve obvious information when such phase jumps interacting with sub-wavelength objects.

T20.30 Ion Transport Effects in Ultra-Low-Pressure Inductively Coupled Plasma Etching of High-Aspect-Ratio SiO_2 Structures

Jiachen Wei*, Gil Young Choi*, Kwang-Ho Kwon* (Korea University at Sejong)
12:05pm – 12:20pm

In high-aspect-ratio contact (HARC) etching processes, ion transport becomes a limiting factor for etching characteristics as the aspect ratio increases; therefore, the directional delivery of ions generated in the plasma to the etch front is essential to maintain the etch rate and achieve profile integrity. In this study, we investigated the SiO_2 HARC etching characteristics using an inductively coupled plasma (ICP) system operating in the ultra-low pressure regime. We systematically analyzed the effects of process pressure, source power, and bias power on etching characteristics, focusing specifically on aspect-ratio-dependent etching (ARDE) and feature-profile evolution. We observed that reducing the process pressure from 20 mTorr to 3 mTorr not only enhanced the etch rate for 60 nm patterns but also suppressed ARDE and minimized the variation in the top critical dimension (ΔCDtop). In contrast, increasing source power primarily enhanced ion flux and neutral species density without substantially altering pattern-size dependency, while increasing bias power moderately improved ARDE by enhanced ion energy. These results indicate that the marked performance enhancement observed under ultra-low pressure conditions cannot be explained solely by changes in plasma density or surface reaction kinetics. Instead, it appears that reduced scattering—caused by collisions within the sheath and presheath regions—preserves ion directionality, thereby facilitating the effective delivery of ions to the bottoms of high-aspect-ratio patterns. These findings demonstrate that ion transport, rather than plasma reactivity, is the critical limiting factor in HARC etching processes and suggest ultra-low pressure ICP processing as an effective approach for next-generation HARC applications.

T20.194 Particle-in-Cell Simulation of Nanoplasma Devices

Chun Yun Kee*, Weiqiang Xu, Mohammad Samizadeh Nikoo, Lay Kee Ang* (SUTD)
12:20pm – 12:35pm

Compact, high-power terahertz sources remain a critical challenge in modern electronics. Nanoplasma devices offer a promising route around the limitations of conventional solid-state electronic and photonic sources, but realizing these miniaturised technologies requires a fundamental understanding of gas breakdown and its dynamics across micro- and nanoscale gaps. We investigate atmospheric-pressure nanogap discharges using one-dimensional particle-in-cell (PIC) simulations that incorporate Fowler–Nordheim field emission and gas-phase collisions. Our findings reveal that reducing the gap spacing below 100 nm drives the discharge into an ionization-limited regime. The breakdown voltage deviates from the predictions of the modified Paschen law widely observed in microdischarge. An overdrive study further resolves the ignition and plasma-formation process. These results provide insight into nanoscale plasma dynamics and inform the design and optimisation of future nanoplasma devices across a range of applications.

T20.110 Adiabatic Cherenkov resonance crossing for free electrons in time-varying medium

Ayan Nussupbekov* (Institute of Advanced Intelligence and Computing, A*STAR)
12:35pm – 12:50pm

We study free-electron radiation in continuously varying temporal media, providing an exact unified framework for temporal transition radiation and dynamical Cherenkov resonance crossings. By modeling the modulation via a smooth profile in the reciprocal permittivity, we obtain the general solution in closed form in terms of generalized hypergeometric ${}_3F_2$ functions. For an adiabatically changing medium, we demonstrate that the radiated

energy scales linearly with the switching time τ when crossing a wavenumber-independent resonance condition, whereas non-resonant modes are exponentially suppressed. Finite-difference time-domain (FDTD) simulations independently confirm our theoretical scaling laws and angular distributions.

T21: Astrophysics and Mathematical Physics

Time: Friday 30 Oct, 2:00pm; Venue: Think Tanks 2&3; Chair: (TBD)
Time allocated for invited talks is 15 min speaking time, plus 5 min Q&A, and time allocated for contributed talks is 12 min speaking time plus 3 minutes Q&A.

T21.166 (INVITED) Coupled Numerical Modelling of Photovoltaic-Urban Heat Interactions in Singapore

Po-Yen Lai*, Xian Li*, Hui Min Lee*, Derrick Low (A*STAR IAIC)
2:00pm – 2:20pm

Photovoltaic systems play an essential role in the clean energy transition; however, their effects on the outdoor thermal environment in hot and humid tropical cities like Singapore remain a significant challenge. The objective of this work is to present an integrated numerical model to examine the impact of rooftop PV deployment on building surface temperatures and outdoor thermal comfort in Singapore. Based on the surface energy balance mechanism, the model accounts for solar and thermal radiation, airflow, and heat conduction, while specifically treating PV panels as dynamic thermodynamic nodes releasing convective heat. Simulation results are compared with field measurements and used to assess different PV layouts for providing a practical guideline for urban planning and renewable energy integration in tropical microclimates.

T21.51 Analysing with(out) noise asymmetries in future space based interferometers

Karel Plets* (National University of Singapore)
2:20pm – 2:35pm

One hundred years ago, Einstein formulated his famous theory of relativity, in which he stated that space and time are unified into a combined spacetime and are curved by matter and energy. He further discovered that moving matter in certain ways causes ripples in spacetime, called gravitational waves (GWs). Next to the measurements we have been able to make with light, this would further enable us to analyse astrophysical events through its direct gravitational effects. For the past decade, we have been able to detect these through a network of interferometers, enabling us to ”listen” to the symphony of the universe. However, with the current network of detectors we can only ‘hear’ the upper tones of the symphony, which is why we are launching another space-based triangle-shaped detector named LISA in 10 years to listen to the lower bass frequencies. Spanning armlengths of ca. 250 million meters, it will consist of three satellites shooting lasers to each other across space.

As LISA has not yet been launched, various approximations have been made in order to prepare for its launch and the subsequent data analysis. One such approximation is the full symmetry of LISA. In the current literature, each of LISA’s three component spacecrafts is assumed to have the same detector noise levels and maintain the shape of an equilateral triangle. However, we already know this not to be true as the planned orbit will not be able to maintain a rigid triangular shape and each of LISA’s detectors will naturally vary in their sensitivity. While the created bias caused by approximating the signal with equal armlengths has already been analysed, a similar treatment had yet to be done on the noise level asymmetries.

In this presentation, I will present my results analysing these effects on LISA using Bayesian analyses and Fisher information matrices.

T21.64 Hysteresis in Urban Traffic Networks: Nonlinear Recovery, Topology, and Relaxation

Dake Wu*, Ling Feng (National Univeristy of Singapore)
2:35pm – 2:50pm

Urban traffic networks can undergo abrupt transitions between free-flow and congested states and exhibit hysteresis: the same congestion-spreading pressure may correspond to different macroscopic congestion levels during loading and recovery. Such history dependence is often interpreted as evidence of multiple metastable states, yet its microscopic origin and persistence remain unclear. Existing spreading models commonly assume that congested roads recover spontaneously. Recent empirical evidence instead suggests that recovery is hindered by congestion on downstream roads, but whether recovery hindrance alone is sufficient to generate hysteresis is unknown.

We study this question using a binary-state network model of congestion propagation and recovery. The local

recovery probability decreases with the number of congested downstream neighbours and continuously interpolates between linear and nonlinear hindrance. Combining mean-field analysis with loading-recovery simulations on directed grids, progressively modified network structures, and real urban road networks, we examine how recovery nonlinearity, network topology, and the time scale of external driving control the collective transition.

Our results identify three distinct controls over traffic hysteresis: recovery nonlinearity, network topology, and time-scale mismatch. Nonlinear recovery can produce a saddle-node bifurcation, whereas linear hindrance remains below the deterministic fold condition and does not generate hysteresis. At the network level, strong downstream branching reinforces collective recovery suppression, while loop-poor or highway-rich structures weaken the feedback and reduce hysteresis. Finite-rate sweeps further produce larger loops under faster driving, while allowing more relaxation contracts the loop. This suggests a contribution from dynamical lag.

By linking microscopic nonlinear recovery to macroscopic collective memory, this work advances the physical understanding of history-dependent behaviour in complex networks, including the distinction between intrinsic multistability and dynamical lag. It also provides a mechanistic framework for assessing the operational limits of traffic capacity and resilience under dynamic demand and network conditions.

T21.49 Supergroup Gauged Linear Sigma Models and their Physical Mathematics

Arif Er*, Zhangcheng Liu, Meng-Chwan Tan (NUS)

2:50pm – 3:05pm

In this presentation, we discuss the physical mathematics that can be derived from the study of the supersymmetric states of 2d N = (2,2) gauged linear sigma models with $U(1|1)^N$ supergauge group possibly with superpotential. In particular, we find a relation between a nonlinear sigma model on a Calabi-Yau complete intersection of hypersurfaces in a super-Grassmannian and a supergauged Landau-Ginzburg orbifold, which can reduce to a regular Calabi-Yau/Landau-Ginzburg correspondence for complete intersections. This defines a super-Grassmannian/supergroup generalization of the correspondence proved by Clader and Zhao. Similarly, we find a relation between a nonlinear sigma model on a Calabi-Yau hypersurface in a product of super-Grassmannians and a hybrid NLSM/supergauged Landau-Ginzburg orbifold, which can reduce to a regular hybrid Calabi-Yau/Landau-Ginzburg correspondence for hypersurfaces in product space. This defines a super-Grassmannian/supergroup generalization of the correspondence proved by Fan-Jarvis-Ruan. We also find that Calabi-Yau supervector bundles over a super-Grassmannian can undergo a physically related mild topology change which is reducible to a regular Atiyah-type flop transition. This defines a super-Grassmannian generalization of a birational equivalence of Calabi-Yau vector bundles in mathematics. Similarly, we find that a Calabi-Yau complete intersection of quadrics in a super-Grassmannian can also undergo a physically related topology change which is reducible to a regular conifold transition. This defines a super-Grassmannian generalization of a homological projective duality for Calabi-Yau quadrics by Kuznetsov-Perry in mathematics. This presentation is based on arXiv:2608.19775.

T21.13 resonant-state expansion for non-relativistic wave equation in one dimension

Abdullahi Tanimu* (Department of Physics, Umaru Musa Yar'adua University, P. M. B. 2218, Katsina state, Nigeria)

3:05pm – 3:20pm

The resonant state expansion (RSE), a rigorous perturbation theory recently developed in electrodynamics, is here applied to non-relativistic wave equation in one dimension. The resonant state (RSs) of a symmetric double quantum well structure superimposed by a combination of delta functions was first calculated. These RSs are then taken as an unperturbed basis for the RSE. The resonant state expansion is first verified for triple quantum well systems, showing convergence to the available analytic solution as the number of basis resonant states increases. The method is then applied to more complicated systems such as multiple quantum well and barrier structures. Results are compared with the Eigen solution in triple quantum wells and infinite periodic potentials, revealing the nature of the resonant states in the studied systems.

6 Committees

Program Committee

Dario Poletti, SUTD

Yee Sin Ang, SUTD

Cesare SOCI, SPMS, NTU

KOH Wee Shing, IHPC, A*STAR

Johnson GOH, TL / NTU

Christian KURTSIEFER, CQT and Physics Dept, NUS

Organizing Committee

Yee Sin Ang, SUTD

Dario POLETTI, SUTD

KOH Wee Shing, IHPC, A*STAR

Cesare SOCI, SPMS,NTU

Christian KURTSIEFER, CQT and Physics Dept, NUS

Sanchali Mitra, SUTD (postdoc)

Rina Rin Binte Sodar, SUTD (Senior Associate)

Irene Zhuang, SUTD (Associate Programme Director)

Author List

Abdillah, Shaik, 78
Acharya, Tejas, 33
Adamo, Giorgio, 27, 39, 66, 80
Adira, Mohitha, 44
Agarwal, Piyush, 13, 15, 16
Aghamalyan, Davit, 45
Ahmad, Azaz, 42
Ahmadi, Morteza, 13
Aimet, Stefan, 49
Aliyev, Vagif, 81
Anders, Janet, 49
Andreani, Lucio C., 65
Ang, Daniel G., 84
Ang, Lay Kee, 85
Ang, Xuan Yi, 13
Ang, Yee Sin, 35, 42, 43, 45, 60, 63
Aolita, Leandro, 24, 54
Arcia Lopez, Andres, 54
Ariando, Ariando, 16
Assad, Syed, 17
Assad, Syed M, 30, 75
Auffeves, Alexia, 82
Avsar, Ahmet, 62
Aw, Clive Cenxin, 41

Bae, Eunok, 75
Bae, Sunghyun, 78
Bai, Ge, 49
Balachandran, Vinitha, 21
Bandurin, Denis, 62
Banerjee, Ayan, 38
Banerji, Anindya, 19, 71
Baum, Christian Alexander, 52
Bayat, Abolfazl, 45
Behera, Mukundadev, 15
Beigi, Salman, 50
Belopolski, Ilya, 6
Berk, Graeme, 40
Bhattacharya, Priyanshu, 84
Bhowmick, Dhiman, 31
Brosseau, Pierre, 80
Budoyo, Rangga Perdana, 26

C. H. Liew, Timothy, 38
Calero Mas, Hector, 29
Calsamiglia Costa, John, 41
Carrazza, Stefano, 18
Casagrande, Heitor, 21
Castro Neto, Antonio Helio, 59
Chan, Eng Aik, 27, 84
Chan, Jun Jie, 20
Chang, Taeyong, 27, 39, 80
Cheah, Bing Wen, 26
Chee Beng, Nelson Lim, 62
Chen, Che-Chin, 84
Chen, George, 13, 14, 78
Chen, Tianqi, 82
Chen, Xu, 28
Cheng, Lin, 37
Cheong, Jian Wei, 20, 22
Chew, Lock Yue, 20, 22
Chiew, Wen Xin, 20
Chin, Jia Boon, 23
Chin, Jiaboon, 19
Chiu, Kuan-Fu, 76
Cho, Young-wook, 27
Choi, Gil Young, 85
Chong, Yidong, 38
Chotibut, Thiparat, 57, 75
Chow, Chang Hoong, 23
Chowdhury, Arya, 19, 71
Chua, Rui Ming, 79
Clark, Lewis, 17
Conlon, Lorcan O., 27
Copetudo, Adrian, 39

Dai, Jiayu, 11
Dangniam, Ninnat, 57
Das, Subhakanta, 28, 52
Das, Swarup, 25
Dasigi, Karthik, 70
de Gliniasty, Gregoire, 82
de Lima Silva, Thaís, 54
Dhyani, Veerendra, 28
Diao, Caozheng, 32
Dieckmann, Kai, 24, 28
Ding, Hai-Tao, 19
Ding, Jiewei, 22
Dini, Kevin, 65
Dmitriev, Pavel A., 70
Dong, Xuan, 22
Dong, Zhaogang, 8, 27, 70
Dorogov, Aleksandr, 29
Du, Jinyi, 13, 14, 28, 78
Duan, Xitong, 80
Dubrovkin, Alexander M., 66
Dumke, Rainer, 20, 26
Dutta Gupta, Subhasish, 38
Dutta, Ronit, 19

Eisert, Jens, 49

Elesin, Leonid, 62
Emeriau, Pierre-Emmanuel, 82
Enshan Koh, Dax, 30, 75
Er, Arif, 88
Ermakov, Alexey, 62

Fadel, Matteo, 49
Fang, Shibo, 42
Fanizza, Marco, 74
Feng, Ling, 74, 87
Feng, Pan, 19
Fischbach, Jan David, 83
Foo, Yan Xi, 45
Foreman, Matthew, 69

Gabardos, Lucas, 47
Gan, Chee Kwan, 18
Gan, Jaren, 13
Gao, Hongwei, 13, 14, 78
Gao, Jia-Yang, 13, 56
Gao, Shuai, 71
Gao, Tianyu, 11
Gao, Yvonne, 39
Gao, Yvonne Y., 29, 32
Garbet, Xavier, 34
Gerace, Dario, 65
Ghazaryan, Davit A., 59
Ghosh, Nirmalya, 38
Ginanjar, Wastu Wisesa, 35
Gluza, Marek, 49, 54, 75
Goh, Kuan Eng Johnson, 83
Gong, Li, 27
Goodarzi, Milad, 50
Gragera Garces, Maria, 50
Gu, Hanfeng, 53
Gu, Mile, 40, 41, 74
Guan, Chunying, 27
Guo, Kaize, 15
Guo, Ruixiang, 80
Guo, Yu, 19, 71
Guo, Zhenyu, 26, 68, 84
Gupta, Puneet, 15
Guéry-Odelin, David, 47

Hakem, Katia, 82
Hanamura, Fumiya, 70
Hao, Hao, 28, 29
Haotian, Song, 28
Haug, Tobias, 24
Haw, Jing Yan, 30, 32
Ho, Pin, 9
Holmes, Zoe, 75
Hon, Marc, 7
Hoogsteder-Riera, Matt, 41
Htet, Thura Kaung, 34
Hu, Mengyao, 38
Hu, Yanglin, 74
Huang, Ding, 21, 81
Huang, Ni-Ni, 39
Huang, Ruo Cheng, 74
Huang, Yiqiao, 13
Hui Kim, Hui, 62
Huynh, Nguyen, 24
Hwang, Sunjun, 23

Ignacio Latorre, Jos'E, 56
Impens, Francois, 47
Ivashko, Oleh, 84

Jamshed, Bilal, 28, 52
Jana, Subhajit, 62
Jaseem, Noufal, 21, 56
Jaya Kumar, Jeykanth, 18
Jeon, Youngsun, 27
Jia, Ridong, 69
Jia, Zhian, 56
Jiang, Mengting, 13
Jiang, Xiao, 43
Jin, Seungwon, 29
Jorba, Pau, 84
Joshi, Manoj Kumar, 48

Kabiraj, Arnab, 60
Kajen, Rasanayagam, 26
Kam, John, 56
Kanchanapusakit, Wittaya, 12
Kang, Yufan, 35
Kapitan, Vitalii, 17
Karuppannan, Senthil Kumar, 62
Kasper, Amon, 39
Kasper, Amon Maria, 39
Kasper, Michael, 35
Kautilyaa Krishnaswami, Gunasheel, 62
Kee, Chun Yun, 85
Khoo, Jun Yong, 18
Kim, Mu Young, 21
Kim, Si Hyung, 13
Kishida, Masako, 84
Klebl, Lennart, 52
Koh, Darren, 36
Koh, Eugene, 21
Koh, Si Yan, 83
Koh, Teck Seng, 18, 56, 57, 76, 83
Koirala, Rishav, 24, 28
Kolpakova, Marina, 20
Kommanaboina, Naga Manikanta, 62

Kong, Jian Feng, 18, 82
Koon, Gavin Kok Wai, 59
Kravtsov, Mikhail, 62
Krishnaswamy, Gunasheel Kauwtilyaa, 63
Krisnanda, Tanjung, 39
Kudriashov, Andrei, 62
Kumar Srivastava, Yogesh, 15
Kumar, Durgesh, 52
Kurtsiefer, Christian, 20, 22, 23, 35, 36, 80
Kwan Jie Wen, Russell, 32
Kwek, Leong Chuan, 23, 33, 45
Kwek, Leong-Chuan, 19
Kwon, Hyukjoon, 75
Kwon, Kwang-Ho, 85
Kwong, Chang Chi, 25, 47
Kwong, Chang Jian, 22

Laha, Arnab, 30
Lai, Po-Yen, 87
Lam, Ping Koy, 27, 30, 75
Lan, Shau-Yu, 25
Lavie, Emilien, 16, 71
Lecamwasam, Ruvi, 27
Lee, Ching Hua, 52
Lee, Darius, 78
Lee, Herman Shiu-Hang, 12
Lee, Hui Min, 87
Lee, Jeff, 32
Lee, Jianwei, 13
Lee, Nigel, 21
Leykam, Daniel, 53, 58, 76
Li, Jianing, 25
Li, Jinxiang, 66
Li, Qiang, 45
Li, Songze, 84
Li, Weiyan, 27
Li, Xian, 87
Li, Xiang, 39
Li, Xiaojing, 51
Li, Xiaotong, 27
Li, Yongqiang, 11
Li, Yue, 28
Lim, En Teng, 13, 14, 28, 78
Lim, Kay Jin, 83
Lim, Kyungtak, 34
Lim, Sharon Xiaodai, 15
Lim, Zi Yao, 18
Lin, Karen Ke, 16
Lin, Shuxin, 43
Ling, Alexander, 13, 14, 16, 19, 22, 23, 28, 32, 71, 78
Ling, Euk Jin Alexander, 23, 78
Liscidini, Marco, 65
Liu, Anthony Yuezhang, 10
Liu, Jianpeng, 11
Liu, Jianwei, 66
Liu, Mengqin, 51
Liu, Mingxuan, 49
Liu, Zhangcheng, 12, 88
Loke, May Chee, 39
Lourembam, James, 13, 15, 16
Low, Derrick, 87
Lu, Youqi, 10
Luchnikov, Ilia, 24
Lumbreras, Josep, 41, 74
Luo, Qinlan, 11
Lye, Adolphus, 73

M. S. Farias, Renato, 54
Ma, Hailan, 41
Ma, Xinyuan, 25
Maddu, Ramu, 28, 52
Maity, Arghya, 56, 57, 76, 83
Manabe, Hidetaka, 53
Mantha, Subrahmanyam Sai Gurunath, 35
Marangi, Marco, 65, 66
Martinelli, Filippo, 65, 81
Mata-Cervera, Nilo, 68
Matsukevich, Dzmitry, 21
Meiller, Tim Collin, 65
Mihm, Moritz, 78
Mingxuan, Liu, 41
Mishra, Pinkesh Kumar, 28
Mitra, Chirantan, 47
Mitra, Sanchali, 35, 60
Modi, Kavan, 56
Moe Thar, Soe, 78
Mohanraj, Sakthi, 28
Mohanraj, Sakthi Sanjeev, 80
Mooi, Hoe Kin, 33
Mostajeran, Cyrus, 54
Mukherjee, Manas, 13, 56
Munro, William, 21
Murapaka, Chandrasekhar, 15
Murtadho, Taufiq, 49

Narasimhachar, Varun, 74
Ng, Boon Long, 23, 71
Ng, Hui Khoon, 83
Ng, Nelly, 49
Ng, Nelly H. Y., 18
Nguyen, Ba Linh, 23
Nguyen, Long Hoang, 26
Novoselov, Kostya, 62

Novoselov, Kostya S., 59
Nussupbekov, Ayan, 85

Obidov, Mukhammad Ali, 62
Omar, Ganesh Ji, 16
Ong, Theodore Kay Chen, 73
Onggadinata, Kelvin, 18, 56, 57, 76, 83
Ou, Jun-Yu, 84

Paka, Tithivich, 75
Pan, Feng, 6, 53
Panda, Sanjeet Swaroop, 27
Patel, Nandan, 71
Paul, Peter, 66
Peng, Bo, 14
Phoong, Jackson, 17
Pimenta Lima, Alexandre, 59
Pira, Lirandë, 10, 50, 58
Piramanayagam, S.N., 28, 52
Plets, Karel, 87
Plum, Eric, 66
Poh, Hou Shun, 35
Poletti, Dario, 21, 33, 54, 56, 57
Pradana, Andri, 20, 22
Prakash, Vindhiya, 23
Principi, Alessandro, 62
Puig, Ricard, 75

Qin, Hao, 32
Qin, Yi, 44
Qu, Yuxuan, 74

Rahaman, Hasibur, 28, 52
Ramesh Nalge, Divij, 34
Ramos-Calderer, Sergi, 56
Reed, Niko, 84
Regnat, Alexander, 84
Ren, Feixiang, 74
Reva, Sergei, 31
Rho, Junsuk, 27
Riechers, Paul, 74
Roncaioli, Connor, 84
Roy, Hrittik Kumar, 15
Roy, Sauvik, 38
Ruan, Yang, 15
Rucker, Felix, 84
Ruiz, Roberto, 54
Rusydi, Andrivo, 32

S., Gauthameshwar, 21, 56
Sachan, Arushi, 16
Sah, Raghav, 35
Samizadeh Nikoo, Mohammad, 85
Santosa, Bella, 76
Sardar Jafar, Sahil, 26
Sarkar, Saubhik, 45
Scarani, Valerio, 40, 41, 47, 49
Schmiedmayer, Jörg, 49
Schut, Martine, 47
Schwinger, Jonathan, 39
Sengupta, Pinaki, 44
Sharma, Ankush, 22, 23
Shen, Yijie, 26, 68, 84
Shen, Yuan, 19
Shettell, Nathan, 82
Shi, Jinhui, 27
Shi, Xiaodong, 28, 80
Shiddiq, Muhandis, 32
Shilov, Artur, 62
Shiotsu, Hallie, 76
Shu, Fangzhou, 31
Sidajaya, Peter, 41
Sim, Glendon Chu Feng, 59
Singh, Isha Le Xue, 74
Soci, Cesare, 23, 65, 66, 80, 81
Song, Haotian, 24
Song, Peng, 59
Song, Pengtao, 32
Sopena, Alejandro, 54
Soret, Ariane, 82
Sornsaeng, Apimuk, 57
Soumyanarayanan, Anjan, 62
Sow, Chorng Haur, 15
Spallek, Jan, 84
Srimahajariyapong, Kasidit, 75
Stilck França, Daniel, 24
Sudheer, Manjima, 66
Sun, Dihang, 26
Sun, Zeen, 19
Suwannachit, Suwannachad, 75
Suzuki, Yudai, 54, 75
Svintsov, Dmitry, 62

Tan, Daniel, 12
Tan, Dawn, 13, 14, 78
Tan, John, 51
Tan, Jun Wei, 52
Tan, Meng-Chwan, 88
Tan, Peng Kian, 36
Tan, Zenn, 13
Tanalikhit, Pattarapon, 12
Tang, Ho-Kin, 22
Taniguchi, Takashi, 62
Tanimu, Abdullahi, 88
Teo, Bryan, 76

Teo, Hau Tian, 66
Tewari, Pratham, 11
Thanasilp, Supanut, 57, 75
Thanos, Dimitrios, 58
Thapa, Bibhuti, 35
Thomale, Ronny, 52
Thompson, Jayne, 40, 41
Tiong, Jackson, 33, 47
Tiwari, Pranay, 19, 71
Tjiptoharsono, Febiana, 62
Tkachev, Sergey, 59
Tomamichel, Marco, 50
Tong, Su, 35, 63
Too, Hon Lin, 73
Touzard, Steven, 70
Trieu, Celine, 39
Tseng, Yu-Heng, 7

Ustyuzhanin, Andrey, 17

Van Horne, Noah, 47
Varshney, Muskan, 78
Verma, Harshit, 75, 82
Verstraelen, Wouter, 45
Vespri, Vincenzo, 49
Vetlugin, Anton, 23, 81
Vetlugin, Anton N., 66, 80
Vijendran, V, 30, 75
Vitagliano, Giuseppe, 49

Walsworth, Ronald, 84
Wang, Benquan, 27, 36, 84
Wang, Botao, 11
Wang, Chengmeng, 25
Wang, Dingzu, 54, 56
Wang, Fan, 42
Wang, Jianhua, 60
Wang, Jiawei, 80
Wang, Kaiyuan, 69
Wang, Sihao, 28
Wang, Xiaojie, 28
Wang, You, 38
Wang, Yu, 84
Wang, Yuchun, 29
Wang, Yuhao, 22
Wang, Zheng Da, 76
Watanabe, Hajime, 25
Watanabe, Kenji, 62
Weber, Bent, 83
Wee, Matthew, 32, 78
Wee, Wen Jun, 17
Wei, Jiachen, 85
Wei, Yating, 69
Wesołowski, Adam, 58
Wilkowski, David, 25, 47, 71
Winter, Andreas, 41
Wo, Kah Jen, 70
Wright, Andrew, 82
Wu, Dake, 87
Wu, Guangxing, 28
Wu, Lin, 30, 31

Xia, Tong-Yan, 71
Xiao, Sicong, 73
Xie, Honglin, 26
Xie, Xi, 84
Xu, Ruyi, 32
Xu, Weiqiang, 85
Xu, Zifang, 22, 23

Yadav, Gyanendra, 36
Yang, Bing, 11
Yang, Huanhuan, 43
Yang, Ran, 27, 28, 80
Yang, Sibin, 44
Yang, Xu-Chen, 11
Yang, Xuchen, 11
Yim, Bernard, 33
Yohana, Lilis Rachel, 26
You, Jiabin, 82
You, Jiacheng, 21
Yu, Kehui, 39
Yu, Wing Chi, 22, 44
Yuan, Haomu, 24
Yuan, Jianmin, 11

Zacheo, Andrea, 65
Zanon, Thomas, 25
Zanotti, Simone, 65
Zeng, Qiyu, 11
Zhan, Yuancheng, 19
Zhang, Ao, 52
Zhang, Baile, 66
Zhang, Ling-Feng, 44
Zhang, Rongjie, 21
Zhang, Xingjian, 78
Zhang, Yingshan, 39
Zhao, Jie, 27
Zhao, Mengyao, 28
Zheludev, Nikolay, 27, 39
Zhou, Jinyu, 71
Zhou, Lin, 28, 80
Zhou, Xiangyu, 62
Zhou, Xin, 62
Zhou, Yuying, 16
Zhu, Bofeng, 68

Zhu, Changyan, 70
Zhu, Di, 28, 80
Zhu, Zeyu, 32

(Notes)
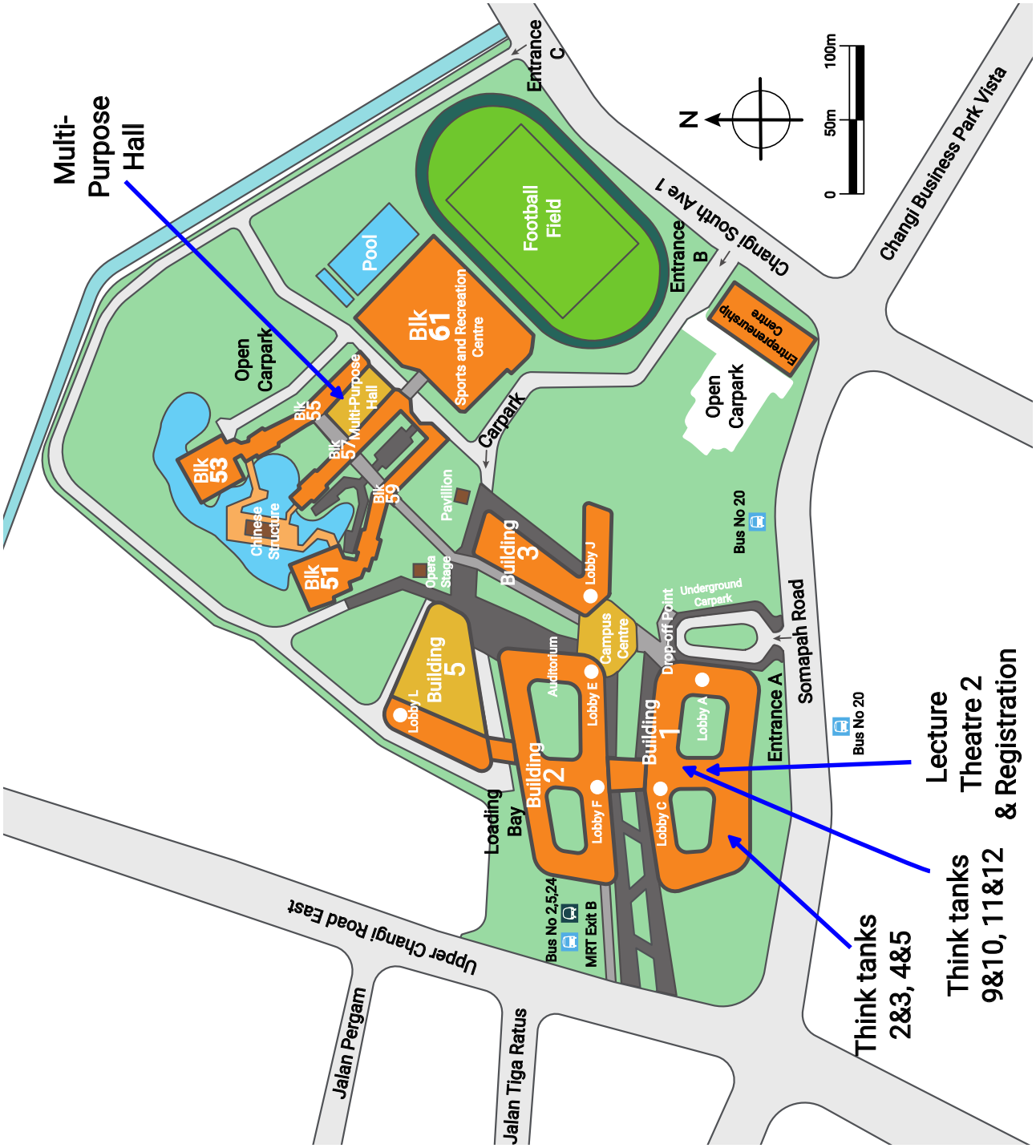
Location Map